INTERACTION OF WINTER FLOUNDER ANTIFREEZE PROTEIN WITH ICE

INTERACTION OF WINTER FLOUNDER ANTIFREEZE PROTEIN WITH ICE

By

ALEXANDER JOROV, B.Sc., M.Sc. IN PHYSICS

A Thesis Submitted to the School of Graduate Studies

In Partial Fulfillment of the Requirements

For the Degree

Master of Science

Department of Biochemistry

McMaster University

MASTER OF SCIENCE (2001) McMaster University

(Biochemistry) Hamilton, Ontario

TITLE: Interaction of Winter Flounder Antifreeze Protein with Ice

AUTHOR : Alexandre Jorov, M.Sc in Physics (St.Petersburg State Technical University)

SUPERVISOR: Professor Daniel S.C. Yang

NUMBER OF PAGES: XIII, 108

Abstract

Interpretation of crystallographic and mutational studies of antifreeze proteins (AFPs) requires molecular modeling of AFPs with ice. Most models proposed so far suggested H-bonds as the major driving force of AFP-ice association. However, the bulk water offers optimal network of H-bonds and van der Waals contacts to the isolated AFP and ice suggesting that corresponding components of free energy would not decrease upon AFP-ice association. In an attempt to resolve this controversy, we Monte Carlo-minimized complexes of several AFPs with taking into account, in addition to nonbonded interactions and H-bonds, the hydration potential for proteins (Augspurger and Scheraga, 1996). Parameters of the hydration potential for ice were developed basing on an assumption that at the melting temperature the free energy of water-ice association is small. Simulations demonstrate that desolvation of hydrophobic groups in the AFPs upon their fitting to the grooves at the ice surface presents the major stabilizing contributions to the free energy of AFP-ice binding. Our results explain available data on structure of AFPs and their mutational analyses, in particular, a paradoxical fact that substitution of Thr residues to Val does not affect potency of Winter Flounder AFP.

Acknowledgements

I would like to thank my scientific supervisor Dr. Daniel S.C. Yang for guiding me during this project. I am very grateful to Dr. Boris S. Zhorov for his help in the modeling studies. I would like to acknowledge the members of my supervisory committee Dr. Vettai S. Ananthanarayanan, Dr. David W. Andrews and Dr. Eric D. Brown. In addition, I highly appreciate the help of Quyen Hoang in almost any issue, as well as of all other members of Dr. Yang's lab.

Table of contents

Abbreviations

3D	-	three-dimensional
AAAA-		the mutated WF AFP with Thr 2,13,24,35 substituted to alanine residues
AFP	-	antifreeze protein
CD	-	Circular Dichroism spectroscopy
H-bond-		hydrogen bond
MCM	-	Monte Carlo Minimization
MD	-	Molecular Dynamics
MEC	-	minimum-energy conformation
NMR	-	Nuclear Magnetic Resonance spectroscopy
SSSS	-	the mutated WF AFP with Thr 2,13,24,35 substituted to serine residues
RVR	-	reduced van der Waals radius
VHS	-	volume of the solvent-exposed hydration shell
VS	-	van der Waals & solvation force field
VVVV-		the mutated WF AFP with Thr 2,13,24,35 substituted to valine residues
WF	-	winter flounder
WT	-	wild type
ZMM	-	Zhorov Molecular Mechanics

List of Illustrations

List of Tables

Chapter 1. Introduction

1.1 What are antifreeze proteins ?

In order to survive the subzero temperatures, living organisms must protect themselves from fatal ice crystal growth (DeVries et al., 1974) . Some of these organisms produce antifreeze proteins (AFPs), which depress the freezing point of their body fluids. The freezing point of a solution at a given pressure is defined as the temperature at which liquid and solid phases have the same free energy. There are antifreeze compounds, such as ethylene glycol, that lower this freezing point by an amount proportional to their molar concentration (colligative effect). In contrast, AFPs depress the freezing point 300-500 times more than one can predict basing on this effect. (Harding et al., 1999). The mechanism of this depression is that AFPs bind to specific surfaces of seed ice crystals, thus inhibiting further ice growth and preventing the freezing of the solution (Wilson, 1994).

First, AFPs were found in millimolar concentrations in the blood of polar fish, which live in sub-zero Antarctic waters (Scholander et al., 1957; DeVries et al., 1980;

DeVries, 1982; DeVries, 1983). Currently, structures of five different types of AFPs has been determined (Davies & Sykes, 1997). Type I AFPs are alanine-rich α-helical proteins of 3.3-4.5 kDa (Duman & DeVries, 1974; Duman & DeVries, 1976; Hew et al., 1985).Type II AFPs are cysteine-rich globular proteins, containing five disulfide bonds (Ng et al., 1986; Slaughter et al., 1981; Ng & Hew 1992) .Type III AFPs are globular proteins of approximately 6 kDa (Jia et al., 1995; DeLuca et al., 1996; SoÈnnichsen et al., 1996; type VI AFPs are glutamate- and glutamine-rich α-helical proteins (Deng et al., 1997); also there are hyperactive insect AFPs (Graham et al., 1997; Liou et al., 2000) (see Figure 1.1 for structural details).

The best studied among them are type I AFPs, which were found in shorthorn sculpin, winter flounder, and other animals. (See Table 1.1 for sequence details).

1.2 Winter Flounder AFP

The winter flounder (WF) AFP HPLC6 (Duman & DeVries, 1974) is a 37 amino residues protein, containing three 11-residue repeats $ThrX_2AsxX_7$, where X is usually alanine. CD and NMR studies of this protein revealed that this protein is 100% α-helical with the exception of the N- and C- terminal residues. High resolution X-ray structure of WF (Sicheri and Yang 1995) (see Figure 1.3), confirmed its α-helical structure and provided a basis for further modeling of WF AFP with ice. The X-ray structure also

showed a N-terminal cap formed by Asp 1, Thr 2, Ser 4, Asp 5 and two water molecules; a C-terminal cap formed by amidated Arg 37. A salt bridge between Lys 18 and Glu 22 apparently stabilizes the protein's α-helix structure. Hydrogen bonds between hydroxyl groups of Thr 13 and Thr 24 and carbonyl oxygens of Ala 9 and 20 respectively are also observed.

1.3 Thermal hysteresis and crystal growth morphology

In general, AFP activity is characterized by the temperature of thermal hysteresis and by the ice crystal growth morphology in a solution containing AFPs. These two characteristics are the major footprints of the AFP activity.

The freezing temperature of the liquid phase at constant pressure is defined as the temperature at which the molecules of the solid and liquid phases have the same free energy. In pure water the freezing and the melting temperature are the same. This temperature can be depressed due to colligative effect by a value proportional to the molar concentrations of solute components. This is purely a thermodynamical effect; it does not depend on the chemical identity of the solute molecules or its dissociated particles.

In contrast to the colligative effect, AFPs apparently create a heterogeneous interlayer between the solid ice and liquid water, consequently distracting thermodynamically favorable growth behavior of the ice crystals. Since the binding of an AFP is specific only to certain crystallographic planes of the ice (Knight et al., 1991), this distraction results in macroscopic changes in morphology of ice crystal growth (Knight et al., 1984). If the concentration of AFP is high enough, ice crystal growth can be completely inhibited even at temperatures below the colligative freezing point. The lowest temperature at which this inhibition may take place is called the freezing temperature of the AFP solution. Unlike the colligative freezing temperature, it is not equal to the melting temperature of AFP solution. The difference between the freezing and melting temperature of the AFP solution is defined as the temperature of thermal hysteresis or simply thermal hysteresis. Thermal hysteresis is considered as the most important characteristic of the AFP activity. The magnitude of thermal hysteresis does not only characterize AFP, but also depends on the concentration of AFP. The thermal hysteresis curve is typically hyperbolic.

Another, perhaps very important characterization of AFP activity is the morphology of the ice crystal growth (Knight et al., 1984). Basically, it is an assessment of the shape of a single growing ice crystal. The specificity of AFP binding to a certain crystallographic plane of ice, when combined with the symmetry features of the ice crystallographic unit cell (see Figure 1.4 for details) results in differential bipyramidal-shaped ice crystal (see Figure 1.2). Practically, this assay is very useful for preliminary

evaluation of AFP activity, however precise analysis of three-dimensional (3D) shape of the crystal may be utilized to identify the ice plane to which AFP specifically binds.

The process of ice growth inhibition is often considered as a "kinetic" in nature (DeVries, 1983), this means that bound AFP molecules physically decrease or completely cover the water-accessible surfaces of ice; thereby preventing the ice crystal growth. However, we believe that this process can also be considered from a thermodynamical point of view. For instance, the freezing temperature of the AFP solution can be defined as the temperature at which the complex of AFP with ice has the same free energy as corresponding number of solvent molecules.

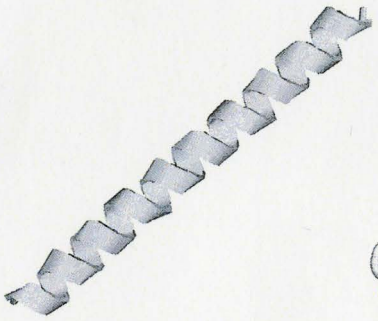

A) Type I
(Yang et al., 1988)

B) Type II
(Ng & Hew 1992)

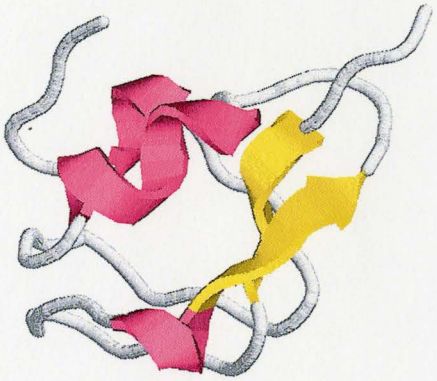

C) Type III
(Jia et al., 1995)

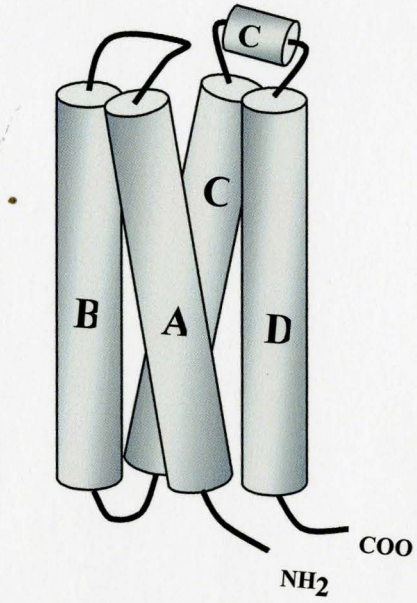

D) Type VI Structural model
(Deng et al., 1997)

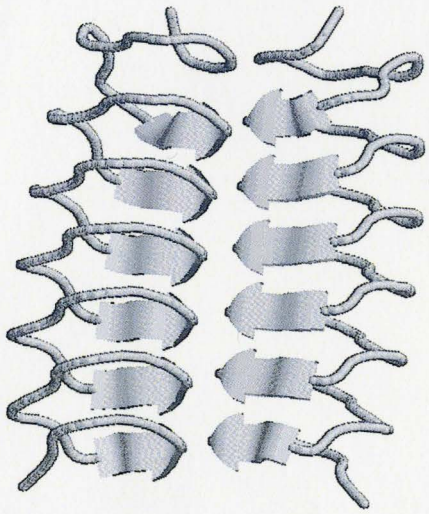

F) Insect AFP
(Liou et al., 2000)

Figure 1.1 Five different types of AFP

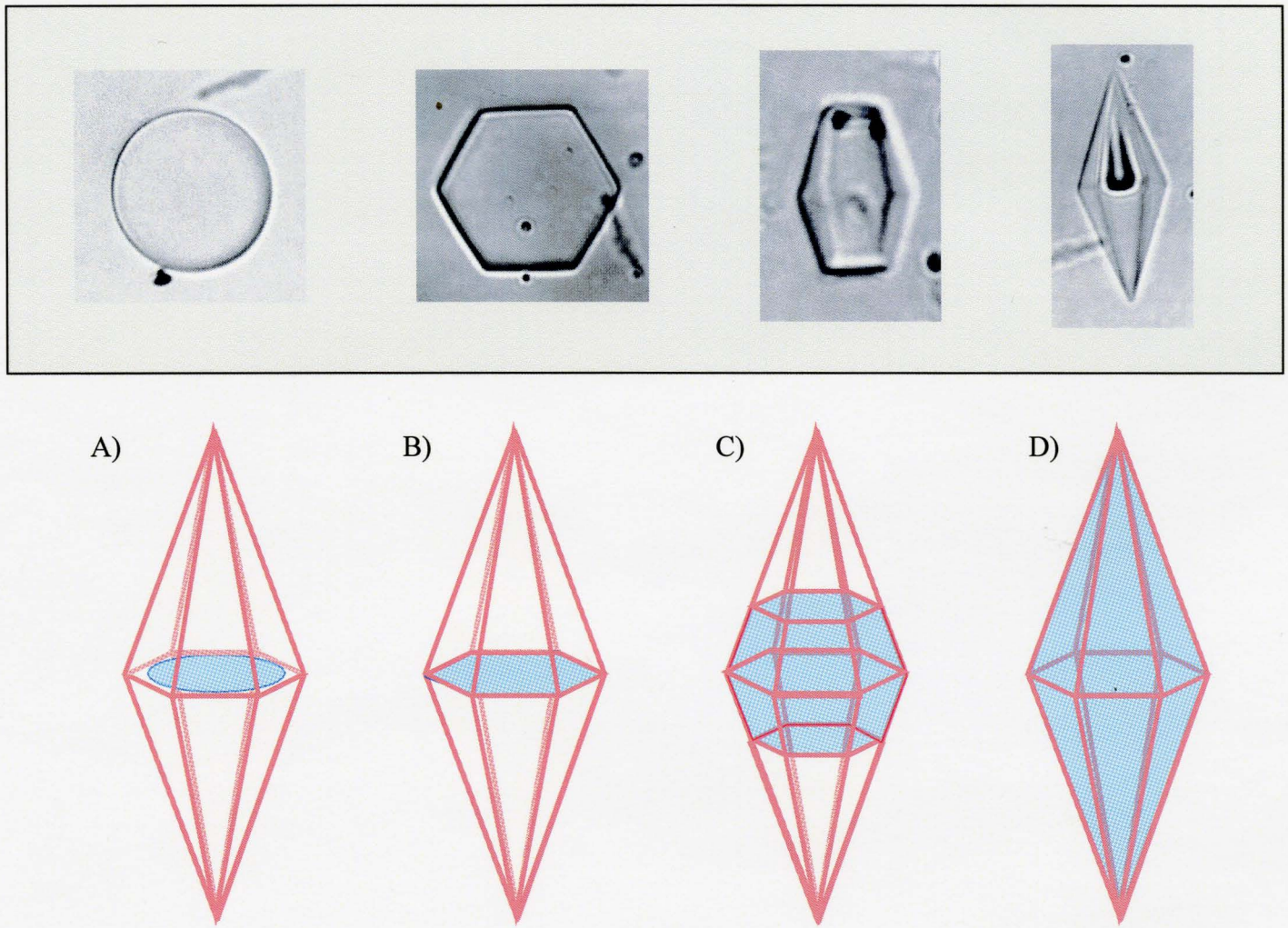

Figure 1.2 Morphologies of ice crystal growth in WF AFP solution and different stages of ice crystal growth in AFP solution. A- circle flat crystal, normally observed in pure water. B-hexagonal flat crystal observed at low AFP concentrations. C, D- bipyramid- shaped crystals observed at high AFP concentrations.

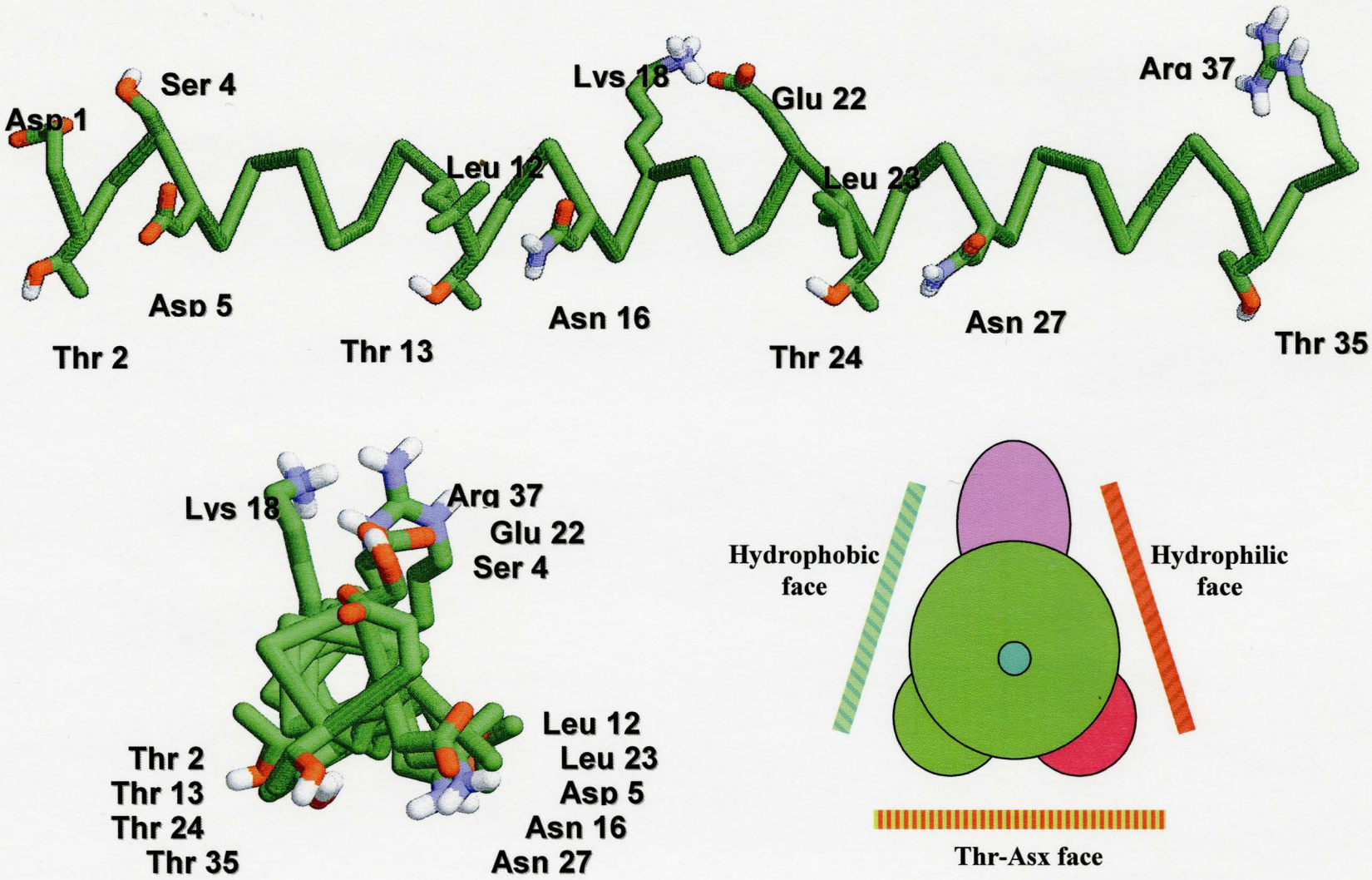

Figure 1.3 X-Ray structure of WF AFP at 1.7 Å resolution (Sicheri and Yang 1995); corresponding schematic representation of WF AFP defines abbreviation for its faces.

Table 1.1 Multiple sequence alignment of type I antifreeze proteins and their temperature hysteresis value. Adapted from (Harding et al., 1999)

Code	Species	Sequence	Hysteresis 10 mg*mL^{-1}	Ref.
HPLC6	Winter flounder	D TASDAAAAAAL TAANAKAAAEL TAANAAAAAAA TAR	0.68	[1]
HPLC8	Winter flounder	D TASDAAAAAAL TAANAKAAAKL TADNAAAAAAA TAR	0.6	[1]
AFP9	Winter flounder	D TASDAAAAAAA TAATAAAAAAA TAVTAAKAAAL TAANAAAAAAATAAAARG		[2]
YTF	Yellowtail flounder	D TASDAAAAAAA TAAAAAKAAAD TAAAAAKAAAD TAAAAAEAAAATAR	0.56	[3]
AP	Alaskan plaice	D TASDAAAAAAA TAAAAKAAAEK TARDAAAAAAA TAAAAR		[4]
SAFP1	Winter flounder	MDAPARAAAA TAAAAKAAAEA TKAAAAKAAAA TKAAAH		[5]
SS3	Shorthorn sculpin	MNAPARAAAK TAADALAAAKK TAADAAAAAAA	0.39	[6]
SS8	Shorthorn sculpin	MNGETPAQKAA RLAAAAALAAK TAADAAAKAAAKAA AIAAAAASA	0.68	[6]
GS5	Grubby sculpin	MDAPAIAAAK TAADALAAAKK TAADAAAAAAKP		[7]
GS8	Grubby sculpin	MDGETPAGKAA RLAAAAALAAK TAADAAAKAAAIAA AAA		[7]
AS1	Arcticsculpin	MDGETPAGKAA RLAAAAALAAK TAADAAAKAAAIAA AAA		[8]
AS3	Arctic sculpin	MDAPARAAAK TAADALAAANK TAADAAAAAAAA		[8]

[1] Duman, & DeVries, 1974; Duman, & DeVries, 1976
[2] Chao et al., 1996
[3] Scott et al., 1987
[4] Knight et al., 1991
[5] Gong et al., 1996
[6] Hew et al., 1985; Fletcher et al., 1982;
[7] Chakrabartty et al., 1988
[8] Yang et al., 1988

Table 1.2 Activity and α-helicity of Winter flounder HPLC6 selected mutants.

	Code	Sequence	Hysteresis (%)to WF AFP at 2mM	Helicity (%)	References
	HPLC6	D TASDAAAAAAL TAANAKAAAEL TAANAAAAAAA TAR	100	98	
	TTTT2KE	D TASDAKAAAEL TAANAKAAAEL TAANAKAAAEA TAR	100	100	[1]
	S23	D TASDAAAAAAL NAATAKAAAEL TAAAAANAAAA TAR	17	95.3	[2]
	TSST	D TASDAAAAAAL SAANAKAAAEL SAANAAAAAAA TAR	0.11	100	[3][4]
	SSSS	D SASDAAAAAAL SAANAKAAAEL SAANAAAAAAA SAR	0	100	[3]
	STSS	D SASDAAAAAAL TAANAKAAAEL SAANAAAAAAA SAR	0	105	[5]
	SSSS2KE	D SASDAKAAAEL SAANAKAAAEL SAANAKAAAEA SAR	0	100	[6,3]
	tttt	D tASDAAAAAAL tAANAKAAAEL tAANAAAAAAA tAR	29	97	[5]
	TVVT	D TASDAAAAAAL VAANAKAAAET VAANAAAAAAA TAR	85	100	[4]
	VVVV2KE	D VASDAKAAAEL VAANAKAAAEL VAANAKAAAEA VAR	100	100	[6]
	AAAA2KE	D AASDAKAAAEL AAANAKAAAEL AAANAKAAAEA AAR	17	100	[6]
	S21	D TASADAAAAAN LAANAKAAAEL TAAAAANAAAA TAR	0	106.2	[2]
	S22	D TASDAAAAAAN LAATAKAAAEL TAAAAANAAAA TAR	30	96.4	[2]
	S41	D TASDAALAAAA TAANLKAAAEA TAANAAAAAAA TAR	0	103	[7]
	S42	D TASDAAAAAAA TAANLKAAAEA TAANAAAAAAA TAR	0	102	[7]
	A17L	D TASDAAAAAAL TAANLKAAAEL TAANAAAAAAA TAR	0		[8]
	A19L	D TASDAAAAAAL TAANAKLAAEL TAANAAAAAAA TAR	80		[8]
	A20L	D TASDAAAAAAL TAANAKALAEL TAANAAAAAAA TAR	100		[8]
	A21L	D TASDAAAAAAL TAANAKAALEL TAANAAAAAAA TAR	10		[8]

[1] Chakrabartty & Hew., 1991
[2] Wen & Laursen., 1992
[3] Haymet et al., 1998
[4] Chao et al., 1997
[5] Zhang & Laursen., 1998
[6] Haymet et al., 1999
[7] Wen & Laursen., 1993
[8] Baardsnes et al., 1999

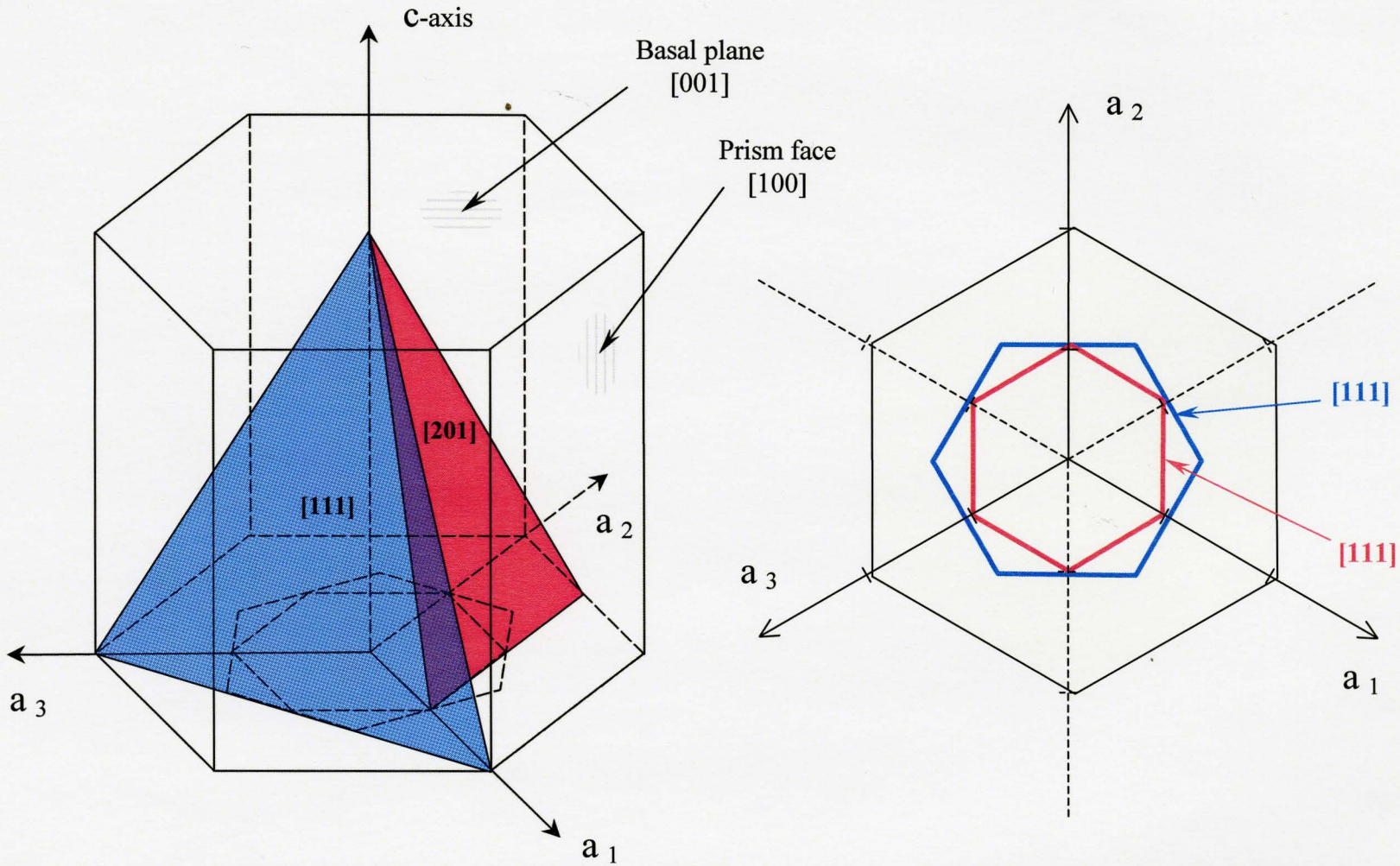

Figure 1.4 Schematic representation of a hexagonal unit cell of ice crystal showing the definition of axis and basal, prism, [201], [111] crystallographic planes. Left – 3D diagram, right – a slab parallel to a –axis. Please note that for simplification i+j vector is omitted in complete [i; j; i+j; k] indexing. This scheme indexes represent the whole set of symmetry related surfaces.

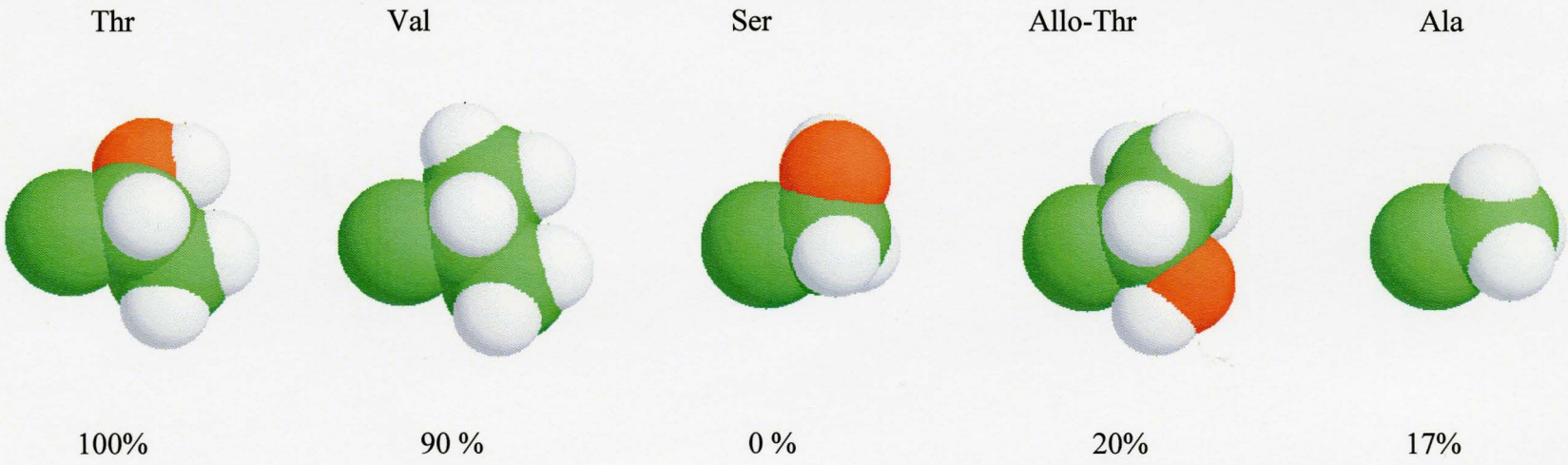

Figure 1.5 Effect of mutation of Thr residues on the activity of WF AFP. The numbers below the space-fill models indicate the activity of the mutants that contain respective residues at positions 2,13,24,35. See also Table 1.2 for mutants activity details.

1.4 Current theory on interaction of AFP with Ice

Based on the morphology of ice crystal growth, WF AFP was initially suggested to bind to the [100] prism face of ice (Raymond & DeVries., 1977). However, a series of ice etching experiments (Knight et al., 1991) showed that WF AFP specifically bound only to the [201] crystallographic plane of ice. These data, along with the X-ray structure (Sicheri and Yang 1995), leaded to the series of models of WF AFP with ice, in which Molecular Dynamics (MD) and Monte Carlo (MC) methods were used to predict the optimal orientation of AFP at the [201] surface of ice and the residues of AFP involved in the binding to ice (See below). The latest models suggested that Thr and Asx (Asp or Asn) repeats are responsible for WF binding to ice. The hydrogen bonding between hydroxyl groups of Thr, Asn, Asp residues and water molecules of ice was suggested as the major driving force of WF AFP binding to ice. Possible role of van der Waals and hydrophobic interaction has been suggested in several molecular modeling studies (Lal et al., 1993; Cheng & Merz, 1997), however no adequate theoretical model regarding this phenomena has been proposed.

1.5 Paradoxes in structure-activity relationships revealed by recent experiments with mutants of WF AFP

Until recently, hydrogen bonding remained the only candidate considered to be responsible for the binding of WF AFP to ice. However, recent experiments on the binding of WF AFP mutants to ice revealed a striking paradox in structure-activity relationships. The substitution of the hydrophilic Thr residues, which were generally thought to form H-bonds with ice (Raymond & DeVries, 1977; DeVries, 1984; Brooke-Taylor et al., 1996; Cheng & Merz, 1997) by the hydrophobic Val residues did not significantly affect the AFP activity (Haymet et al., 1999), whereas the substitution of these Thr residues by Ser residues eliminated AFP activity (Zhang & Laursen, 1998).

Another evidence against the theory that H-bonds are the major driving force of AFP-ice association was obtained when alanine residues in positions 17,19,20,21 of the WF AFP were simultaneously mutated to the bulky leucine residues (Baardsnes et al., 1999). The experiment showed that the WF AFP activity was seriously affected only when leucine residues have been substituted in positions 19 and 21, at the hydrophobic side of the AFP helix. The results of this experiment suggested that the "hydrophilic" face of WF AFP helix (see Figure 1.3) was not involved in the AFP binding to ice.

Because of the contradiction between the results of recent mutations and "H-bond" theory, the importance of other forces, such as van der Waals and hydrophobic

interactions were suggested. However no adequate explanation was provided for the physical origin of these forces in the AFP-ice system.

1.6 Molecular modeling and dynamics studies of WF AFP

Molecular modeling and dynamics studies of antifreeze proteins and WF AFP went through a long process of evolution, starting from the earliest intuitive models, where AFP was suggested to H-bind to the prism face of ice (Raymond & DeVries., 1977; DeVries & Lin., 1977; DeVries.,1984), to the latest and most advanced computer model, in which a proposed hypothesis that van der Waals interaction is the driving force of WF AFP binding to ice was tested (Dalal & Sonnichsen, 2000).

The first models (Raymond & DeVries, 1977; DeVries & Lin, 1977; DeVries, 1984) were primarily based on the ice crystals growth morphology studies and the knowledge of ice crystal structure. Since at low concentrations AFP modifies round and flat ice crystals into hexagonal ones, it was suggested that AFP binds to the prism faces of ice, and consequently inhibits ice crystal growth through those faces. As evidence, a 4.5 Å match between Thr and Asp, Asn amino residues of WF AFP and the distance between oxygen atoms of ice on the prism face was provided. However, this model did not explain the specificity of AFP binding to the prism face, since the 4.5 Å distance can be found in many different crystallographic faces of ice.

All subsequent models were based on the results of ice etching studies (Knight et al., 1991), which demonstrated that WF AFP specifically bound to the [201] crystallographic plane. In the absence of a high resolution X-ray data, molecular modeling studies were focused on the prediction of WF conformation. After the investigation of side chain conformation of WF AFP using Monte-Carlo simulating annealing and energy minimization protocol in vacuum, WF was suggested to bind to the [201] crystallographic face of the ice "in a zipper-like fashion" by H-bonding between the hydroxyl groups of Thr and oxygen atoms of ice. In this model, the predicted 16.1Å distance between Thr residues matched the 16.7 Å distance between oxygen atoms repeats along {0 1-1 2} vector on [201] face of ice (Chou, 1992). In a different molecular dynamics study, which was done for 0^{o} C and included solvent molecules, resulted in an average 16.6 Å distance between Thr residues and proposed a very similar mechanism of AFP binding to ice via H-bonds (Jorgensen et al., 1993). Another two molecular dynamics simulations of WF were reported at the CRYO'92 meeting also suggesting similar binding mechanisms to ice. (Haymet & Kay, 1992; McDonald et al., 1992).

The next very important step was the introduction of the ice surface to the computational experiment. One of the first groups, which successfully approached this kind of modeling, used COMMET software, which combined both MC and MD approaches (Lal et al., 1993). This research explored two possibilities of binding AFP to [201] and [001] faces of ice in vacuum. The results of this experiment showed that Thr, Asn and Asp of WF AFP formed H-bonds with ice surfaces, however they also

highlighted the importance of steric complementarity between AFP and ice, suggesting the contribution of van der Waals interaction to the free energy of AFP-ice binding. It was shown that the difference in AFP-ice H-bonding energy between [201] and [001] ice surfaces was not significant, while the difference in van der Waals potential was huge. Consequently, van der Waals interaction or "the lock and key mechanism" was proposed to be responsible for high affinity of WF AFP to [201] ice surface. The predicted binding energy –84 kcal/mol of WF AFP to ice [210] surface was suggested by the authors to be overestimated since the solvating effect was not taken into account.

Another group (Brooke-Taylor et al., 1996) focused on the behavior of water molecules surrounding the WF AFP. The results of this MD simulation, which was carried out with parameters corresponding to 0^{o} C, showed that water molecules around the hydrophobic regions of AFP are more flexible than near hydrophilic polar groups where water molecules tend to form organized H-bonded structure. The binding mechanism was proposed, in which WF AFP interacts with the ice through H-bonds, formed by polar groups, while the hydrophobic region "restricts the binding of further water molecules and keeps them in a flux, thus preventing further growth of ice". Contradiction of the results of this simulation with modern theory of hydrophobicity, according to which water molecules around hydrophobic groups restrict themselves in "water cages" formations, consequently resulting in the entropy penalty for free energy of the whole system, apparently did not influence author's conclusion.

MD simulations of WF AFP in gas, water and ice [201] interface (Cheng & Merz, 1997), despite introduction of water in the model, did not suggest anything new in terms of H-bonding concept involving polar groups of Thr, Asp and Asn. However this simulation failed to achieve the same level of steric complementarity as the model by Lal et al. (1993). Apparently, this is the result of overestimation of the energy of hydrogen bonds, which leads to trapping MD convergence trajectory in a local minimum, formed by strong hydrogen bonds. The authors of the paper also did say that activity of AFP is related to free energy of binding, however they did not comment on a value of -157 kcal/mol for the AFP binding energy to ice in water, which is roughly two times stronger than the already huge energy provided by Lal et al. (1993). More importantly, the reported value of -1062 kcal/mol of the combined energy of AFP interaction with ice surface and water molecules, in the case of bounded AFP, was higher than -1167.4 kcal/mol energy of interaction only with water molecules, in the case of fully solvated AFP. Despite this fact directly suggested that within proposed model and the energy estimation parameters, the binding of AFP on ice surface could not take place, it was left without any adequate explanation. This model also showed that the methyl groups of the Thr and Leu residues governed by van der Waals interactions tend to direct toward the groves on the ice surface. This is a rather controversial result, since it is reasonable to suggest that bulky waters theoretically should offer stronger van der Waals potential than ice, leaded authors to the important conclusion that hydrophobic interactions may contribute to the AFP binding. The authors suggested that interaction between hydrophobic groups of Thr and Leu with already organized ice, reduced the hydrophobic-

effect penalty of placement of those groups in water solution and therefore may contribute to the free energy of binding.

The most recent reported computer modeling studies of WF AFP (Dalal & Sonnichsen., 2000) tested the hypothesis, that van der Waals interactions are the dominant driving force of AFP- ice association. According to the authors, the importance of van der Waals interaction was based on experimental evidence, particularly on mutation studies of Thr substitution to Val (Zhang & Laursen, 1998; Haymet et al., 1999). Basically, in this computation, the rigid-body WF AFP was randomly positioned above the ice surface, and then the energy of the whole system was minimized. After a quarter of million of these cycles, the set of best energy conformations was selected. Using this relatively simple but elegant approach, the authors demonstrated that the minimum energy of van der Waals interactions corresponded to the conformation, in which AFP aligned along the {1-10-2} vector and bonded to the [201] surface of ice by its Thr-Ala-Asn face. The results of this study suggested that van der Waals interactions are not sufficient to explain recent experimental results on AFP binding specificity.

1.7 Our general approach and results

In this study, we analyzed all contributing forces to the interaction of AFP with ice and concluded that hydrophobic interactions between AFP and ice is the major driving force of AFP-ice interaction. We analyzed the activity curve of the WF AFP, and came to the conclusion that the free energy of AFP-ice binding does not exceed 5 kcal/mol.

We also consider the AFP-ice binding free energy as a small difference of two large values: energy of AFP hydration and energy of AFP-ice association in vacuum. Standard computational approaches, requiring the introduction of a large number of explicit water molecules to hydrate AFP and ice, are not expected to reproduce the small energy of AFP-ice binding, mainly because of two reasons. First, the parameters of the force fields used to simulate interactions of explicit water molecules with ice and with AFP, naturally, have limited accuracy. Second, introduction of at least a thousand explicit water molecules necessary to hydrate the large surfaces of AFP and ice would require additional 6,000 degrees of freedom. While modern computers allow using so many variables, simulation by the conventional molecular dynamics (MD) method would not move the system far from the starting point set up by the user.

To resolve this problem, we have employed non-standard computational approaches, namely Monte Carlo minimization (MCM) (Li and Scheraga, 1987) in the

space of generalized coordinates and calculation of hydration effect by using method of Augspurger and Scheraga, (1996) that involves "implicit waters". Since these methods had not been implemented in commercially available molecular simulation programs such as Discover (Biosym/MCI, USA), we used the program ZMM developed by Dr. B. S. Zhorov (Department of Biochemistry, McMaster University).

To test the above hypothesis that hydrophobic interactions are the major driving force in AFP-ice interactions, we built several computational models of AFP-ice system. We also adjusted parameters used in the method of Augspurger and Scheraga (1996) with the aim to make the method applicable for simulations of interactions of ice and protein with the solvent at the equilibrium freezing temperature of water. With the use of these parameters, the search for the optimal orientation of WF AFP on the ice surface was performed by numerous MCM "hands free" docking experiments from randomly generated starting points.

Finally, we analyzed the partitioned energy of AFP-ice interactions to determine individual atom-atom interactions that provide the largest contributions to the AFP-ice binding and discussed structure-activity relationships of known WF AFPs and their mutants in view of the results obtained. Importantly, our model explained most of the available experimental data on structure-activity relationships of WF AFP. In our model, WF AFP binds to the ice surface with its hydrophobic face. Unlike in other models, methyl groups of threonin residues were oriented inside the grooves on surface of ice,

while the hydroxyl groups remained in water. We also showed that this interaction is driven by the hydrophobic force of desolvation of WF AFP's hydrophobic groups. We demonstrated that WF AFP not only bind to the [201] surface of ice, but also to the [111] plane with slightly weaker binding energy.

Chapter 2. Binding energy of WF AFP and methods for its computing

2.1 Energy of AFP interaction with ice is approximately 5 kcal/mol, which contradicts with 80-150 kcal/mol shown in previous computation studies.

Understanding of AFP activity requires computational modeling of AFP complexes with ice. Ideally, such models should predict free energy of binding of AFP to ice ($\Delta G_{AFP\text{-}Ice}$). However, experimental values of $\Delta G_{AFP\text{-}Ice}$ are not available in the literature. Thermal hysteresis ΔT, which is defined as the difference between the "freezing temperature" of ice in the AFP solution and its "melting temperature", is the most common experimental characteristics reported. Figure 2.1 shows a typical concentration-dependent hyperbolic-like thermal hysteresis curve. The objective of this chapter is to derive $\Delta G_{AFP\text{-}Ice}$ from ΔT.

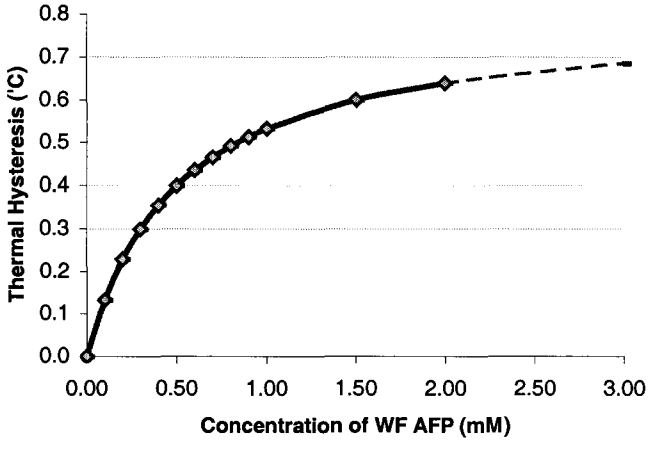

Figure 2.1 ΔT of Winter Flounder AFP.

The system under consideration consists of an AFP at concentrations C_{AFP}, which binds to the surface of ice.

$$AFP + Ice \underset{k-}{\overset{k+}{\rightleftharpoons}} AFP \equiv Ice$$

Conditions for a typical thermal hysteresis evaluation experiment are: 0.1mM - 3mM AFP in ~1mm size of the solution drop. The total binding surface of AFP is estimated to exceed that of ice by three orders of magnitude [£]. Therefore the fractional amount of AFP bound to the ice surface θ and AFP concentration in solution C_{AFP} is negligible to the total ice surface area. Consequently, θ should be thermodynamically defined by free energy of binding of AFP to ice surface.

By definition, at equilibrium the number of molecules of AFP that bind to the ice surface N_{+k} is equal to the number of AFP molecules that dissociate from the ice surface N_{-k}:

$$N_{k+} = N_{k-} \qquad (2.1)$$

According to Langmuir (1918) and Burcham et al., (1986) who first applied Langmuir approach to an AFP system, equation (2.1) rearranges to equation (2.2).

$$k_{+} \times (1 - \theta) \times C_{AFP} = k_{-} \times \theta \quad (2.2)$$

where θ is a fraction of the surface of ice covered by the AFP, C_{AFP} is concentration of AFP in solution, k_{+} and k_{-} are rate constants of the direct and reverse reactions.

Definition of association constant (K_a) and equation (2.2)gives us equation (2.3):

$$K_a = \frac{k_+}{k_-} = \frac{\theta}{(1-\theta)\times C_{AFP}} \qquad (2.3)$$

and, simple rearrangement yields to equation (2.4), in which K_d is the dissociation constant

$$\theta = \frac{K_a C_{AFP}}{1+K_a C_{AFP}} = \frac{C_{AFP}}{K_d + C_{AFP}} \qquad (2.4)$$

Fractional hysteresis activity (ΔT_F) can be defined as the ratio between the temperature of the thermal hysteresis at certain concentration (ΔT_C) and the maximum temperature of thermal hysteresis observed at the saturation concentrations (ΔT_{max}). We assume that ΔT_F depends on θ or, in other words, ΔT_F is a function of θ

$$\Delta T_F \equiv \frac{\Delta T_C}{\Delta T_{max}} = \psi(\theta) \qquad (2.5)$$

where ψ is an unknown function. Combination of equation (2.5) and equation (2.4) gives us equation (2.6) in which the temperature of thermal hysteresis (ΔT_C) is a function of AFP concentration (C_{AFP}).

$$\Delta T_C = \Delta T_{max} \psi \left[\frac{C_{AFP}}{K_d + C_{AFP}} \right] \quad (2.6)$$

The simplest representation of the function ψ, with which the theoretical equation (2.6) perfectly fits the experimentally observed thermal hysteresis curves, is given by equation (2.7)

$$\psi(x)=x \qquad (2.7)$$

Thus, combination of equations (6) and (7) gives us the final equation for ΔT_C

$$\boxed{\Delta T_C = \Delta T_{max} - \frac{K_d \Delta T_{max}}{K_d + C_{AFP}}} \quad (2.10)$$

From equation (2.10) it is easy to derive that K_d is equal to concentration at which ΔT_C is equal to half of ΔT_{max} : see equation (2.11). On the other hand, $\Delta G_{AFP\text{-}Ice}$ is related to the K_d by the fundamental Arrhenius equation (2.12).

$$C_{\frac{1}{2}} : \langle \Delta T_{C\frac{1}{2}} = \frac{1}{2} \Delta T_{max} \rangle$$

$$K_d = C_{\frac{1}{2}} \qquad (2.11)$$

$$\Delta G = RT \cdot Ln(K_d) \quad (2.12)$$

The Experimental value $C_{1/2}$ of, for example, Winter Flounder AFP is about 0,5mM (Baardsnes et al., 1999). Since R≈1,99 cal mol^{-1} K^{-1} and T ≈ 273 K thus :

$$\Delta G^{WF}_{FP-Ice} \approx 1{,}99 \times 273 \times Ln(5 \cdot 10^{-4}) \approx -4{,}1 \cdot kcal \cdot M^{-1}$$

All earlier modeling of AFP predicted binding energy at the level of hundreds kcal/mol (e.g., Cheng & Merz, 1997). We believe, such values are not reasonable.

£ Under typical for thermal hysteresis evaluation experiment conditions: 0.1mM - 3mM of AFP concentrations and about 1mm size of the solution drop, the total binding surface of AFP exceeds that of ice by three orders of magnitude.

Let us consider an ice crystal with radius r embedded in a drop with radius R of 1mM AFP solution. The volume of this drop has order of value ~ R^3 mm^3 and the surface area of ice crystal has ~ $r^2 mm^2$.

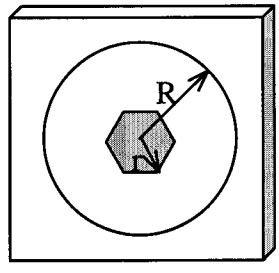

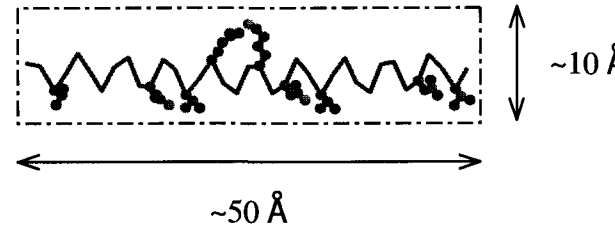

An approximate surface area which can be covered by an individual molecule of WF AFP is ~500 $Å^2$=$5 \cdot 10^{-12}$ mm^2. Consequently, it is possible to accommodate ~$2 \cdot 10^{11} \times r^2$ molecule of AFP on the surface of this ice crystal. On the other hand, there are $10^{-9} \times R^3$

Mol of AFP or ~ $6 \cdot 10^{14} \times R^3$ molecules in the drop with radius R mm of 1mM AFP solution.

Thus, in this system, the ratio between quantity of AFP molecules and that of available AFP binding sites on the surface of ice will be :

$$\frac{6 \cdot 10^{14} \cdot R^3}{2 \cdot 10^{11} \cdot r^2} \sim 10^3 \cdot \frac{R^3}{r^2}$$

if the ice crystal occupies the whole volume of the drop, in typical hysteresis assay (R~1mm) this ratio is 10^3 .

2.2 The necessity of water in the computational model

The contradiction between experimental results and recent molecular models of WF AFP clearly shows that it is impossible to predict the behavior of this system using a conventional force field in vacuum. Water, an equally important member of interaction, was factored out from the consideration. In modeling studies on ligand-protein interaction omitting of water effects may not lead to serious consequences. However AFP-water-ice system practically compares water with ice, which is basically the rigid organized water. Therefore, omission of water would be totally unacceptable. One should be able to demonstrate the difference between interaction with the rigid and solid water.

2.3 Explicit and implicit water

In general, two approaches are possible for introduction of solvent effect to the computer molecular system: explicit and implicit waters. Explicit water is basically just water molecules randomly incorporated to the computer system of ice and AFP with certain density. Theoretically it is a way to account for water effects on the system, however this approach demands enormous amount of computing resources. This method is practically impossible to implement for our task due to the large number of variables,

such as positions and orientations of water molecules. On the other hand, a much more efficient method had been developed to take water into account, that is implicit water. This method, in contrast to explicit water method, does not deal with individual water molecules, instead it uses the term "solvation potential". This potential, multiplied by the volume of the solvating shell of an atom group, is equal to the energy of transferring the group from vacuum to water. The parameters for this method, such as potential and volume of solvating shell, are derived from experimental observations. This method allows relatively easy estimation of the solvation effect during binding process. For instance, solvation component of binding energy of two atomic groups would be equal to the solvation potential of each group multiply by the volume which both solvating shells exclude from each other upon binding.

2.4 Necessity of implicit water for computation

The implicit water method provides reliable, but more importantly, obtainable solution for including the water factor into AFP-ice system. Instead of substantially increasing the complexity of the computing system by many additional members of interactions, it just add one new energy component to the existing ones. Molecular dynamics simulation of AFP binding on ice using the explicit waters method (Cheng & Merz, 1997) clearly demonstrated complete inability of this approach to simulate water effect in such a large system. Despite the fact that reported value -1062 kcal/mol of

combined energy of AFP-ice and AFP-water interaction, in the case of AFP bound to ice, was higher than -1167.4 kcal/mol energy of AFP-water interaction of fully solvated AFP, the computing system remained biased to starting conformation. Monte-Carlo simulation with explicit waters approaches apparently would face the same problem in this complex system. Explicit waters necessary for solvating AFP would increase the space of variable coordinate by 6000 degrees of freedom. This would make practically impossible the global energy minimization in such a system.

Another important aspect of computations is the estimation of hydrophobic interactions. Theoretically, MD simulation combined with explicit water method should predict free energy and, in particularly, hydrophobic interactions by statistical analysis of conformational ensembles of the system, which moves according to Newton's law, and enthalpy forces with speed relevant to temperature of the solution. However, practically it would require a very large quantity of water molecules necessary to form water cages around hydrophobic groups and also huge time of simulation to wait while those cages would disappear upon merging of hydrophobic groups. Molecular mechanics approach with explicit waters utilizing, for example, MCM protocol, in addition to the system overcomplicating problem would require assigning new solvation potential to account for entropy effects, which otherwise could not be computed using this method. On the other hand, after solvation potential is introduced, there is no more need for explicit waters, if this potential would also include enthalpy component of interaction with the solution. Consequently, it would be already the implicit water method.

Nowadays there are only two options to include water is this system: adding explicit waters and subsequent long MD simulation of the system or using implicit water approach with molecular mechanics. Apparently only the implicit water method is suitable for the AFP-ice system.

2.5 Nature of the driving force of AFP-ice binding.

From the physical point of view, AFP-ice-water is a very interesting and unique system. What we know for sure is that AFP binds to ice, but we also have a major question: why? What is the driving force of AFP-ice association? In other words, what ice can offer to AFP that water could not? From the molecular point of view, water and ice are identical. However, water has an advantage of all enthalpy components of interactions; since it is flexible, it is reasonable to suggest that water can offer closer and consequently stronger contact. On the other hand, ice is rigid and has lower density, consequently it could not possibly provide stronger van der Waals interactions with AFP than water does. Similar reasoning can be provided for H-bonding, especially taking into account that for H-bonding not only distance but also direction is important. Flexible water will always find better conformations to satisfy AFP in terms of H-bonds. Therefore, neither van der Waals nor H-bonding interaction could be the driving force of AFP-ice association, since AFP potential for both these interaction is already fully realized in water. In the absence of ionizable groups in AFP and ice, the electrostatic

interactions are relatively small. Therefore, solvating effects remain the only candidates for the driving force in AFP-ice interaction.

It is entropically unfavorable, when water molecules are immobilized into organized water cages near hydrophobic groups of AFP. The process, when AFP-ice binding expels these immobilized waters to the "free" water, apparently is the driving force of AFP ice interaction, since ice is already organized and entropical penalty for this is paid.

Chapter 3. Two alternative WF-binding surfaces of ice

3.1 Ice etching assay

In the ice etching assay (Knight et al.,1991) a sphere made of a single ice crystal is exposed to 10^{-2} mM WF AFP solution and allowed to grow (see Figure 3.1 A) In the sphere, all microscopic crystallographic planes are exposed to the solution and molecules of AFP cover those planes to which AFP binds better. After been exposed to the AFP, the sphere is allowed to sublime in air at -10^{o}C. During the sublimation process, those areas of surfaces, which have been covered by AFP and, therefore, preserved from even sublimation, became matte, while uncovered surfaces remained glance. Thus, by analyzing the matte spots on the surface of the sphere, it is possible to identify those crystallographic planes to which AFP binds primarily.

This assay has been done with WF AFP solution (Knight et al., 1991) (Figure 3.1B) and the [201] crystallographic plane was found to be a plane at which WF AFP preferably accumulated.

3.2 Ice growth morphology

In the ice growth morphology assay (D. Yang unpublished), a single ice crystal is grown in an AFP solution and then photographed. The purpose of this assay is to identify the crystallographic plane where AFP accumulates.

The assumption is that AFP, when bound to an ice plane, would prevent the growth of ice on that plane. Therefore, the ice crystal would eventually form a bipyramid, designated by the crossing of 12 equivalent crystallographic planes. The bipyramidal shape is defined by the symmetry operator of the ice crystallographic group (see Figure 3.2.A).

In order to identify this plane, careful examination of the angles of the bipyramid was performed. The results have shown that in all experiments the angle is very stable and has a value of 39 ° +-0.5 °, which corresponded to the 111 crystallographic plane (see Figure 3.2B).

3.3 The contradicting results of these two assays.

Ice etching assay is precise enough to distinguish the difference between [201] and [111] surfaces. On the other hand, the growth-morphology assay is also able to show the difference between bipyramid, formed by the [111] plane with peak angle of 39 °, and

bipyramid, formed by the [201] plane with the peak angle of 34°. The huge difference of 5 ° is very easy to detect. The peak angle of the ice bipyramid may appear bigger for observer than it is in reality only if the vertical axis of ice bipyramid is constantly beveled to the observer (see Figure 3.2 C for details). Simple trigonometric calculations show, that in this case the bevel angle must be 30 °, so [111] and beveled [201] bipyramid will appear the same. But in this case, in different morphology experiments bevel angles should be different and, consequently, the error should be at least ±5°, which is not observed in these experiments.

In practice, because the ice crystal is lighter than water, the bipyramid tends to remain parallel to the surface of water drop. Therefore, if we choose for observation the ice bipyramids in the geometrical center of the drop, where the surface is parallel to the horizon, the vertical axes of the bipyramid should remain perpendicular to the observer (see Figure 3.2.D for details).

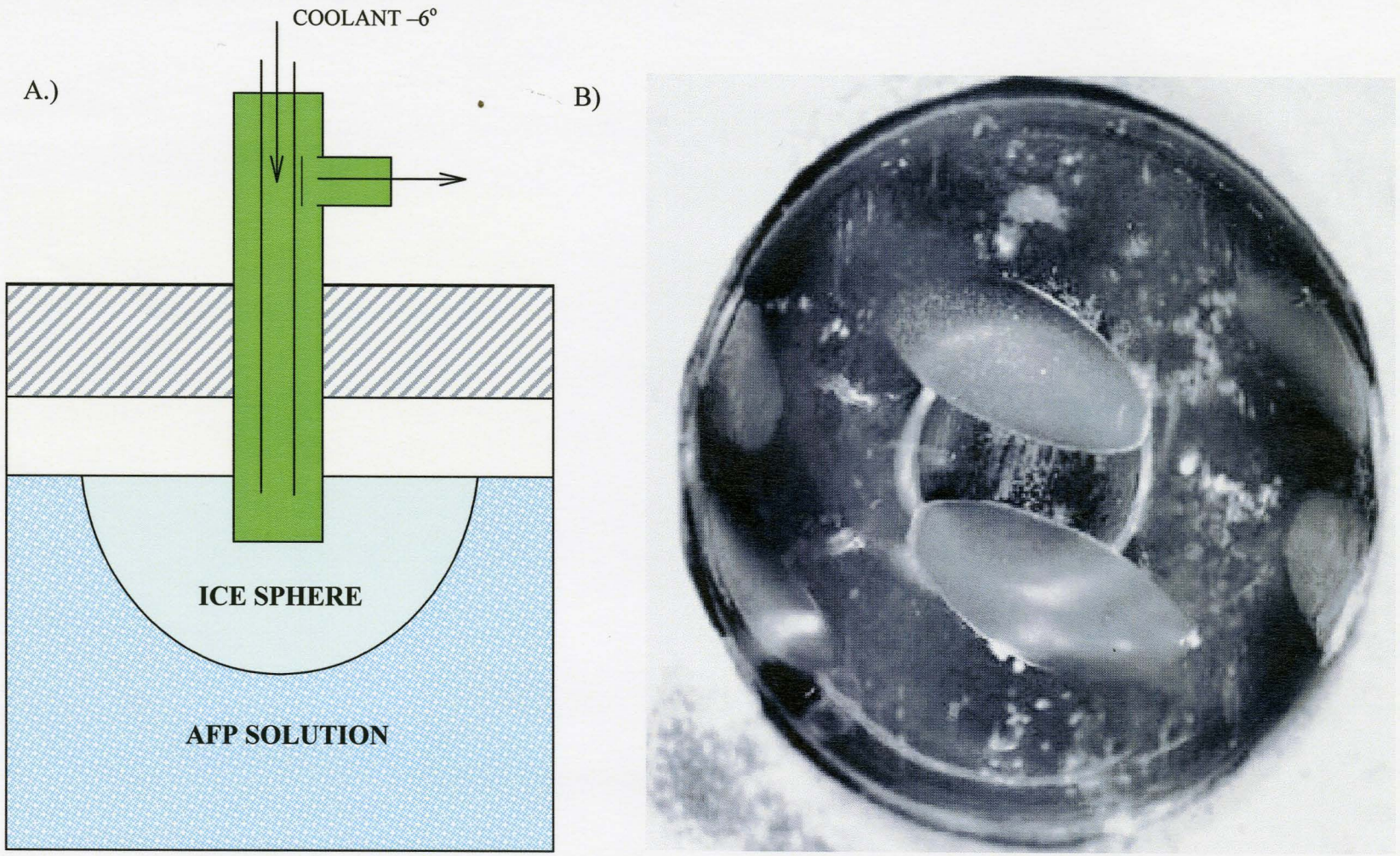

Figure 3.1 A. Scheme of ice etching assay. B. Ice sphere exposed to WF AFP solution; matte spots indicate presence of bound AFP to [201] and symmetric identical crystallographic ice planes. (Provided by C. Knight)

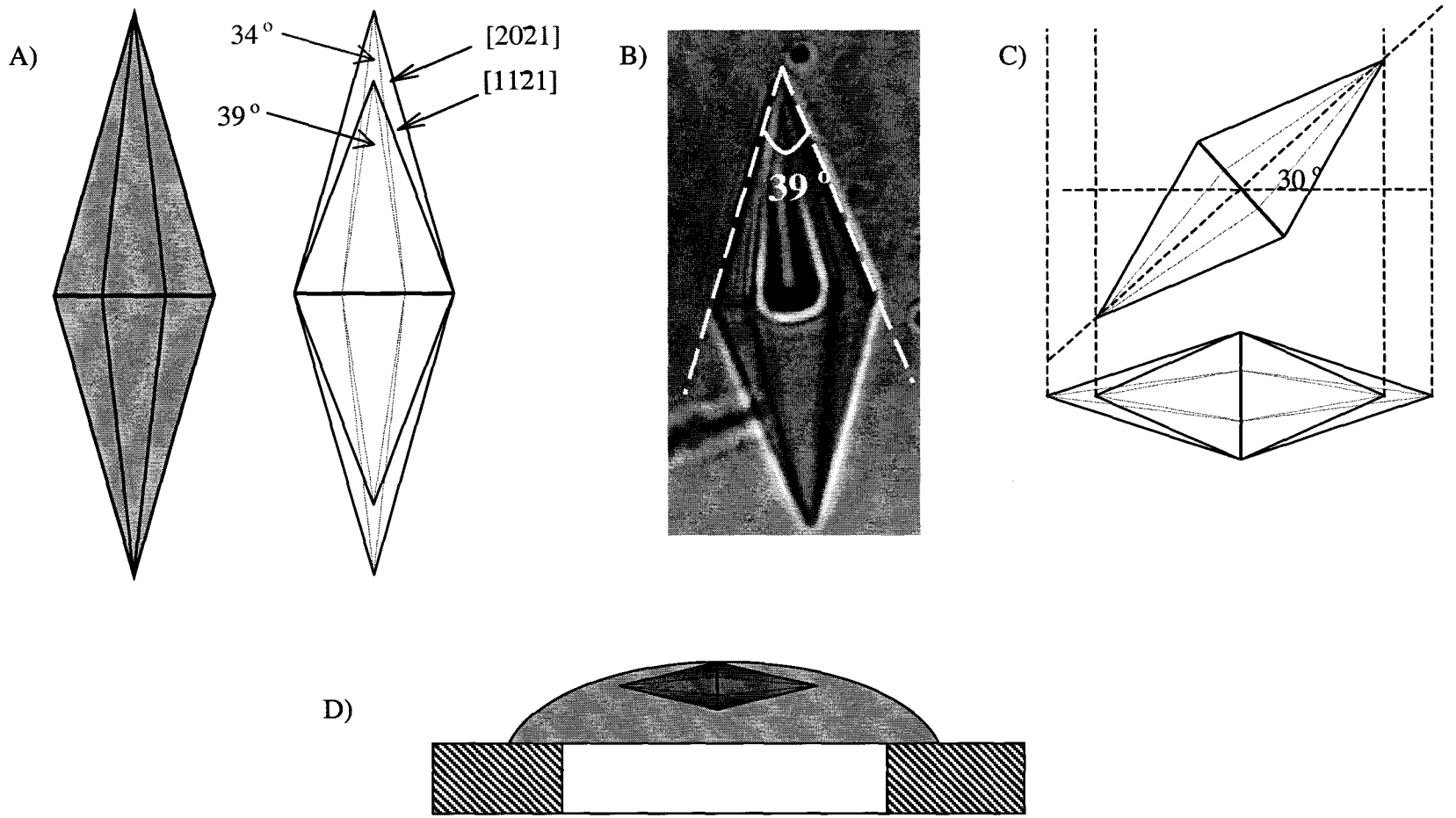

Figure 3.2 A. Ice bipyramid formed by 12 equivalent crystallographic planes [201] and [111]. B. Growing ice crystal in WF AFP solution. C. The ice crystal formed by [201] plane should be beveled on 30 ° to appear for the observer the same as the crystal formed by [111] plane. D. The ice crystal bipyramid is parallel to the horizon

3.4 Two surfaces are possible, but when do we see them? And why?

The results of the experiments described above suggesting that WF AFP may bind to both [201] and [111] crystallographic planes. However, why we see either [201] or [111], and never see both planes together?

We propose that WF AFP binds to the [201] plane slightly stronger than to [111] plane. Let's assume the difference in free energy of binding to be about 1-2 kcal/mol and the total free binding energy about –5 kcal/mol (see Chapter 2). In this case, the density of WF AFP on the surface of ice sphere in the ice etching assay is related to free energy of WF AFP binding to the different ice planes by the fundamental Arrhenius equation (2.12) and equation (2.4). Therefore, WF AFP in ice etching study should be 10 times more dense on the [201] plane than on the [111] plane surface. This could explain why we do not observe WF AFP on the [111] plane surface on sphere: the WF footprint on the [111] plane is simply too dim to be detected when comparing to [201] plane. But if WF AFP binds stronger to the [201] plane, why do we observe bipyramids formed by [111] plane in the morphology assay?

To answer this question we have to consider that most crystals formed in nature have very basic stereometrical shapes, such as parallelogram, prism, pyramid, bipyramid. This is because nature is always trying to minimize the surface energy of the crystals. In all crystallization the processes of loosing the entropically favorable degrees of freedom

of "free" molecules are compensated by the gaining of enthalpically favorable energy of association or, in other words, the bonding energy. Consequently, the more bonds a molecule forms on the surface of crystal, the bigger is the energy gain. In nature, we observe crystals formed by simple crystallographic planes, such as [001], [011], [111] because these planes have the maximum number of bonds per surface area. This could explain why we do not see crystals formed by [201] plane.

We suggest that both the surface energy of the crystal itself and the energy of AFP binding to a particular plane are important for determination of the ice crystal growth morphology. Their combination, rather than one of those factors, is responsible for shaping crystals of ice in the AFP solution. Apparently, the [111] surface is a product of compromise between the most efficient from bonding energy point of view [001] face and [201] to which WF AFP have strongest binding affinity. But why WF AFP is "designed" by nature to bind to the [201] plane? Why did not Winter flounder produce AFP which binds stronger to [111] plane? We will address these questions in Chapter 6 (Discussion).

Chapter 4. Methods of computations

4.1 Model of ice

Ice etching assay (Knight et al., 1991): WF AFP accumulates primarily on the [201] crystallographic plane. Morphology of the ice crystal growth (D. Yang, unpublished): ice bipyramids, formed in solution of WF, represent the [111] crystallographic surface (Figure 3.2 B).

We suggest that WF can interact with both [201] and [111] planes, however the affinity to the [201] plane is stronger, making it observable in the ice etching experiments. While the miller index designate a unique crystallographic plane, many unequal crystalline surfaces can be formed that are parallel to each other. The number of unique surfaces depends on the space group. The [201] and [111] surfaces designates four and two equivalent surfaces respectively. Although they are identical from the crystallographic point of view, the physical surface profiles are different, (see Figure 4.1 for details) which is crucial for the modeling. In this situation we choose the surface, where each surface molecule of water forms a maximal possible number of H-bonds (Figures 4.1A; 4.1E); the reason for this has been discussed earlier.

Ice was modeled as a cylindrical slab with the diameter of 80 Å and thickness of 7.5 Å. The slab was created to be large enough to accommodate a 50Å long WF AFP with some extra area for translational freedom. Coordinates of the oxygen atoms of this slab were generated using program MACO (D. Yang unpublished). The ZMM software was used to add hydrogen atoms and to assign random Euler angles to all water molecules. Then the whole slab was Monte-Carlo-minimized with fixed positions of oxygen atoms. The system converged rapidly and the energy of the system decreased dramatically during 10000 steps. The MC- minimized structure of ice was used in the subsequent models as a rigid body.

We decided not to add any water molecules onto the surface of ice, which could potentially improve the binding of WF AFP to the surface of ice as have been done in two latest modeling studies of WF AFP (Cheng & Merz, 1997; Dalal & Sonnichsen, 2000) (see Figure 8.E for details). In our system the ice was rigid, without any water "pillow" between the ice and AFP. Each water molecule on AFP binding surface of ice has at least two H-bonded neighboring water molecules. We believe that this is unbiased approach, because otherwise we could loose any sense of surface at all, by adding and subtracting the molecules of water wherever we needed to do so in order to improve binding affinity.

4.2 Model of WF AFP and AFP mutants

We used the X-Ray geometry of WF AFP (Sicheri and Yang, 1995) as an initial structure for the modeling (see Figure 1.3 for details). Hydrogen atoms were added using ZMM package. To eliminate possible conformational strain effect, which could occur due to the crystal packing, the energy of the WF X-ray structure was minimized. The conformational energy dropped from –237.6 kcal/mol to –277.7 kcal/mol and as the result of the energy minimization, the α-helix of AFP was straighten up due to a slight change of the torsion angles in the main chain. An additional hydrogen bond was formed between the hydroxyl group of Thr 35 and the carbonyl oxygen of Ala 31, consequently all four Thr were aligned with χ_1 torsion angle equal to -60° (see Table 4.1 for details). The obtained structure was used in all subsequent computational experiments. The information on generalized coordinates of the initial and minimized structures is presented in Table 4.1. This structure was also used to build mutants of WF by implementing homology modeling method in ZMM software.

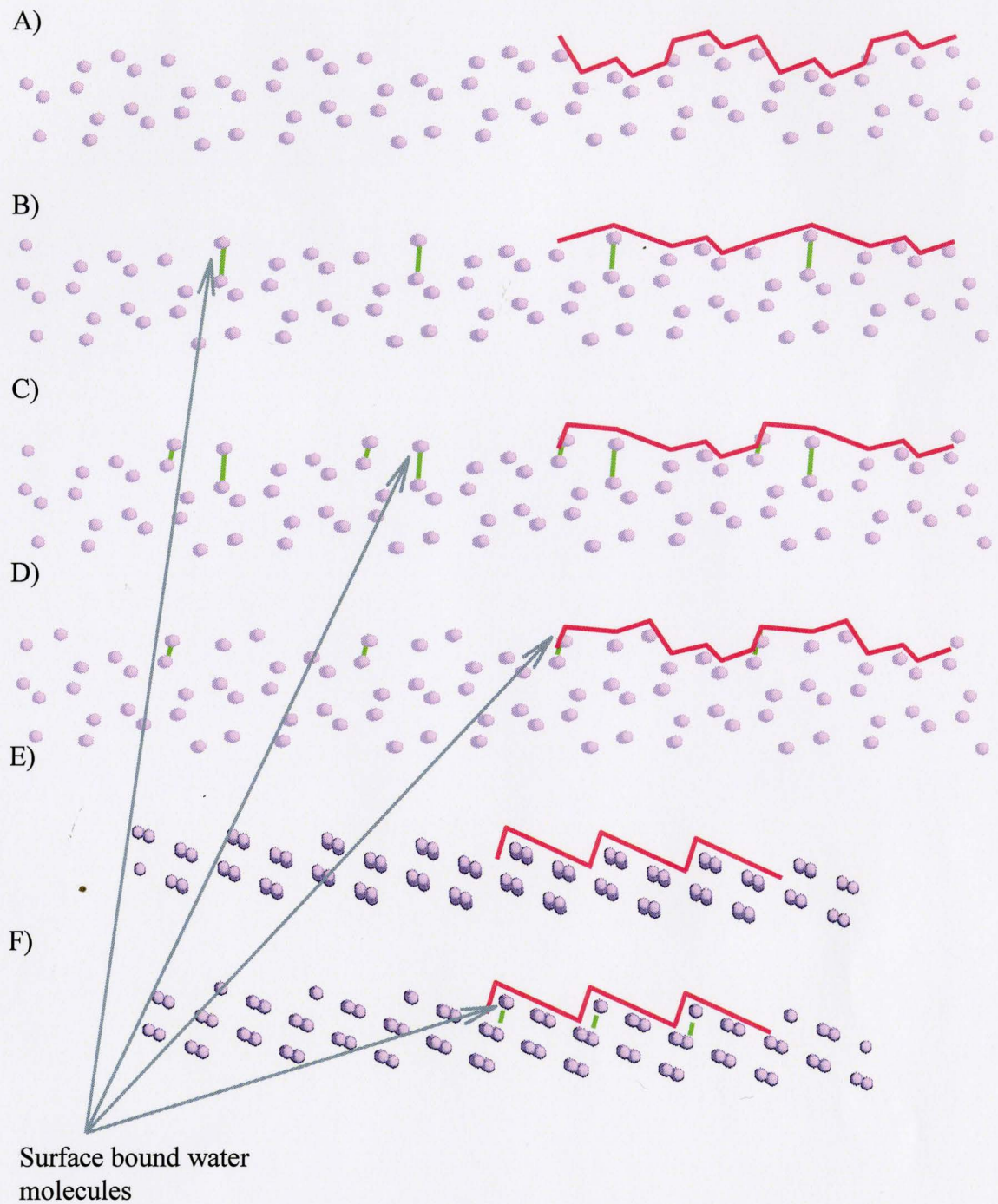

Figure 4.1 Different ice slabs. A-D are crystallographically equivalent to the [201] plane, E and F to the [111] plane. For our modeling we choose surfaces A and F because they do not have surface- bound water molecules.

Table 4.1 Torsion angels of the X-ray and energy-minimized X-ray structure of WF AFP

Number and name of residue		Torsion angels of X-ray structure						Torsion angels of minimized X-ray structure					
		φ	ψ	χ_1	χ_2	χ_3	ω	φ	ψ	χ_1	χ_2	χ_3	ω
1	ASP	0.805	2.292	3.089	1.119	3.142	3.132	0.793	2.335	3.044	1.227	3.110	3.020
2	THR	-1.040	-0.840	-0.692	-2.596	3.142	-3.120	-0.954	-0.835	-0.801	-2.627	-3.057	
3	ALA	-1.093	-0.727	3.072				-1.187	-0.847	3.072			
4	SER	-1.115	-0.704	-0.925	-1.130	-3.141		-1.109	-0.688	-1.006	-1.129	3.095	
5	ASP	-1.172	-0.682	-1.220	-0.120	3.142	3.114	-1.148	-0.686	-1.218	-0.114	-3.136	3.077
6	ALA	-1.195	-0.709	3.064				-1.164	-0.760	3.064			
7	ALA	-1.027	-0.775	3.066				-0.983	-0.810	3.044			
8	ALA	-1.063	-0.748	3.087				-1.036	-0.795	3.072			
9	ALA	-1.032	-0.717	3.101				-1.055	-0.755	3.095			
10	ALA	-1.197	-0.736	-3.140				-1.121	-0.799	3.108			
11	ALA	-1.081	-0.862	3.112				-1.031	-0.849	3.096			
12	LEU	-1.138	-0.694	3.066	1.002	3.127		-1.100	-0.759	3.122	1.063	3.114	
13	THR	-1.089	-0.796	-1.142	1.439	3.142	3.136	-1.049	-0.836	-1.065	1.394	3.127	
14	ALA	-1.119	-0.694	3.136				-1.102	-0.728	-3.135			
15	ALA	-1.189	-0.692	-3.119				-1.194	-0.734	3.107			
16	ASN	-1.221	-0.625	-1.279	-0.238	-3.105	-3.134	-1.163	-0.674	-1.169	-0.229	-3.129	-3.137
17	ALA	-1.238	-0.652	3.101				-1.176	-0.795	3.134			
18	LYP	-1.159	-0.753	-2.935	2.903	-2.921	-1.060	-1.077	-0.821	-3.068	2.974	-3.040	-1.119
19	ALA	-1.037	-0.771	-3.123				-1.029	-0.747	3.085			
20	ALA	-1.110	-0.688	3.113				-1.069	-0.741	3.118			
21	ALA	-1.150	-0.624	3.110				-1.084	-0.732	3.122			
22	GL-	-1.108	-0.809	-1.490	2.892	0.724	3.104	-1.073	-0.881	-1.258	2.907	0.829	3.142
23	LEU	-1.002	-0.801	-2.508	1.906	3.070		-0.976	-0.841	-2.668	1.839	3.067	
24	THR	-1.087	-0.745	-0.959	1.477	3.142	3.126	-1.026	-0.792	-1.017	1.445	3.073	
25	ALA	-1.135	-0.705	3.062				-1.097	-0.723	3.088			
26	ALA	-1.037	-0.772	3.089				-1.048	-0.829	3.090			
27	ASN	-1.129	-0.722	-1.311	-0.564	-3.097	3.123	-1.089	-0.726	-1.384	-0.605	3.140	3.102
28	ALA	-1.189	-0.583	3.098				-1.150	-0.675	3.120			
29	ALA	-1.132	-0.832	3.116				-1.105	-0.817	3.111			
30	ALA	-1.011	-0.739	-3.127				-1.036	-0.822	3.110			
31	ALA	-1.165	-0.677	3.140				-1.117	-0.720	3.056			
32	ALA	-1.134	-0.756	-3.136				-1.038	-0.755	3.087			
33	ALA	-1.189	-0.721	3.117				-1.130	-0.763	3.091			
34	ALA	-1.180	-0.646	-3.064				-1.128	-0.570	3.133			
35	THR	-1.154	-0.657	-2.619	-2.734	3.142	3.129	-1.248	-0.798	-1.033	1.400	-3.096	
36	ALA	-1.201	-0.333	-3.085				-1.323	-0.498	-3.086			
37	ARG	-1.782	3.142	-1.350	2.810	-3.090	1.355	-1.765	3.142	-1.216	2.918	3.132	1.481

4.3 Energy components

4.3.1 Energy contribution of the solvation effect

Implicit waters method (Augspurger and Scheraga., 1996) was used to take into account the solvating effect. In contrast to the explicit waters method in which large number of water molecules is added to the system, in the implicit water method the energy of solvation effect for each solute group is assigned in addition to the other atom to atom forces such as, van der Waals, electrostatic and H-bonding terms. The energy of solvation effect is, by definition, the energy of transferring the molecular group from vacuum to solvent. In our case, the solvent is water. The empirically determined energy naturally combines contributions from all types of interactions between the solvent and solute including: van der Waals, electrostatic, hydrogen bonding and hydrophobic effect. This energy is usually negative, since it represents a huge gain in the van der Waals potential, however it is very different for hydrophobic and hydrophilic groups (see Table 4.1). When two groups of atoms interact in solution, their solvating shells overlap, consequently excluding some volume from each other. This creates a desolvation penalty (gain) which is proportional to the solvation potential multiplied by fractional volume of the overlapped solvation shell.

The total free energy of interaction of protein with water ΔG_{hyd} is considered as the sum of contributions from individual atoms:

$$\Delta G_{hyd} = \sum_i \delta_i (VHS)_i \qquad (1)$$

δ_i is an empirically determined hydration energy density of atom i (A_i), and $(VHS)_i$ is the volume of the solvent-exposed hydration shell of A_i (shaded area at Figure 4.2).

$$VHS_i = V(R_i^h) - V(R_i^v) \qquad (2)$$

$V(R_i^h)$ is the volume of the first hydration shell of A_i, and $V(R_i^v)$ is the volume of the van der Waals spheres of A_i and its covalent neighbors, R_i^h is the radius of the first hydration shell of A_i, and R_i^v is the van der Waals radius of A_i. Analytical expression for the exact calculation of VHS_i includes overlapping volumes of two, three, and four van der Waals spheres of atoms bound to A_i. Since this expression is not differentiable, an algorithm for the approximate computing of VHS_i was proposed that involves only double overlaps between spheres whose van der Waals radii are reduced to compensate ignoring of triple and quadruple overlaps. Thus,

$$(VHS)_i = \frac{4\pi}{3}(R_i^{h^3} - R_i^{v^3}) - \sum_{j \neq i} [D(r_{ij}; R_i^h, R_j^r) - D(r_{ij}; R_i^v, R_j^r)], \quad (3)$$

where $D(r_{ij}, R_i, R_j)$ is the volume of intersection of two spheres of radius R_i and R_j, whose centers are separated by the distance r_{ij}, and R_j^r is the reduced van der Waals radius of A_j

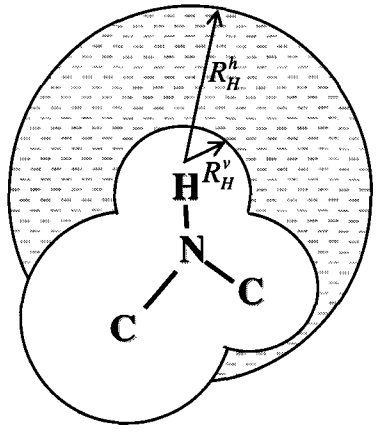

Figure 4.2 Solvent-exposed volume of the first hydration shell of radius R_H^h (shaded area) around the amide hydrogen that has van der Waals radius R_H^v. Atoms N, C^α and C' occupy part of the volume of the first hydration shell, thus decreasing the solvent-exposed volume (Based on Augspurger and Scheraga, 1996).

To ensure the VHS differentiability, the hard van der Waals spheres were substituted by the softer "Gaussian spheres" the volume of intersection between which is given by the following formula:

$$D_G(r_{12};R_1,R_2) = A^2\left(\frac{\pi B}{R_1^2+R_2^2}\right)^{3/2} R_1^3 R_2^3 \exp\left(\frac{-r_{12}^2}{B\left(R_1^2+R_2^2\right)}\right) \qquad (4)$$

The reduced van der Waals radii R_j^r are pre-calculated for each molecular system via Monte Carlo integration of the corresponding van der Waals volume reduced by overlaps with atoms covalently bonded to A_j. Empirical parameters A = 1.88 and B = 0.52 were

adjusted to minimize the difference between results of calculations of VSHs made with the exact (but not differentiable) and approximate differentiable expressions.

The hydration energy densities δ_i were determined by least squares fitting of the computed and experimental energies of gas-to-aqueous transfer of various organic molecules. The parameters are given in Table 4.2.

The major problem of application of the above algorithm to the AFP-ice system is the lack of parameters $\delta_{I,}$, R^v and R^h for the ice hydrogen and oxygen and certain unfit of parameters in Table 4.2 for simulation of the system at the melting-ice temperature, since they were derived for room temperature. Derivation of proper parameters would be a large stand-alone project therefore, we decided to use existing parameters with complete understanding of their limitations. We also addressed the question of adjusting solvation parameters in chapter five.

Table 4.2 Empirical solvation parameters (Augspurger and Scheraga, 1996)

	Atom type	δ_i x 10^3 kcal/(mol Å^3)	R_i^v (Å)	R_i^h (Å)
1	Hydroxyl, amino	-10.35	1.415	4.17
2	Acid H	-3.206	1.415	4.17
3	Amide H	-7.714	1.415	4.17
4	Thiol H	2.709	1.415	4.17
5	Aliphatic CH_3	1.319	2.125	5.35
6	Aliphatic CH_2	0.2374	2.225	5.35
7	Aliphatic CH	-1.271	2.375	5.35
8	Aliphatic C	-2.297	2.06	5.35
9	Cyclic CR	0.3827	2.25	5.35
10	Cyclic CH	0.2890	2.375	5.35
11	Aromatic CH	-0.2137	2.10	5.35
12	Aromatic CR	-1.713	1.85	5.35
13	Branched aromatic C	-1.910	1.85	5.35
14	Aromatic COH	-0.6063	1.85	5.35
15	Carbonyl C	2.696	1.87	5.35
16	Primary amine N	-1.149	1.755	5.05
17	Secondary amine N	-10.28	1.755	5.05
18	Aromatic N	-10.48	1.755	5.05
19	Amide N	-7.332	1.755	5.05
20	Hydroxyl, ether O	-7.396	1.62	4.95
21	Acid, ester O	0.07897	1.62	4.95
22	Ketone carbonyl O	-15.70	1.56	4.95
23	Acid, amide carbonyl O	-15.56	1.56	4.95
24	Thiol, disulfide S	-4.706	2.075	5.37
25	Water H	0	1.415	4.17
26	Water O	0	1.62	4.95

4.3.2 Total energy function

The energy was presented as the sum of six components. Van der Waals interactions were calculated using the AMBER force field (Weiner et al., 1984) with a cutoff distance of 8 Å and a shifting function (Brooks et al., 1985). The standard partial charges at the atoms of AFP (Momany et al., 1975) and a distance-dependent dielectric parameter (Weiner at al., 1984) were used to calculate the electrostatic energy. The partial charges at the water molecules were assigned the values of –0.5 for oxygen atoms and 0.25 for hydrogens. Energy terms also included hydrogen bonding, solvation effect (Augspurger and Scheraga, 1996), torsion energy, and flat-bottom constraints. To analyze the results, the energy can be subdivided into internal and ligand-receptor (AFP-ice) energy.

4.3.3 Imperfection of our energy calculations

The imperfection of our approach is the use of solvation parameters which were derived for room temperature of 25°C to simulate the system at the temperature of 0°C. We expect that at lower temperatures the hydrophobic effect becomes weaker and hydrophilic forces slightly stronger, than at the room temperature. However we hope that

we were able to compensate for this temperature effect by adjusting reduced van der Waals radius of ice, thus avoiding overestimation of the hydrophobic effect.

4.4 Starting geometry

AFP: X-ray structure of WF AFP with idealized alpha-helix

Ice: Generated by the program MACO (D. Yang)

Positions and orientations of AFP: Random

4.5 Generalized coordinates

Molecular mechanics calculations were performed with the ZMM program package (Zhorov, 1981, 1982). ZMM allows conformational searches in the space of arbitrarily specified generalized coordinates: torsion and bond angles, positions of free molecules (Cartesian coordinates of their root atoms) and the orientation of the molecules (Euler angles of the local systems of coordinates centered at the root atoms). WF AFP consists of 308 atoms whose positions were specified by 924 Cartesian coordinates. In the space of internal coordinates, only 154 variable torsion angles, position and orientation of AFP may specify the geometry of the system. Other geometrical parameters, namely, bond lengths, bond angles, positions and orientations of water molecules in the ice slab were kept fixed. While these parameters were used to calculate the Cartesian coordinates of atoms, they did not appear in the list of variable geometrical

parameters, because ZMM allows to fix any parameters without imposing special constraints. Bond lengths and bond angles between atoms of the backbone were fixed. Bond lengths and bond angles involving hydrogen atoms were fixed at their standard values (Momany et al., 1975).

4.6 Monte Carlo Minimization Method

The Monte Carlo-minimization (MCM) protocol (Li and Scheraga, 1988) was used for the search of optimal conformations. Trajectories were calculated at T = 600 °K. The subsequent starting point in a trajectory was obtained by randomly selecting a generalized coordinate of the previous point and changing it by a random increment. The energy was minimized from the starting point until the norm of the energy gradient fell below 1 kcal mol^{-1} rad^{-1} or until the limit of 300 calls of the procedure of calculation of energy and gradient was exceeded. The resulting minimum-energy conformation (MEC) was accepted in the trajectory if its energy E fell below that of the preceding point of the trajectory E_p or if a random number $n \in (0, 1)$ was less than $\exp(-(E-E_p)/RT)$. The obtained MEC was added to a stack of MECs accumulated during the search if its energy was within 7 kcal/mol from the apparent global MEC held in the stack and if it was geometrically distinct from any MEC already accumulated in the stack. Two MECs were considered distinct if they had at least one generalized coordinate different by 0.1 Rad. An MCM trajectory was terminated when the last N consecutive energy minimizations did not lower the energy of the apparent global MEC in the stack nor added a new MEC

to the stack. In most of our computational experiments, the parameter N was set to 1000. A trajectory was also terminated after 10,000 energy minimizations in case the above criteria of convergence were not satisfied. One energy minimization of this system usually converged in less than 200 iterations and took 1 - 2 minutes on a Pentium III 450 mHz processor.

4.7 Constrains

To prevent movement of AFP beyond a definite distance from the ice slab, distances r between specified atoms of AFP and ice were restrained within the boundaries $d_l < r < d_h$ by using the function $E_r = s(r)*f(r)$. In the last equation, s(r) is a switching operator (Brooks et al., 1985) and $f(r)$ is a quasiparabolic penalty function defined as follows:

$$s(r) = \begin{cases} 1 & \text{if } r \le d_l - x \\ [(d_l + x - r)^2(d_l + x - 3(d_l - x) + 2r)]/(2x)^3 & \text{if } d_l - x < r \le d_l + x \\ 0 & \text{if } d_l + x < r \le d_h - x \\ [(d_h - x - r)^2(x - d_h + 3(d_h + x) - 2r)]/(2x)^3 & \text{if } d_h - x < r \le d_h + x \\ 1 & \text{if } d_h + x < r, \end{cases}$$

$$f(r) = C(r - d_h/2 - d_l/2)^2.$$

The switching distance x was set to 0.2 Å and the force constant C was set to 100 kcal mol^{-1} $Å^{-2}$.

4.8 Software

For energy calculations and MCM search we used ZMM software package. ZMM is a molecular modeling package for conformational analysis and modeling of biomolecular systems.

ZMM searches the energetically optimal structures in the space of internal coordinates: torsion and bond angles, bond lengths, positions and orientation of free molecules or ions. Rigid fragments that are not expected to undergo significant conformational rearrangements may be specified in such a way that interactions within each rigid fragment are completely excluded from computational protocols. This essentially facilitates modeling of complex molecular systems. For example, in docking experiments, the ice slab may be considered as a rigid body.

Most well-known molecular modeling packages, e.g., AMBER, DISCOVER, CHARM and XPLORE minimize energy in the space of Cartesian coordinates of atoms. Corresponding algorithms for molecular mechanics and molecular dynamics calculations are relatively simple compared to those of internal coordinate systems. However, the price for the simplicity is a large number of variables, many of which move collectively during energy minimization. For example, rotation of a phenyl ring around the C-Ph bond in the Cartesian coordinate space involves the collective movement of 30 variables (Cartesian coordinates of atoms), whereas this rotation may be described by one torsion

angle in the generalized-coordinates space. The energy minimization in the space of torsion angles is used in several other programs, including the ECEPP package (H. A. Scheraga and coworkers). However, ECEPP is difficult to use when bond angles and/or bond lengths should be treated as flexible, e.g., for docking of certain drugs in proteins. In many cases, only few atoms of a ligand should be considered as flexible, whereas valence geometry of the protein and the remaining part of the ligand may be considered as rigid. An example is curare alkaloids, in which bond angles of few carbon atoms in the macrocycle essentially deviate from the tetrahedral values (Zhorov, 1993; Zhorov and Brovtsyna, 1993). Usually, the valence geometry of a tetrahedral atom is described by six bond angles, which are not independent and, hence, are not generalized coordinates. The latter may be chosen as polar angles in a vector model of a tetrahedral atom (Zhorov, 1983). A unique feature of ZMM is that any part(s) of the system may be specified as rigid, while the flexible part(s) may contain any variables (torsions, bond angles, lengths).

ZMM implements well-known force fields such as AMBER (Weiner et al., 1984) and ECEPP/2 (Nemethy et al., 1983) The following methods of conformational search are realized in the ZMM:

- Energy minimization in generalized coordinates (Zhorov, 1981, 1983)

- Nested rotations with building multidimensional grids

- Monte Carlo minimization (MCM) (Li & Scheraga, 1987)

- MCM in the space of scaled collective variables (Noguti & Go, 1985; Maurer et al., 1999)

- Biased MCM (Abagyan & Totrov, 1994)

- Nested MCM protocol (Zhorov, unpublished).

- Predicting loop-closing conformations of macrocycles (Go & Scheraga, 1970).

- Computing MC-minimized energy profile a ligand in a protein (Zhorov and Lin, 2000)

- Computing multidimensional MC-minimized energy map of a ligand in a protein (Zhorov, unpublished)

ZMM is a file-operated package with molecular structures and controlling parameters specified in input files, and results delivered to output files. Advantage of the file-operated systems (e.g., compilers for programming languages) is the 100% reproducibility of results, a possibility to debug input data and to clone homologous jobs. Molecular graphics programs such as RASMOL, INSIGHT, MVM, etc., may be used concertedly with ZMM that exports and imports PDB files. ZMM includes utilities to build input files automatically and to analyze large number of minimum-energy conformations accumulated in a conformational stack during conformational search.

For visualization purposes we primarily used RASMOL program, we also used Insight II software package to generate starting conformations of AFP binding on ice surfaces for some early models.

Chapter 5. Results of computational experiments

5.1 Overview of our initial approaches

5.1.1 Conventional force field computations

In the initial approach, we used conventional AMBER force field without taking into account any solvating effect, since we were not sure about the physical nature of AFP-ice interaction at that time. Our first objective was to repeat published theoretical studies of AFP-ice system, with the hope that this experience would give us new ideas of how to improve the model.

In this first step of our modeling study, we developed new methodological approaches, primarily for the model of ice. We systematically considered different ice slabs (see Figure 4.1), and also developed approaches for generating coordinates of ice hydrogen atoms. We also found that despite using the MCM method for the global minimum-energy conformational search, the final conformation correlated with the starting conformation. The preliminary analysis have shown that this effect was due to formation of strong hydrogen bonds between ice and AFP. These bonds prevented further substantial changes in conformation. Basically, the negative energy of hydrogen bonds

between AFP and ice created deep local energy minimum, which was very difficult to overcome. Generally, the energy of the local minima was comparable with the energy of apparent global minimum, however the binding geometry of AFP-ice complex was essentially different.

Soon after the model was built, we realized that our minimum-energy conformations were, in principal, very similar to those reported in previous modeling studies. In our structures, AFP was bound to ice by hydrogen bonds formed between waters of ice and polar groups of Thr, Asp and Asn. (see Figures 5.1; 5.2)

Although our model shows apparently better binding characteristics than previous models, it had the same disadvantage as these models, namely, it did not explain the main mutation paradox, in which Thr replaced by Val did not affect the AFP activity, while replacement by Ser did. The need to consider water effect became apparent.

5.1.2 Trajectory convergence problem

The correlation between the starting and final conformation indicated that our search for the global minimum was biased with the "hand-made" starting conformation. Due to strong H-bonding interactions between AFP and ice, the trajectory was "trapped" in deep local minimums created by these forces and did not converge to the global minimum. Therefore, we had to develop a new search strategy. That could have been

either sequential consideration of all possible starting conformations, or generation of random starting conformations with subsequent statistical analysis of the results.

5.1.3 Complementarity concept

At this point we started to look for the physical nature of the driving force of AFP-ice interaction. We suggested that the AFP-ice binding is driven by decrease of water-accessible nonpolar surface of AFP. The main reason for this suggestion has been discussed above. One of the major requirements for this type of binding is a surface complementarity between AFP and ice. Otherwise, loss of van der Waals energy after transferring the AFP binding surface from the "soft" water to a non-complimentary ice surface would not allow the binding to take place at all. Therefore we decided to search for the conformation which corresponds to the maximal steric complementary binding of AFP to ice. We expected that this search would narrow the set of possible binding conformations, and that further individual assessment of multiple conformations would eventually lead us to the unique one which correlated with experimental data.

Structures with maximum binding complementarity may be found by optimizing the energy of van der Waals interactions between ice and AFP. Therefore, we MC-minimized the structure of AFP-ice complex without taking into account H-bonds and electrostatic energy, consequently the only contribution to the energy of binding was van

der Waals interactions. We found out that the conversions of MCM trajectory were much better than in case of MC minimizing of complete energy function. The absence of strong electrostatic and H-bonds interactions has made the energy profile of the AFP-ice complex substantially smother, which increased efficiency of MCM protocol.

At this stage our level of bias to the starting point dramatically decreased, since we observed major binding conformational changes without "stacking" within the starting point which was inevitable in case of MC minimizing of complete energy function. However, since our objective was to explore all possible binding conformations rather than finding the most complementary one, we were interested in creating an energy profile map which would provide us with relative values of binding van der Waals energy, which is relevant to steric complementarity, for all possible binding conformation geometries. Theoretically this map has to be 6 dimensional, designated from 3 Euler angles of rotation and 3 degrees of translation. Creating of this kind of 6 dimensional map with 10^{o} rotational and 1Å translational resolution would require computing of approximately 10^{8} conformations, most of which would have small or no binding complementarity at all. Therefore we limited our map to only one dimension, which was the degree of rotation φ around α-helix axis (see Figure 5.3 for details). To build this map, rotation of AFP around φ was restricted by using flat bottom quasi-torsional constrain within 20^{o} step, while all other degree of freedom were allowed to vary. To keep AFP within the dimensions of the ice slab, flat bottom constrains were imposed between Ala 19 of AFP and the imaginary axis which perpendicularly crossed the

geometrical center of the ice slab disc. Then van der Waals, torsion and bond energy components of the AFP-ice system were MC-minimized with the fixed main chain of AFP. Consequently, the maximum complementarity conformation was found for each step of φ. The result of this computational experiment as a dependence of relative value of van der Waals binding energy on the angle φ is presented on Figure 5.4. We found that regardless of the value of φ in the range 80°-280°, the maximum complementarity binding geometry of WF AFP was aligned parallel to [20-11] vector on [201] surface of ice. The global energy minimum of van der Waals interactions between AFP and ice corresponded to the conformation in which WF AFP bound to ice by its "Thr, Asp, Asn" face (see Figure 5.5). Conformations in which AFP interact with ice by its "hydrophobic" and "hydrophilic" faces were found to have weaker van der Waals energy than the global minimum conformer by 20% and 30% respectively (see Figures 5.6; 5.7) However, since complementarity is also related to the total binding surface area, these two binding faces should not be excluded from future consideration as candidates for real binding face.

After visual examination of all three conformations allowed by complementarity requirement based on hydrophobic concept of AFP-ice interaction, the "hydrophobic" face was proposed to be the binding surface of AFP. This proposal was later supported by independent mutations studies (Baardsnes et al., Dec. 1999). However we needed more quantitative way to demonstrate the difference between "hydrophobic", Thr, Asp, Asn and "hydrophilic" faces to be less biased in our conclusions. After this stage of our study we decided to introduce water into the system.

5.2 Optimization of parameters

5.2.1 Solvation parameter of ice

The solvation method of Augspurger-Scheraga (Augspurger and Scheraga, 1996) lacks parameters for computing hydration energy of ice. These parameters include density of free energy to remove water from hydration shell of water molecules forming ice δ_{ice}, radius of the solvation R^{h}_{ice} shell and reduced van der Waals radius (RVR) of water molecules forming the ice R^{v}_{ice}. We have developed these parameters based on the three following postulates: (i) the free energy of ice melting at 0° C (melting, freezing) is 0 kcal/mol; (ii) upon binding the α-helix of WF AFP to ice, relatively similar amount of water is excluded from the ice surface, regardless of AFP binding face; (iii) the free binding energy of AFP to ice is about 5 kcal/mol (see Chapter 2). To simplify our computational model, we ignored desolvation energy of ice, assuming that it is relatively similar for all productive binding conformations of WF AFP on ice. A series of computational experiments demonstrated that the hydration component of free energy of binding of AFP to ice is extremely sensitive to the value of RVR. We varied the value of RVR in the range of 1.5 to 2.0 Å and performed MCM search for each value of RVR. We found the value, which correctly reproduced the experimental data for binding energy to be 1.95 Å. Using this value, we performed next series of computation experiments with MC-minimizing the energy from different starting points. We found that the resulted

conformations had an important common feature: AFP helix interacted with ice by the "hydrophobic" face (see Figure 5.13). Importantly, we also found that the hydrophobic methyl, rather than the hydrophilic hydroxyl group, is exposed inside the grooves of the ice surface. This finding explains the most important mutations. However, the convergence of MCM trajectories was very poor: from 50 different starting points only 5 conformations were found within 3 kcal/mol from the apparent global minimum. We analyzed this problem and found, that the poor convergence was due to the strong electrostatic interactions, which trapped some trajectories in the local minima with relatively high energy. In an attempt to solve this problem, we increased the dielectric constant ε and found that the final MCM orientation of AFP on ice was low-sensitive to this parameter, whereas the conversion of MCM has improved dramatically. Based on this finding, we decided to ignore the electrostatic component in subsequent computations. This required a new calibration of RVR, which was found to be 1.9 Å. We repeated the computational experiment with the new parameters and found that 40 out of 50 starting points converged to the structures within 3 kcal/mol of the lowest energy conformation. Although the insensitivity of AFP orientation to the electrostatics is surprising, it may be explained by simple physical considerations. In a real system, the orientation of AFP would be governed by three major types of forces: van der Waals, solvation effect and electrostatics, including H-bonds. However, H-bonding of polar groups of AFP to liquid water is always energetically (entropically and enthalpically) more favorable. In this system, desolvation forces are stronger than H-bonds. Thus calculations with and without electrostatics provide similar results, while computations

without electrostatics yield much better convergence of MCM. For future references we would call energy minimization using AMBER force filed, excluding electrostatic component, combined with solvation potential – minimization in van der Waals & solvation (VS) force field.

5.3 Typical computational experiment

The typical computational experiment was set as follows: no bias was imposed for the starting position and orientation of WF AFP near the surface of the ice slab. This means that the starting Euler angles and translational position of AFP were randomly generated.

To keep the AFP within the ice surface, two constrains were imposed (see Figure 5.9). The center of helix was constrained within 5Å to an axis normal to the surface and passing through the geometrical center of the slab. To prevent unproductive parting of AFP far from the ice surface, N and C terminus of AFP helix were constrained within 15 Å from the plane. Both types of these constrains were flat bottom. Although these constraints did not bias our results, they dramatically improved the convergence of MCM trajectories due to preventing the movements of AFP away from the slab.

During the search, the AFP backbone was fixed, while all side chain torsions were allowed to vary. This approach preserved the α-helix of WF AFP from possible distortion due to binding on ice during MCM protocol.

The maximum length of trajectories was limited to 10000 of MCM steps. A file with coordinates of atoms was delivered each time when the energy of the system decreased below the value of the current minimum. Figure 5.10 shows typical superposition of the lowest-energy conformers, obtained in the course of MCM trajectory. AFP rapidly approached the ice surface and then searched the optimum orientation on the ice surface. Usually it took about 3000 MCM steps to find the optimal orientation on the surface, however extra 7000 steps were allowed to make sure that the best orientations are found (see Figure 5.11)

5.4 Ice surface [201] with wild type of WF AFP and "Val","Ser","Ala" mutants

MC minimization of WF AFP and its mutants to find the optimal binding conformations on ice surfaces was performed from 100 starting points, in which the position and orientation of AFP in space around the ice surface were randomly generated. These trajectories yielded ensemble of minimum energy complexes within 1 kcal/mol

from the apparent global minimum. Figures 5.13-5.16 show the typical structures from this ensembles.

The typical binding conformation of wild type WF AFP has the following characteristics. AFP is oriented along [01-12] vector and bound to the ice surface by its "hydrophobic" face (see Figure 5.13). Methyl groups of Thr form hydrophobically favorable contacts with the grooves on the ice surface while hydroxyl groups are exposed to the solution. Side chain conformation of the threonines $\chi_1 = -60^o$ allows formation of hydrogen bond between the hydrogen atom of the hydroxyl group and the carbonyl oxygen of the main chain. This conformation is also consistent with the energy minimized X-Ray structure of WF AFP. Hydrophilic groups of Asp, Asn together with all the other hydrophilic groups of side chains of WF AFP remain in water. Entire α-helix of the AFP forms tight steric contact with the ice surface.

Binding conformation of "Valine" mutant generally shares the same features with the wild type, however, since Val does not have hydroxyl groups both methyl groups can be involved in hydrophobically favorable interactions with ice surface (see Figure 5.14). This resulted in lower than wild type AFP-ice binding energy. Binding conformation of "Alanine" mutant is very similar to the "Valine" in terms of orientation and binding face of AFP (see Figure 5.16). However, due to the absence of bulky hydrophobic side chain alanine was unable to form favorable contact with the ice grooves, which resulted in

lowering steric complementarity and increasing desolvation energy component. (See Table 5.1)

In contrast to the wild type, "valine" and "alanine" mutants, "serine" analog did not show any consistent binding affinity. Relatively weak binding energy was primarily due to hydrophobically favorable interactions between Leu 12, Leu 23 and ice surface.

5.4 Ice surface [111] with wild type of WF AFP and "Val","Ser","Ala" mutants

Binding conformations of wild type WF AFP and its three mutants on the ice [111] surface revealed mostly the same binding characteristics as the corresponding conformations on the [201] ice surface (see Figures 5.17-5.20). AFPs interacted with the ice surface by their "hydrophobic" face, with the exception of "Serine" mutant. AFPs aligned on the ice surface so that the distance between grooves on ice surface matched the distance between threonine residues. However, binding energies were relatively higher than those of the corresponding conformations on [201] surface, except "alanine" mutant which was demonstrated to have similar binding affinity for both surfaces (see table 5.1).

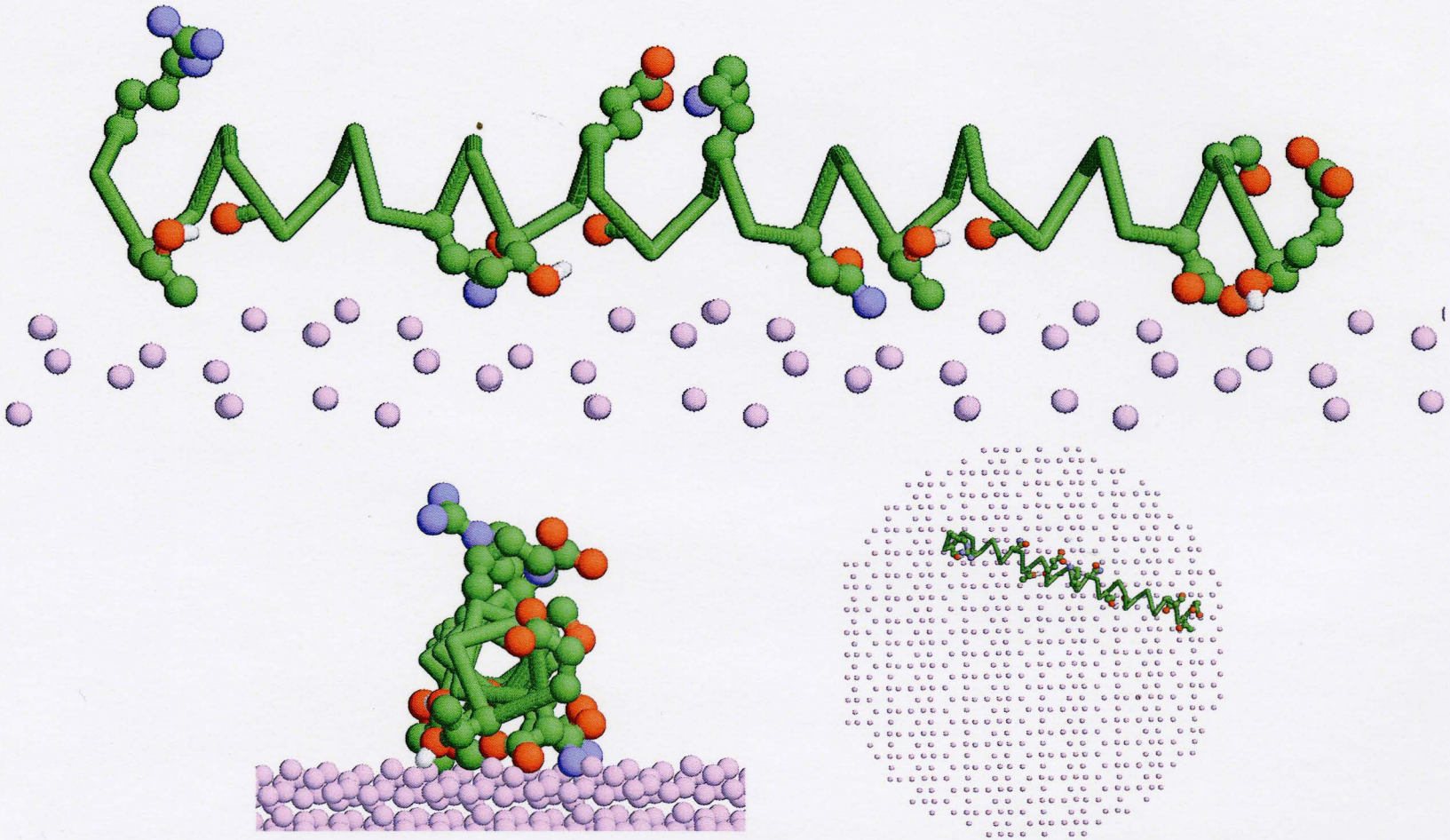

Figure 5.1 MC-minimized binding conformation of WF AFP on ice [201] surface obtained by using AMBER force field in vacuum. Binding energy is –57.3 kcal/mol. AFP interacts with the ice surface by its "Thr, Asp, Asn" face, thus allowing formation of hydrogen bonds between polar groups of Thr, Asp, Asn and water molecules of ice. This particular binding conformation also shows alternative binding geometry of Thr amino residues. See figure 5.2 for details.

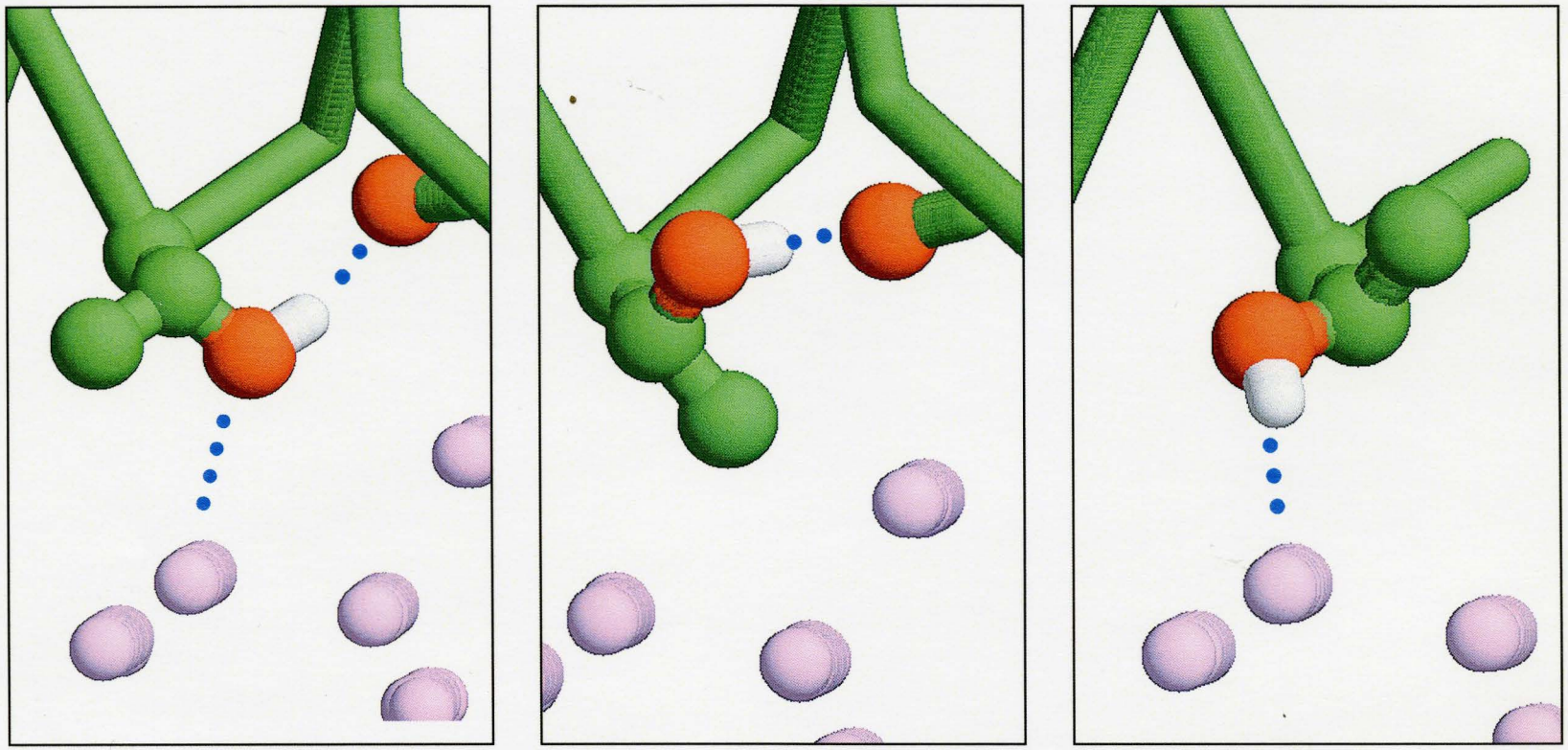

Figure 5.2. Results of MC-minimizations of WF AFP binding conformations on the ice [201] surface in vacuum, showing alternative binding geometries of Thr residues. Possibilities for hydrogen bonds are shown by blue dotted\ lines. Torsion angles χ_1 of these Thr conformations are equal to -60^o, $+60^o$ and 180^o left to right respectively. Analysis of these conformations suggested geometry $\chi_1 = -60^o$ to have strongest binding potential in vacuum. Hydroxyl group of Thr is able to accept hydrogen bond from water of ice and also donate one to the carbonyl oxygen of the residue four position upstream, while bulky methyl group is involved in van der Waals interaction with ice.

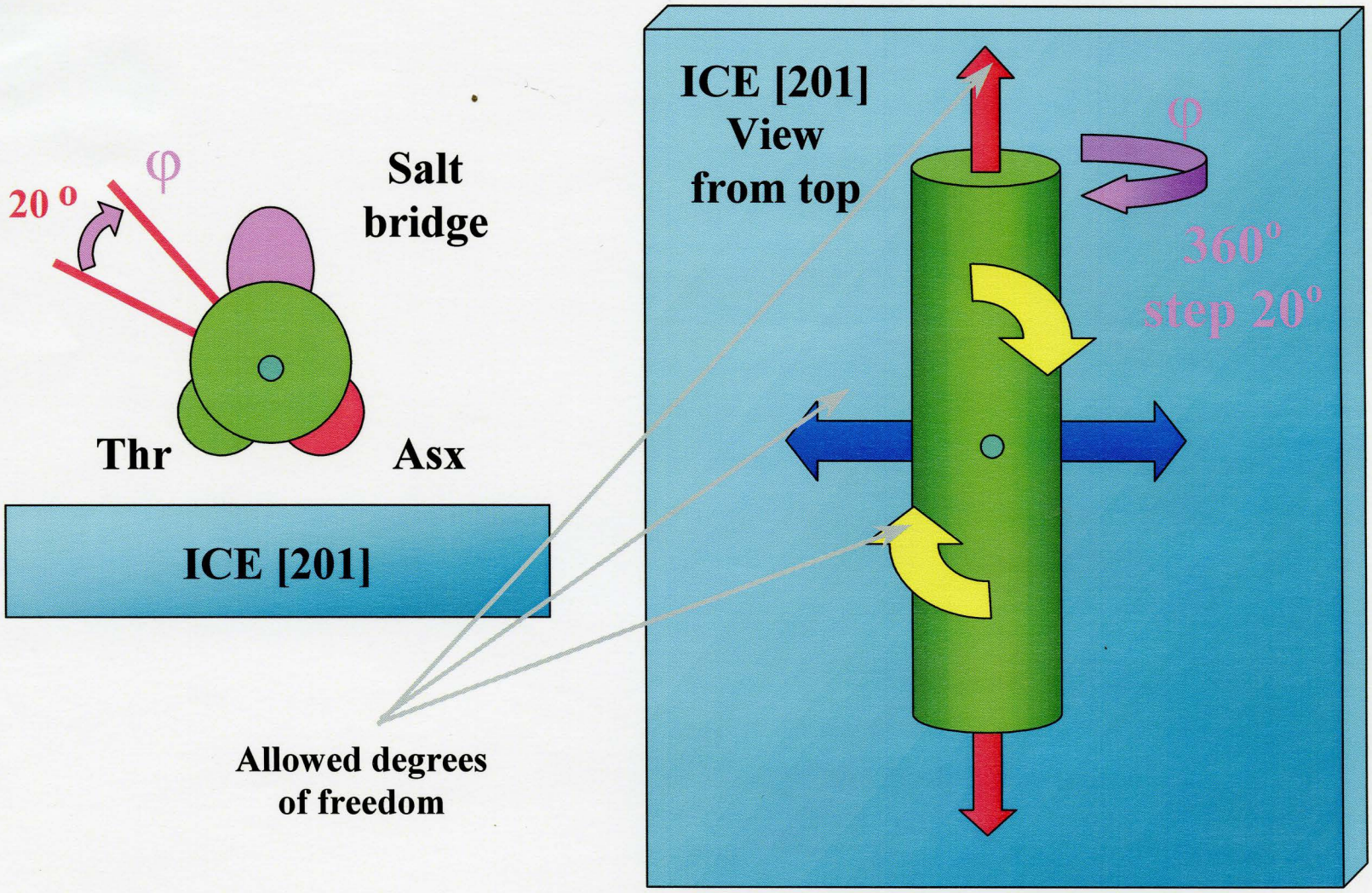

Figure 5.3 The scheme of computational experiments. Search for the highest van der Waals complementarity was performed with different values of angle φ.

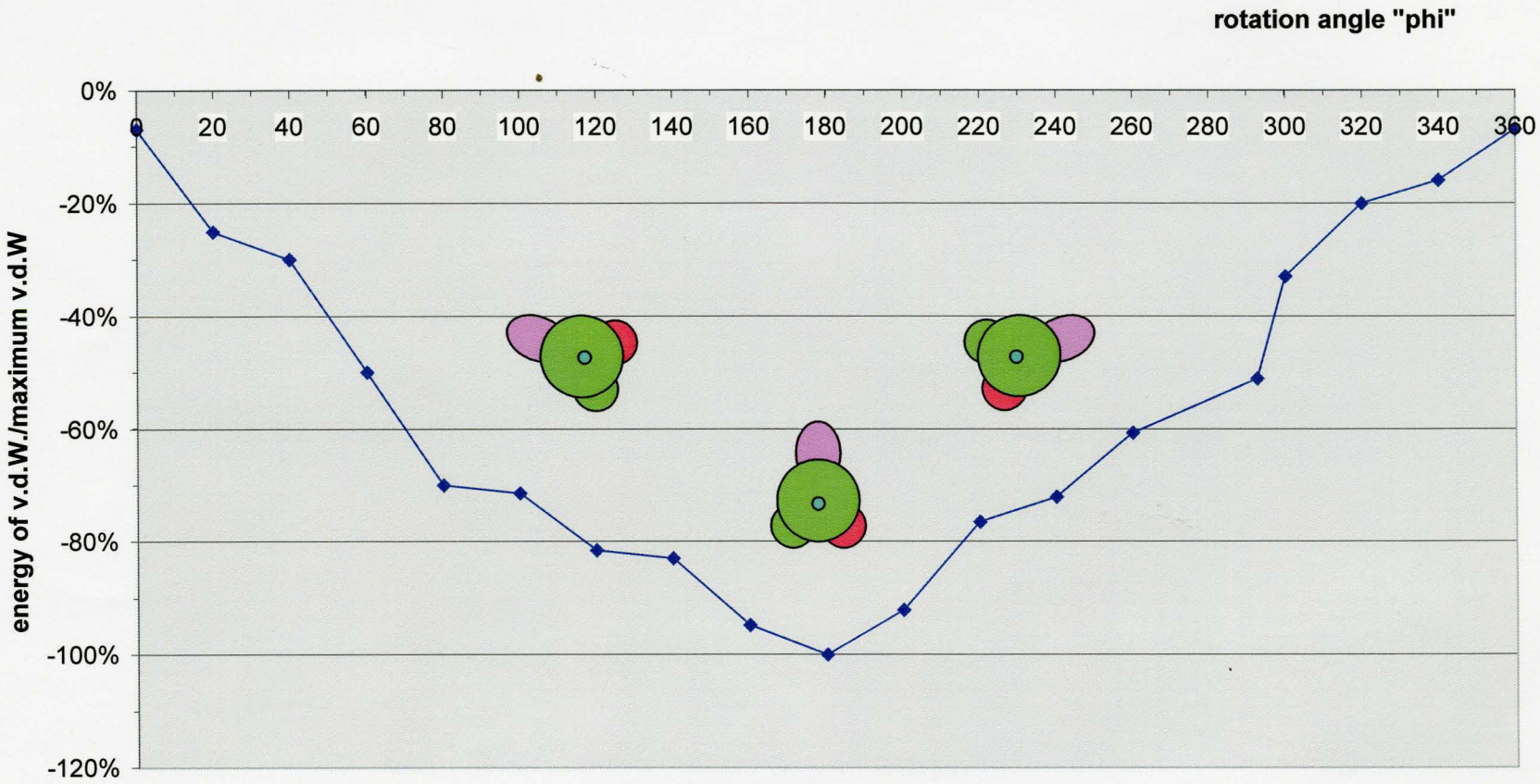

Figure 5.4 Relative value of MC-minimized energy of AFP-Ice van der Waals interaction as the function of angle φ.

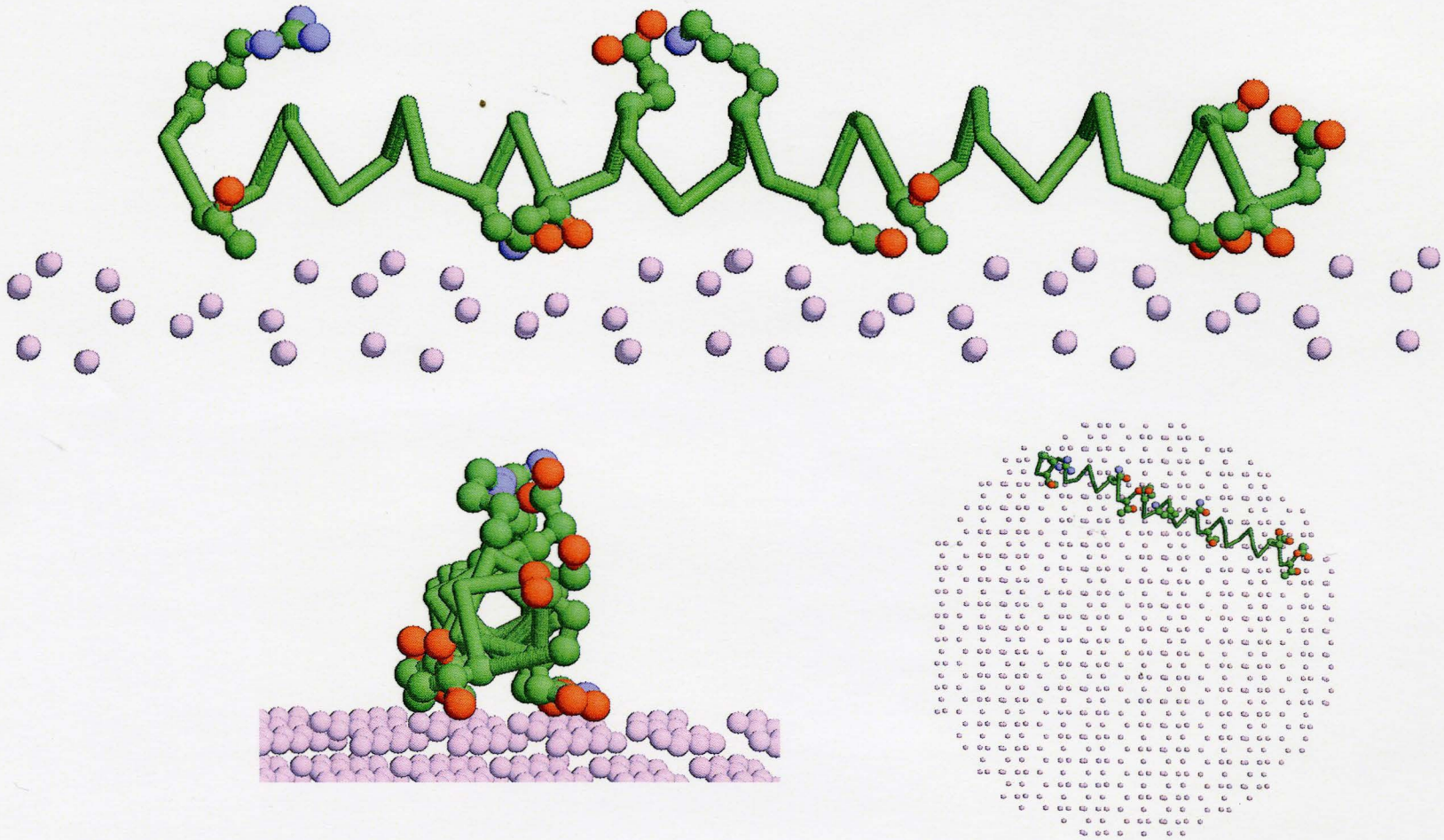

Figure 5.5 Binding conformation of WF AFP on the ice [201] surface, which involves strongest van der Waals interaction between AFP and ice. Binding van der Waals energy is –35.2 kcal/mol. AFP interacts with the ice surface by its "Thr, Asp, Asn" face. Both methyl and hydroxyl groups of Thr are involved in binding interaction. AFP aligns along [01-12] vector on ice surface.

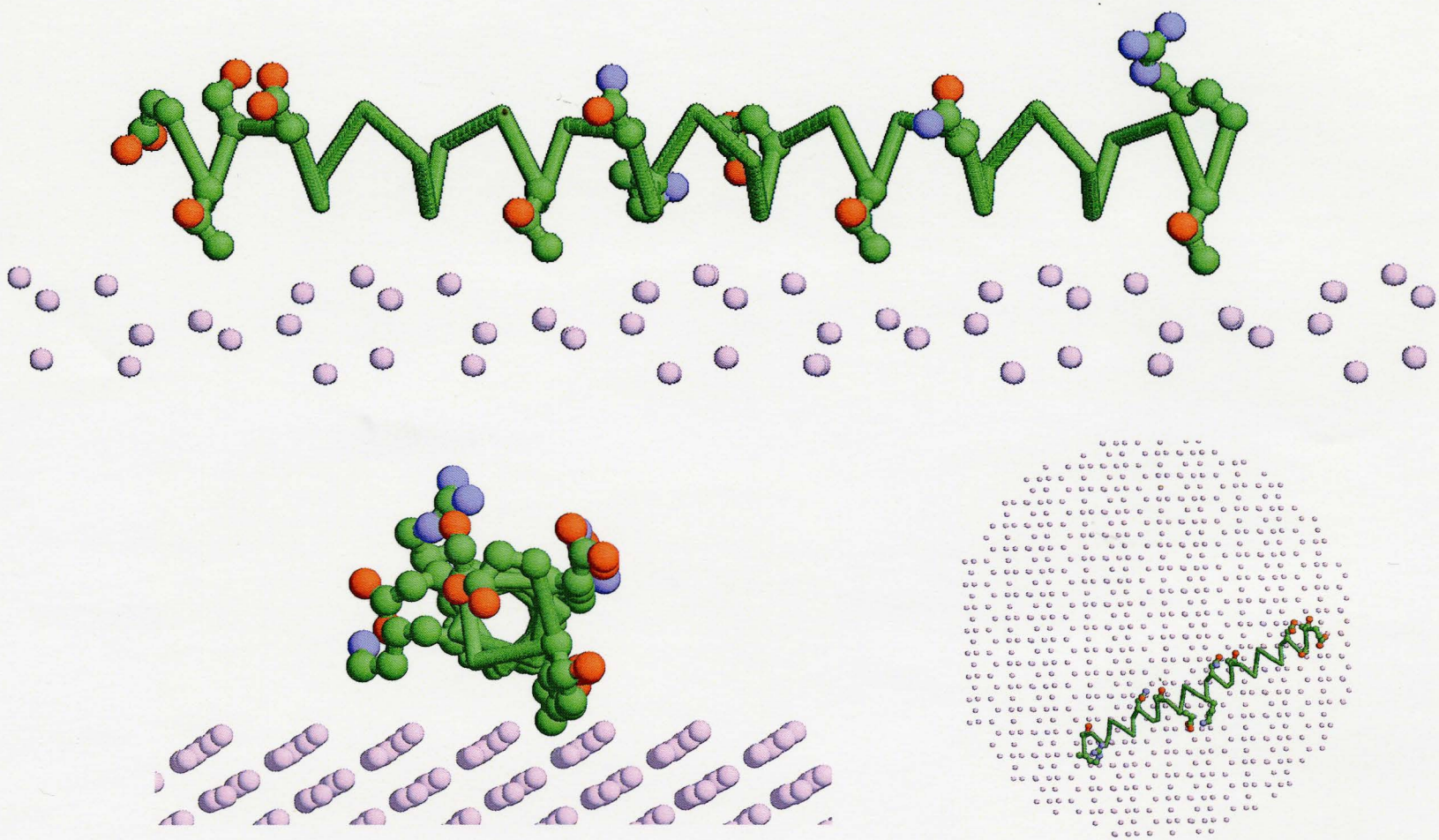

Figure 5.6 One of the possible binding conformations of WF AFP on the ice [201] surface which is allowed by the concept of complementarity between AFP and ice . Binding van der Waals energy is –24.7 kcal/mol. AFP interacts with the ice surface by its "hydrophobic" face. Bulky methyl of Thr is involved in the binding interaction.

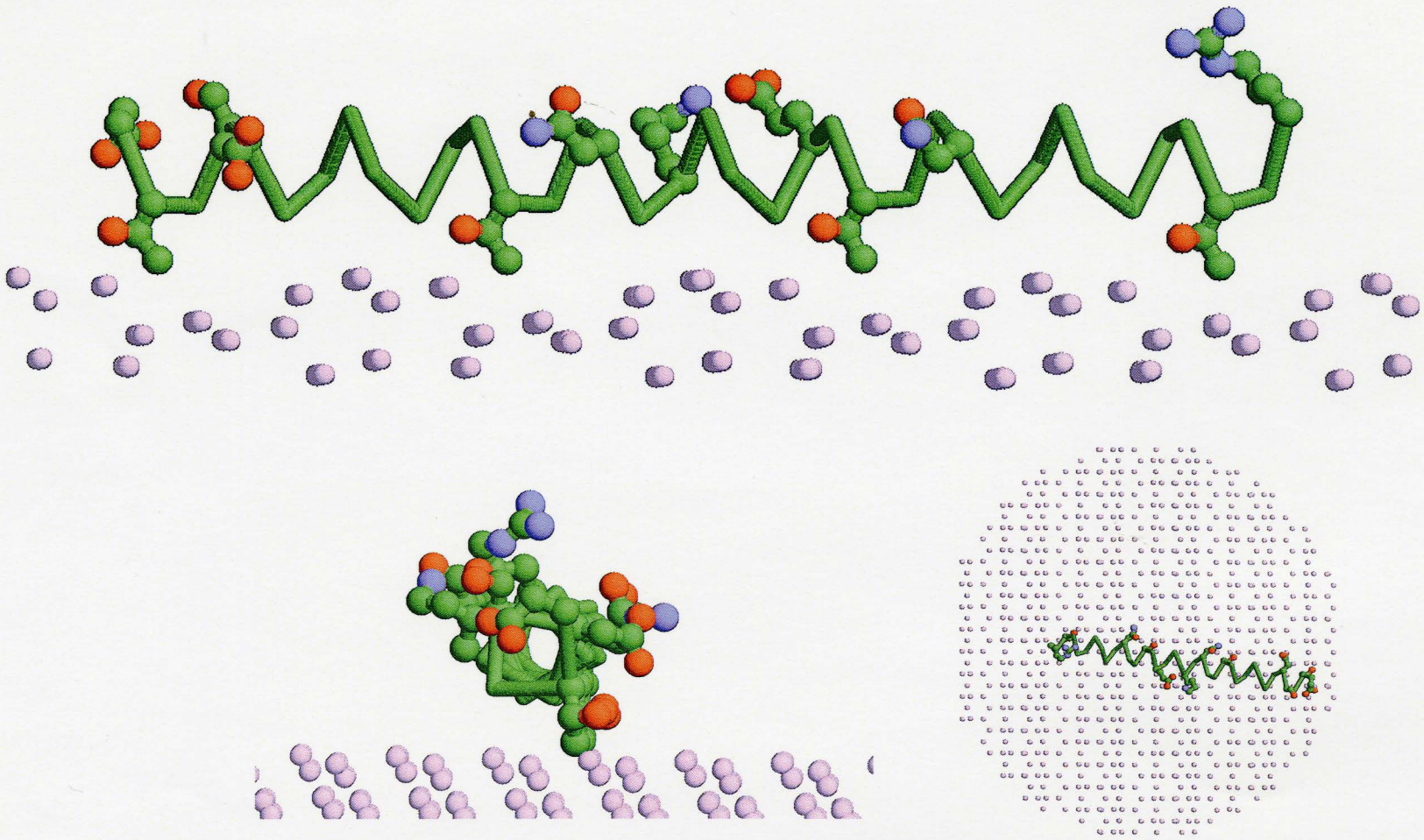

Figure 5.7 Another possible binding conformations of WF AFP on the ice [201] surface which is allowed by the complementarity concept. This figure demonstrates unspecificity of this approach to the hydrophobic or hydrophilic interactions. Binding van der Waals energy is –22.0 kcal/Mol. AFP interacts with the ice surface by its "Hydrophobic" face. Both hydrophobic methyl and hydrophilic hydroxyl groups of Thr are involved in the binding interaction.

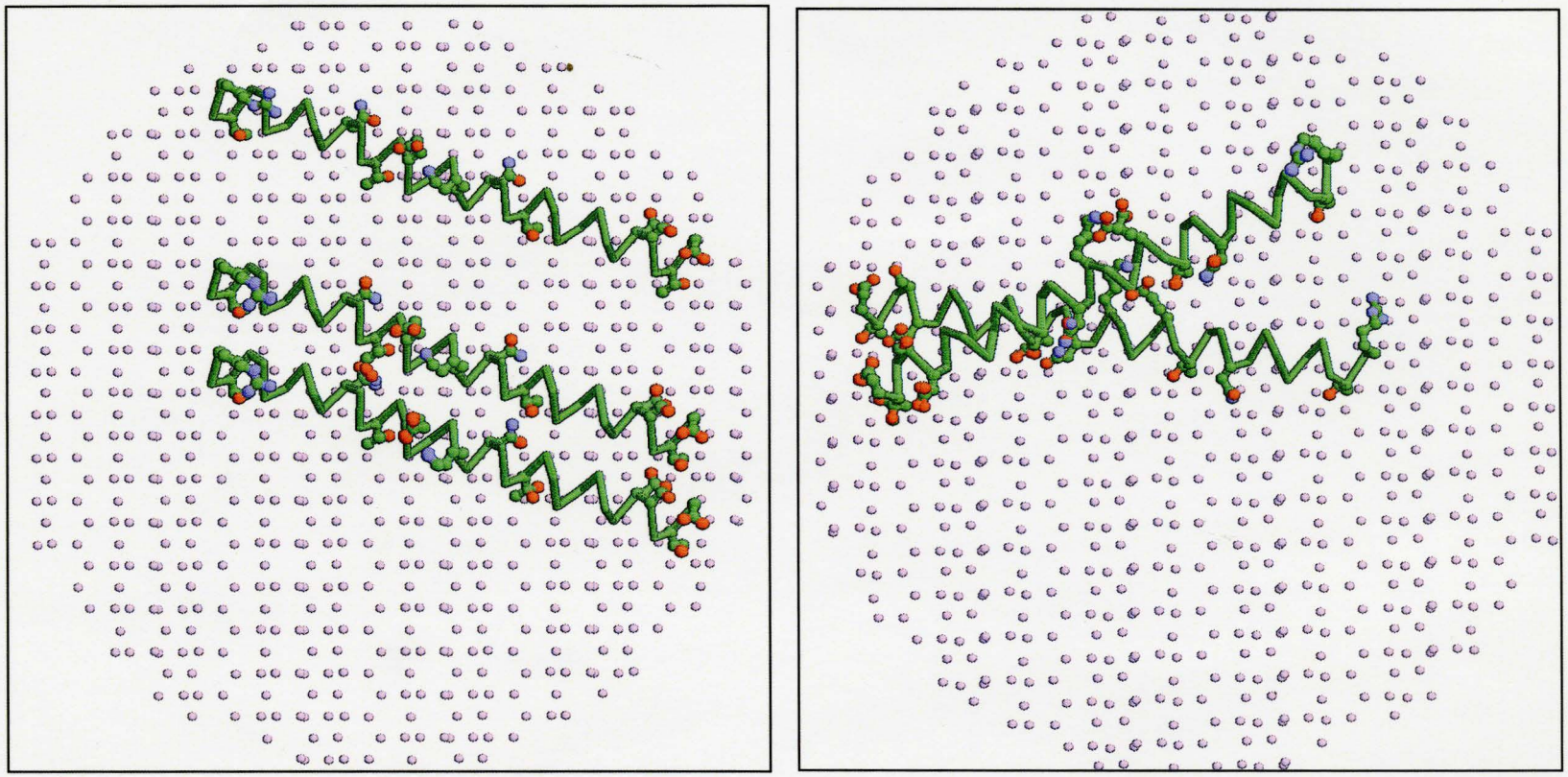

Figure 5.8 Visualization of a few points from MC—minimization trajectory of binding simulations of WF AFP on ice [201] surface. This figure illustrates possibility of substantial translation and rotation of AFP during MCM protocol.

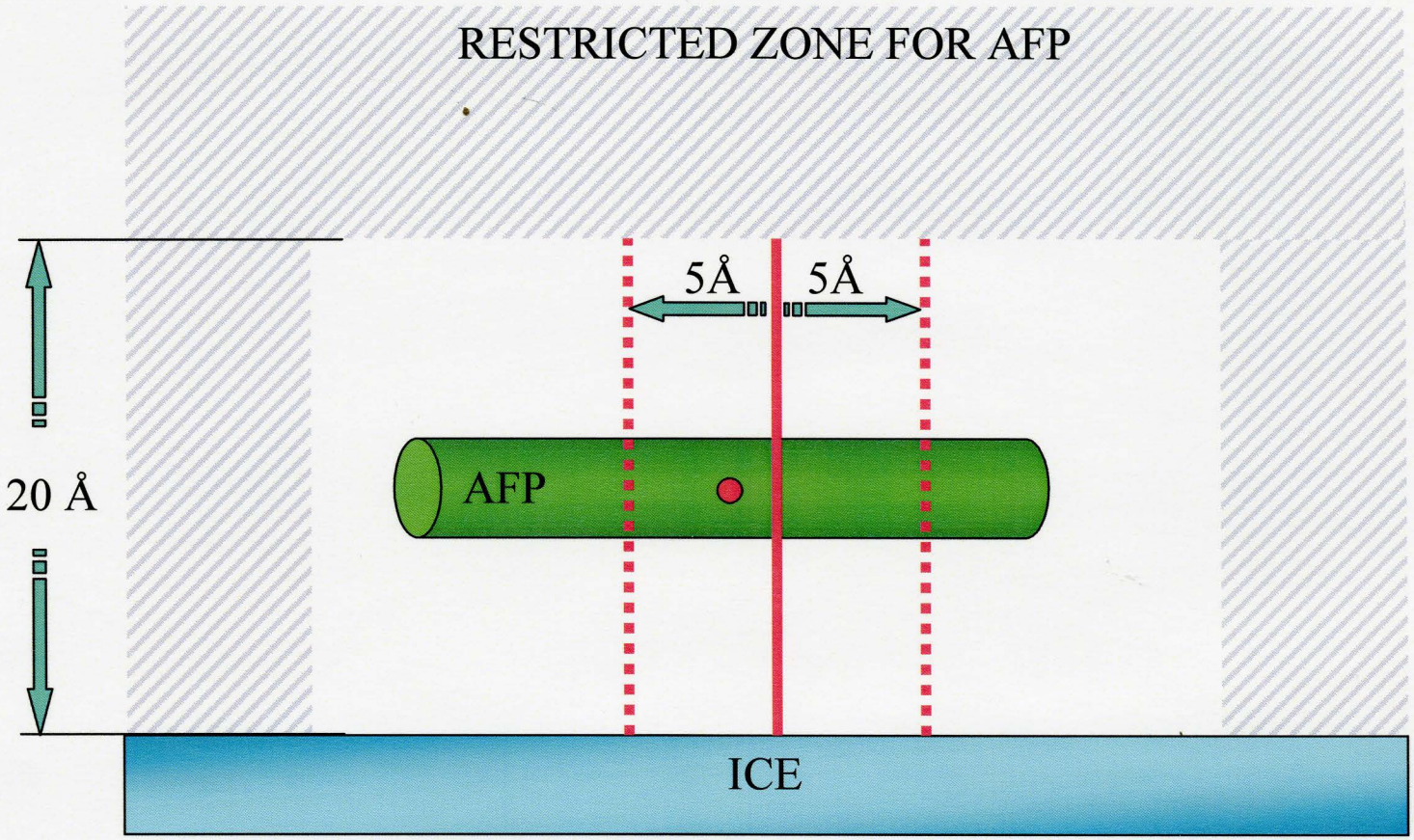

Figure 5.9 Constrains in typical computational experiment. In order to minimize unproductive MCM search in areas not relevant to the binding conformations and also to keep AFP on the ice surface to exclude possibility of binding on the edge of ice, following flat bottom constrain were introduced. 1) Flat-bottom constraints between N- and C-terminal CA atoms and ice surface. The bottom width = 20 Å. 2) 1. Flat-bottom constrains between the center of AFP and a normal to the ice surface passing through the center of the ice slab. The bottom width = 10 Å.

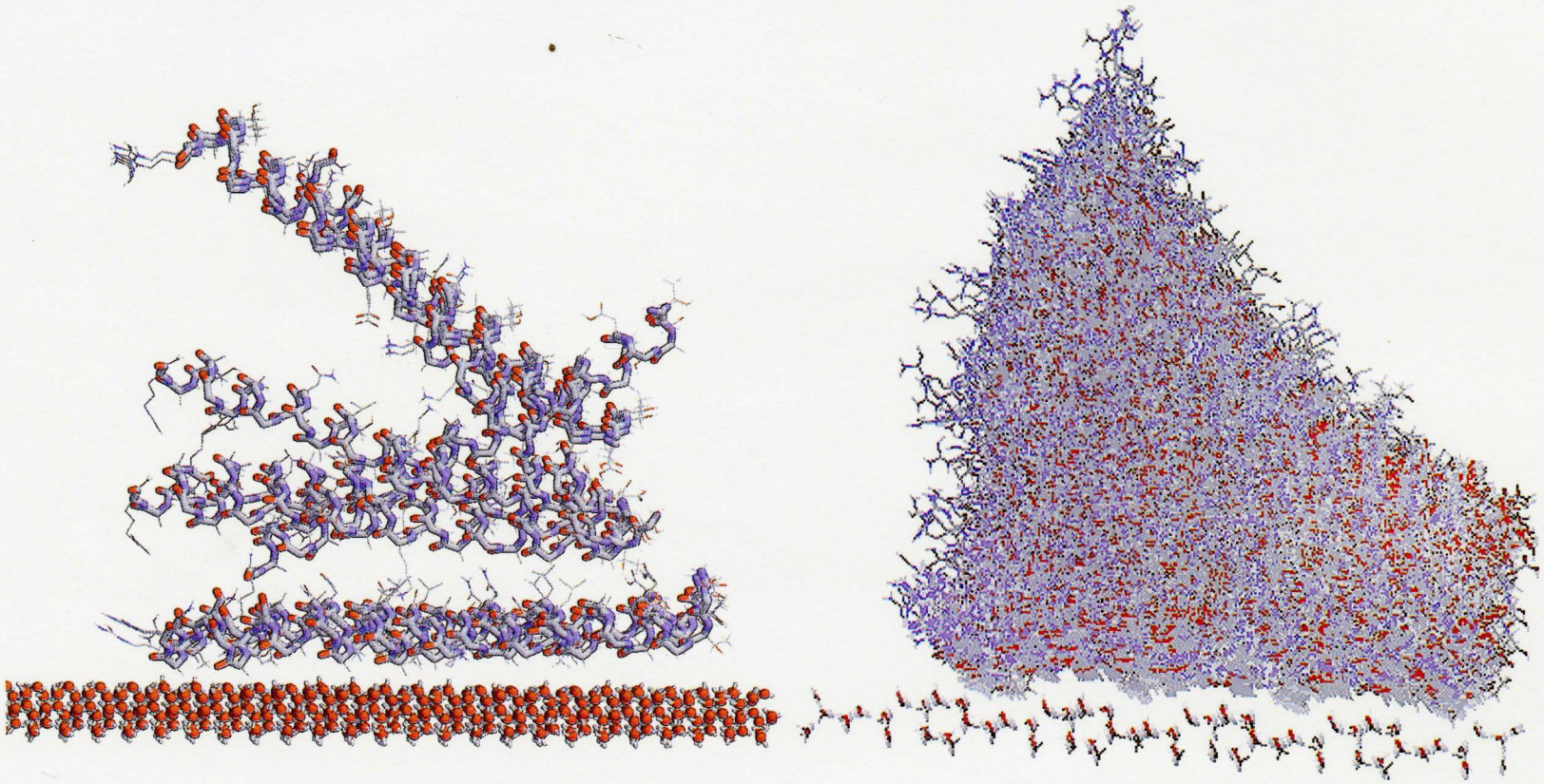

Figure 5.10 Convergence of an MCM trajectory from a random starting point (left) and from multiple randomly generated starting points (right).

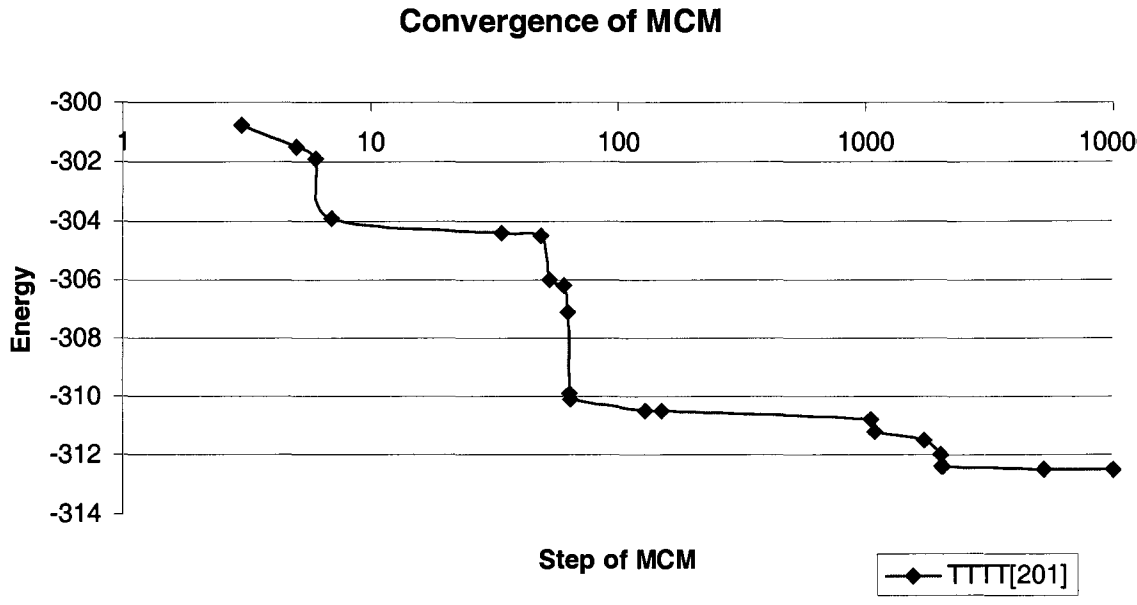

Figure 5.11 Typical MCM convergence trajectory.

Ice surface	AFP	v.d.W. energy AFP-ice	Solv. Energy AFP-ice	Total AFP-ice	System
Ice [201]	TTTT	-18.4	13.5	-4.9	-313
	VVVV	-20.3	12.4	-7.9	-294
	SSSS	-4.8	2.3	-2.5	-316
	AAAA	-15.9	12.4	-3.5	-302
Ice [111]	TTTT	-12.9	9.1	-3.8	-309
	VVVV	-15.1	7.9	-7.2	-290
	SSSS	-7.6	5.1	-2.5	-312
	AAAA	-17.9	14.5	-3.4	-300

Table 5.1 The binding and total system energy of WF AFP and its mutants on the [201] and [111] surfaces of ice

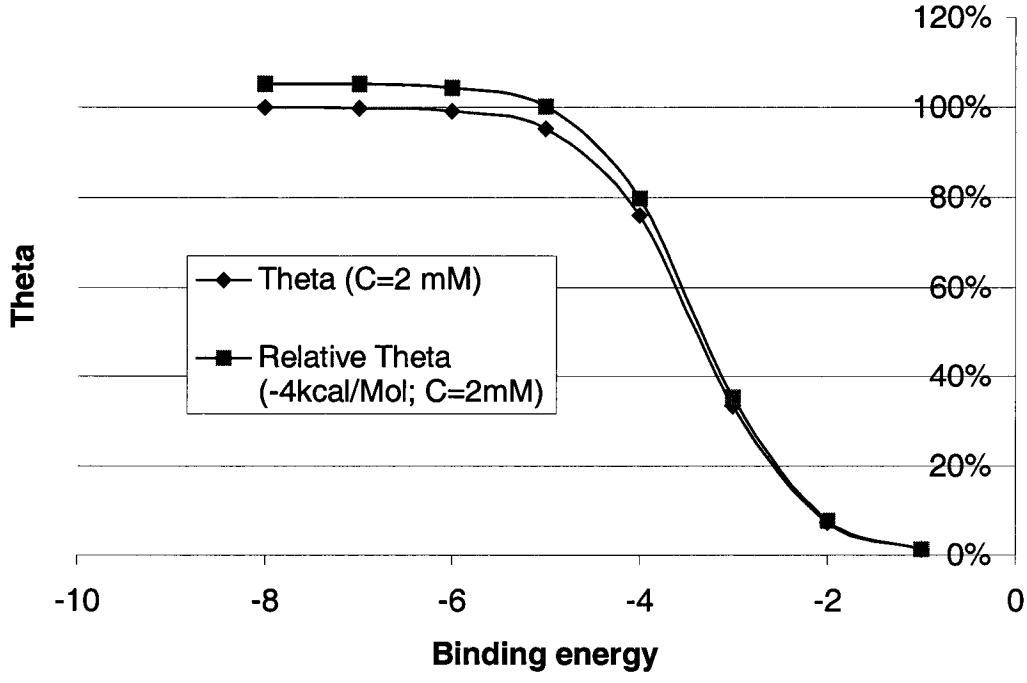

Figure 5.12 The dependence of fractional amount of AFP on ice surface θ (Theta) on the binding energy, at 2mM AFP concentration (activity saturation). Based on equation 2.4.

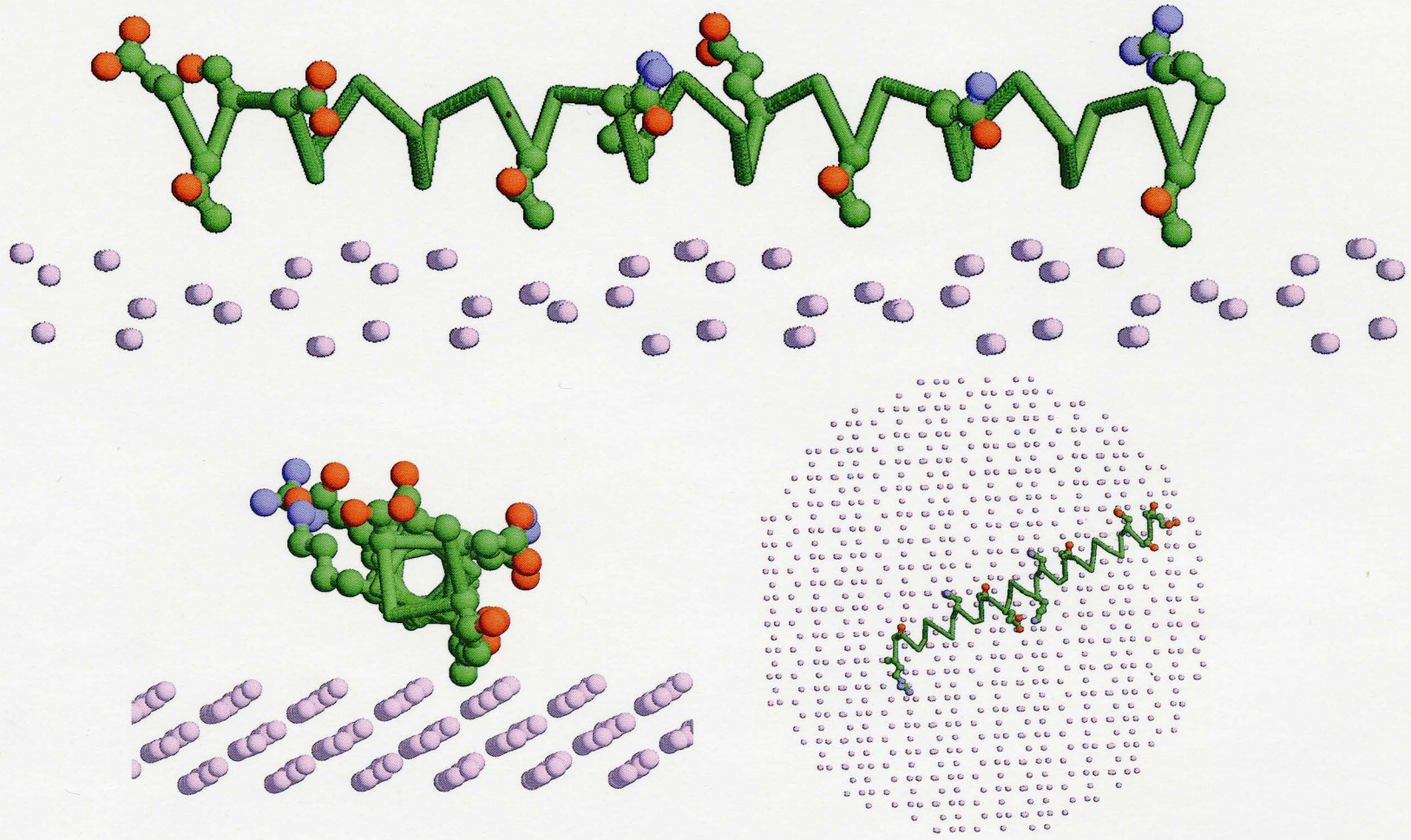

Figure 5.13 MC- minimized WF AFP – ice [201] system obtained by using van der Waals & Solvation (VS) force field. The conformation of this system shares the same key features with the system minimized by using the force filed which included both VS and electrostatic component. Hydrophobic methyl groups of Thr oriented insight ice grooves while hydroxyl groups of Thr and Asp and Asn residues remains in water. AFP aligns along common [01-12] vector on ice surface.

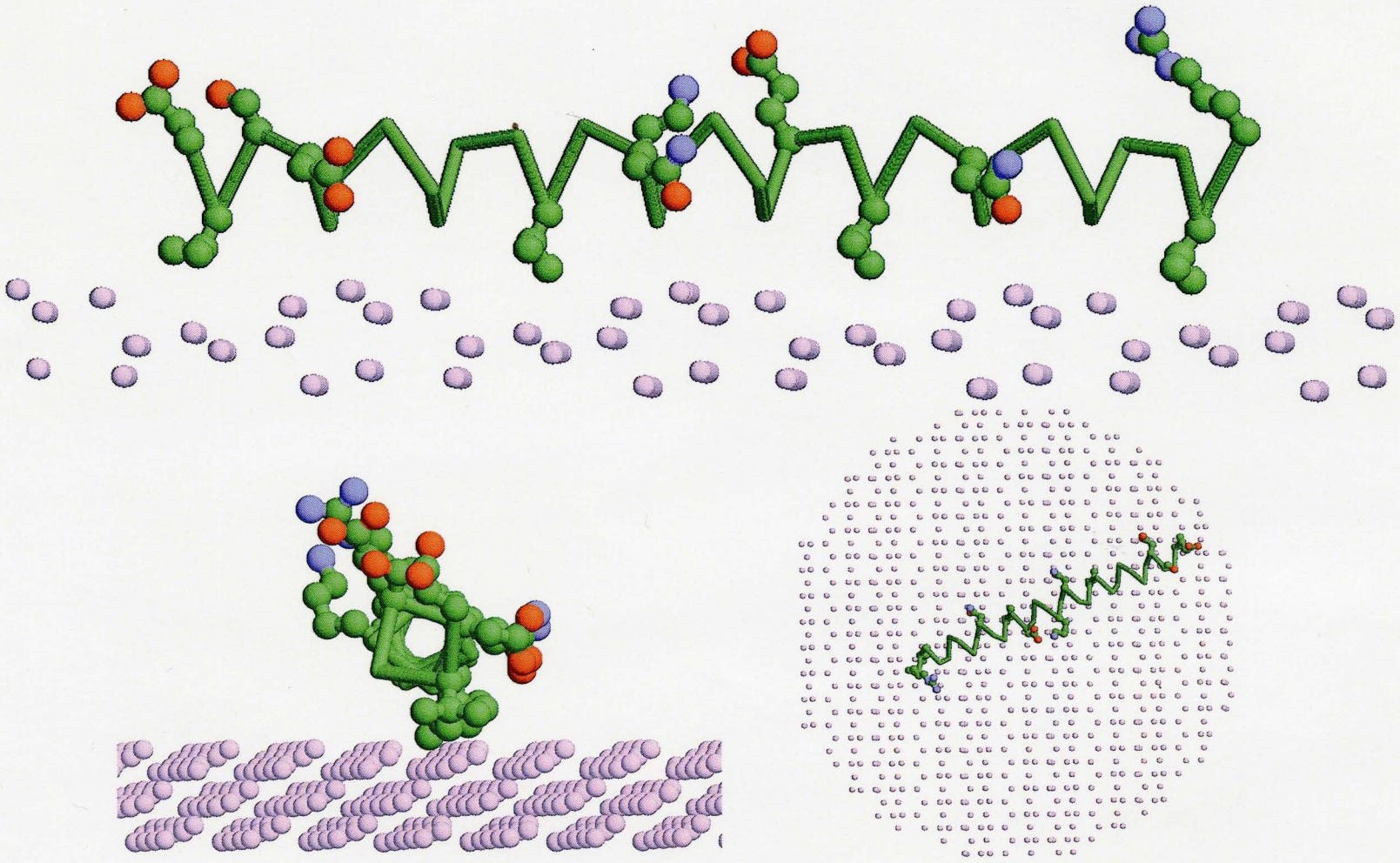

Figure 5.14 MC-minimized in VS force field binding conformation of "Valine" mutant of WF AFP on the surface of ice [201] generally reproduced binding geometry of the wild type WF AFP. However, due to additional methyl group it shows stronger binding affinity.

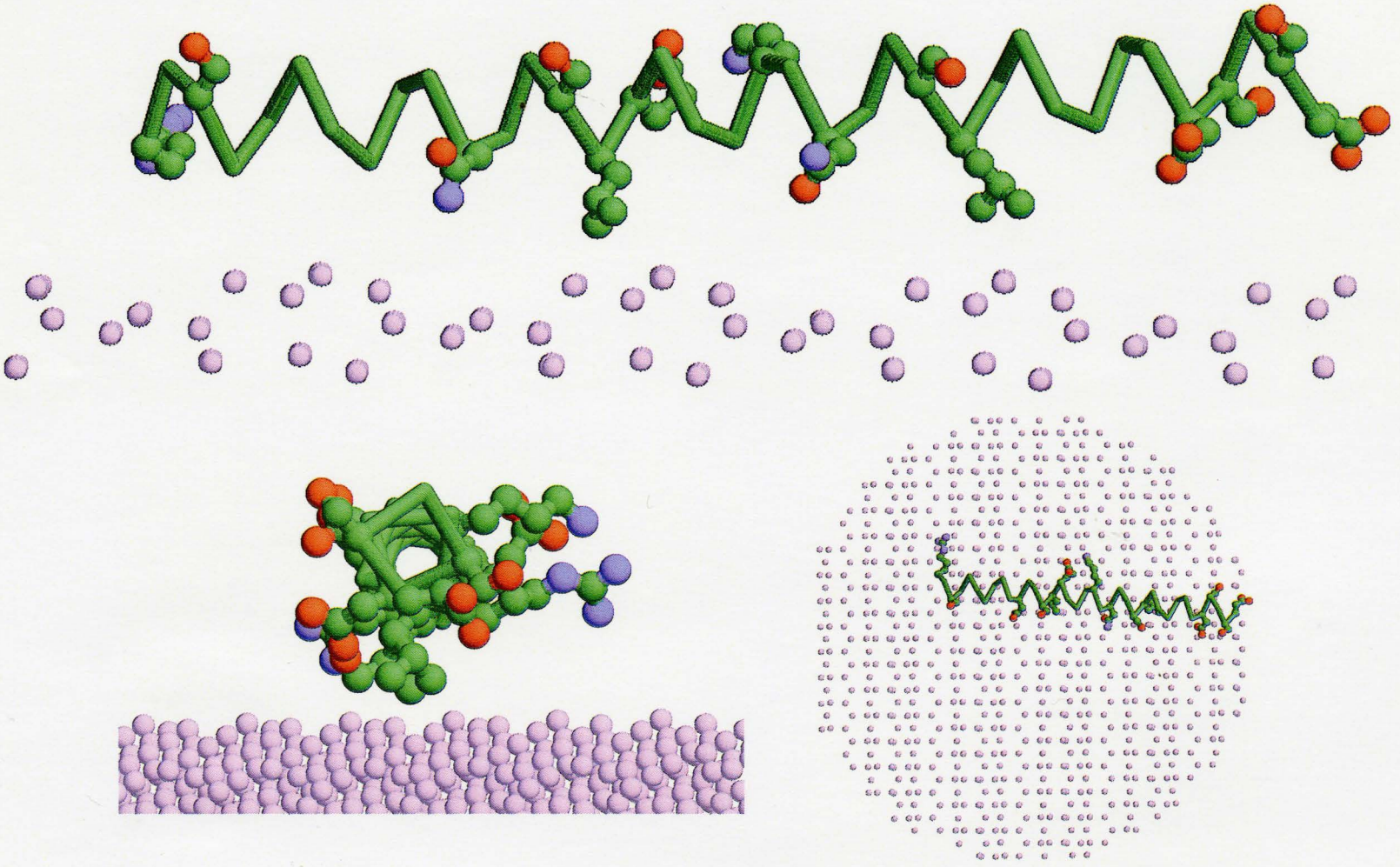

Figure 5.15 MC- minimized binding conformation of "Serine" mutant of WF AFP on the surface of ice [201], in contrast to the "Wild Type" and "Valine" mutants, does not show any specificity to the ice. Binding energy is week primarily due to Leucines interactions with ice.

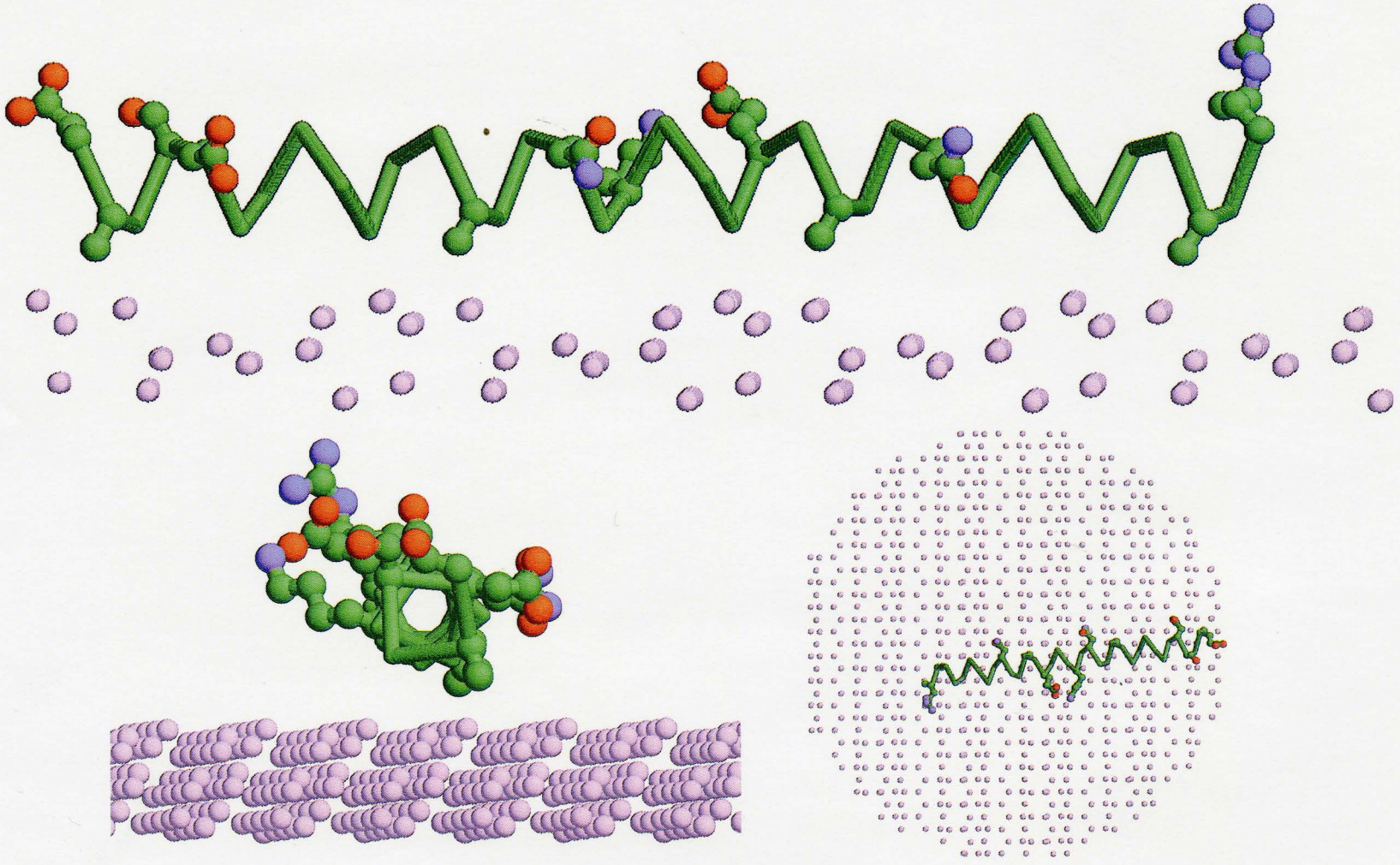

Figure 5.16 MC- minimized binding conformation of "Alanine" mutant of WF AFP on the surface of ice [201] shows higher binding affinity than "Serine" mutant, however, in contrast to the "Wild Type" and "Valine" mutants, methyl groups of Ala are unable to interact with ice grooves which resulted in weaker van der Waals contact with ice.

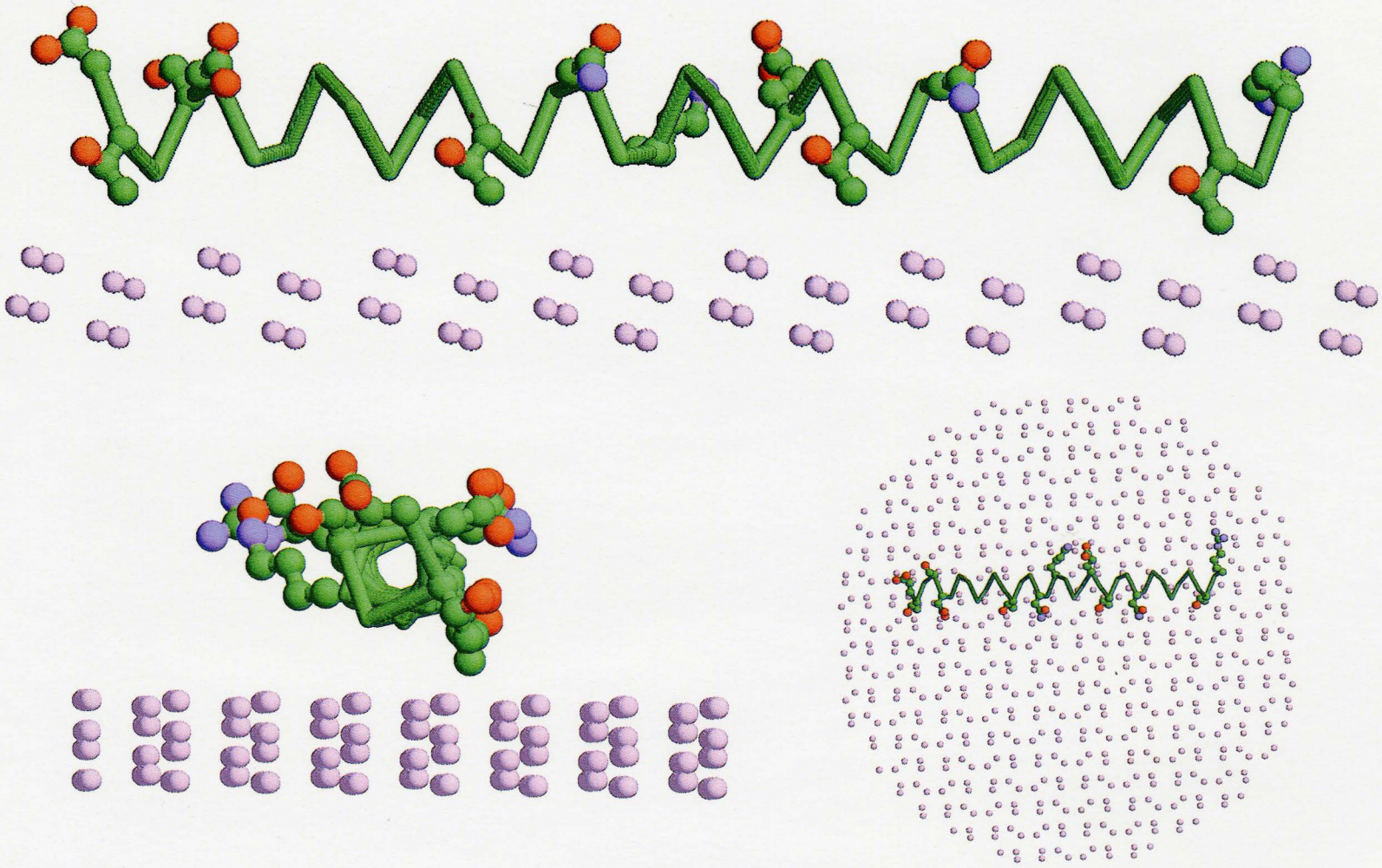

Figure 5.17 MC- minimized WF AFP – ice [111] system obtained using van der Waals & Solvation (VS) force field. Methyl groups of Thr fitted insight ice grooves which are smaller than on [201] surface. Binding affinity is slightly weaker than on [201] surface due to less specific van der Waals contact. (See Table 5.1)

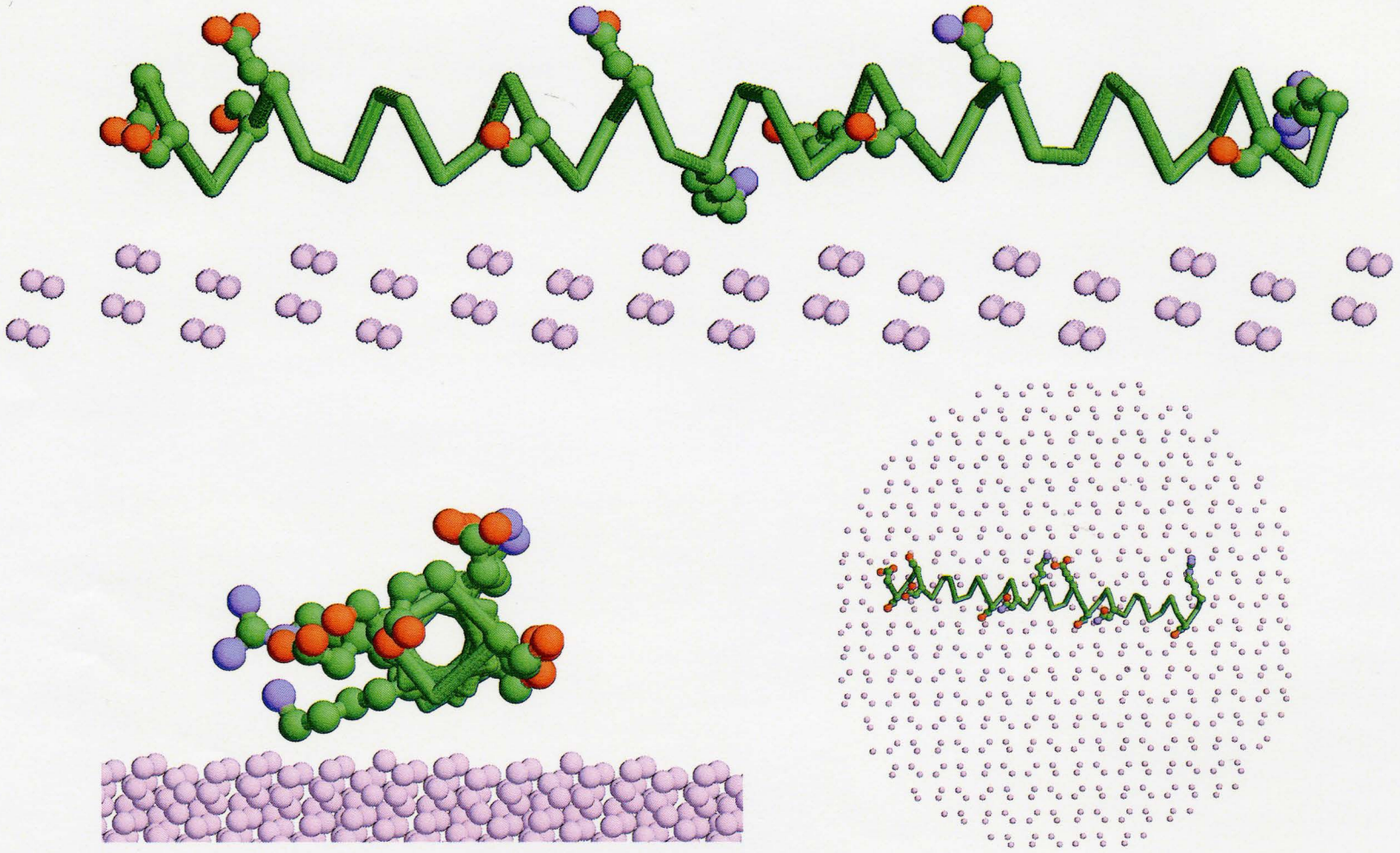

Figure 5.18 MC- minimized binding conformation of "Serine" mutant of WF AFP on surface of ice [111] demonstrate very poor binding affinity as in case of binding on [201] ice surface. Orientation on the ice surface is uncertain and varies randomly depending on the starting point in the trajectory.

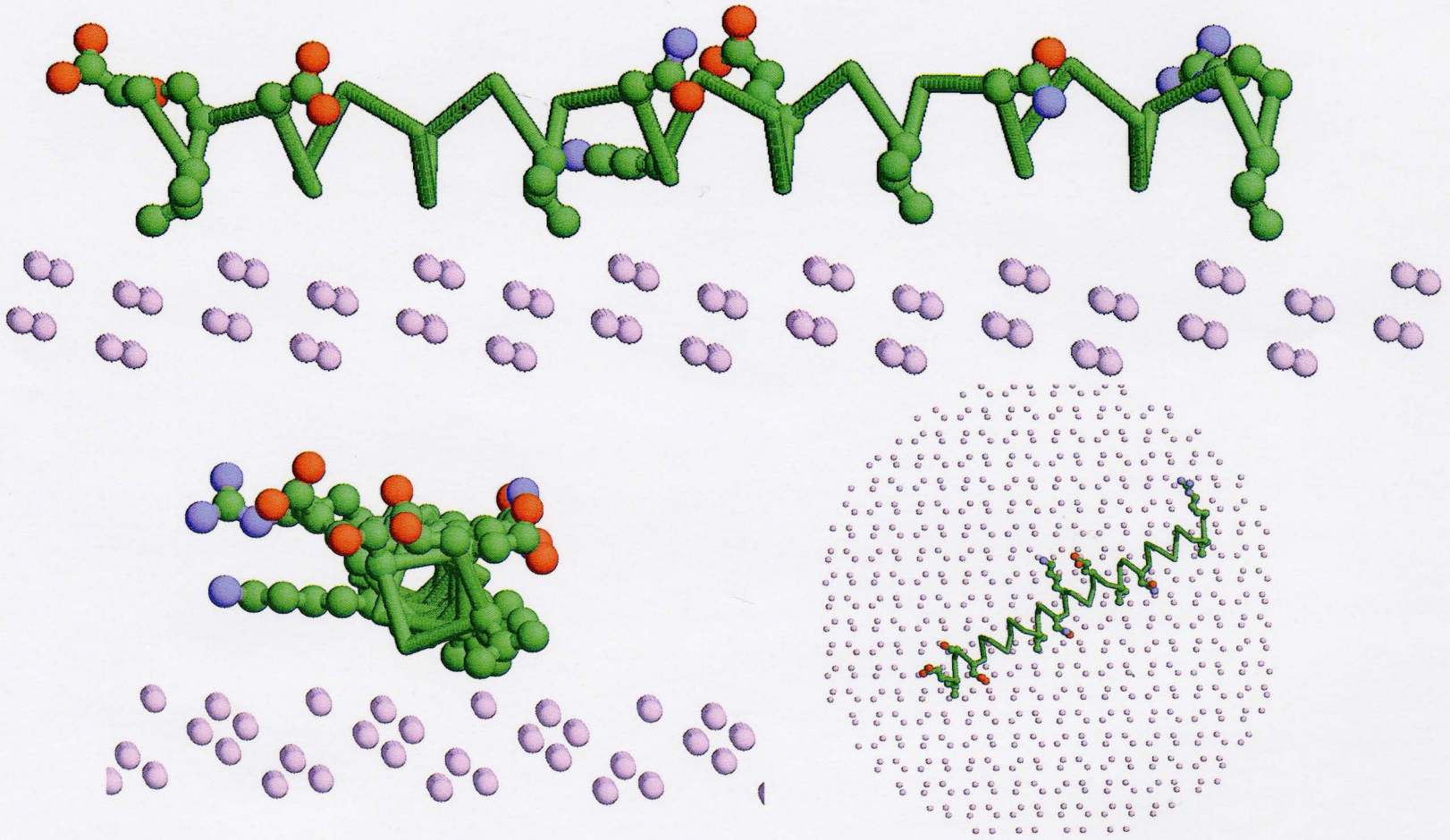

Figure 5.19 MC- minimized in VS force field binding conformation of "Valine" mutant of WF AFP on surface of ice [111] demonstrates strongest binding affinity among mutants and "Wild type" due to absence of hydroxyl groups on binding surface. However, the binding on the [111] ice surface is weaker than on the [201] surface.

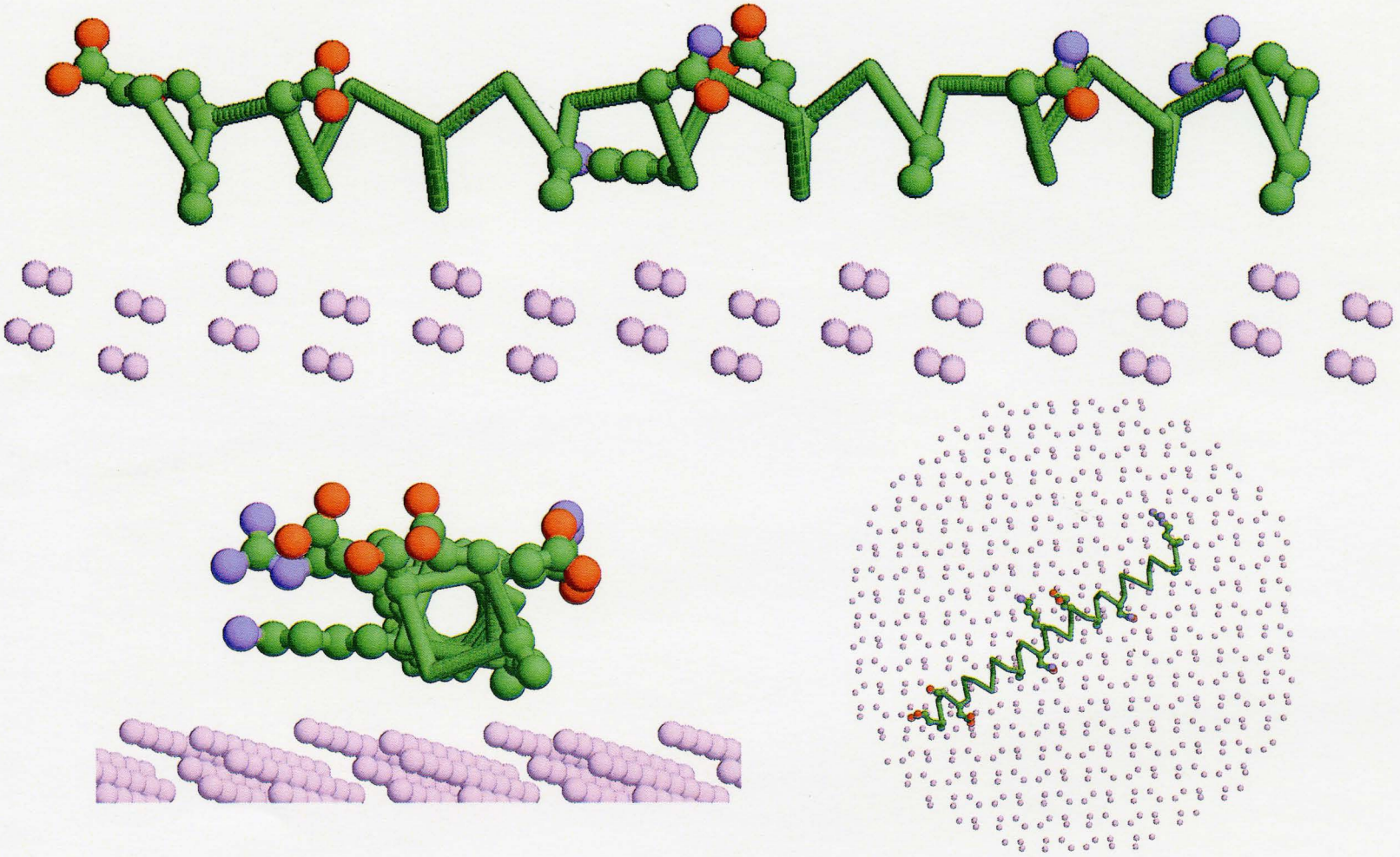

Figure 5.20 MC- minimized binding conformation of "Alanine" mutant of WF AFP on surface of ice [111] shows higher binding affinity than on [201] surface. Flat poly-alanine surface of the mutant has more steric complementarity with relatively flat [111] surface than with [201] surface.

Chapter 6. Discussion

6.1 Critical review of previous theoretical studies of WF.

During the last decade more than seven groups of scientist attempted computer modeling of WF AFP binding to ice surfaces. Due to the relatively large apparent binding surface area, these models predicted huge binding energy (80-160 kcal/mol). Such a large value of the binding energy was observed because either conventional force fields approximation were used in vacuum or explicit water molecules were introduced in the system. The major components of the calculated energy of interaction of AFP with ice, not surprisingly, were hydrogen bonds and electrostatic interactions. However, these calculations did not take into account an important component of interaction, namely the binding surface hydration of AFP and ice.

Although attempts have been made to include explicit water molecules in the model (Cheng & Merz., 1997) they did not lead to any substantial advance in understanding the mechanisms of AFP-ice interaction, because the dramatic increase of the number of variables had made global energy minimization of the system practically impossible. Obviously, the huge system involving AFP, ice, and explicit water molecules

was trapped during molecular dynamics simulations in the vicinity of the local minimum, nearest to the starting point. Therefore that kind of modeling was biased to the initial "hand –made" binding, and consequently produced results that were expected.

6.2 Why hydrophobic interaction are crucial ?

Presumably, antifreeze protein binds to ice, implying that a part of AFP less favorably interacts with the surrounding liquid water than with the ice surface, the rigid organized water. But what ice has to offer to AFP? It is likely to be neither hydrogen bonds nor the van der Waals potential, because both of them are already completely realized in water. The inflexibility of ice may also reduce these forces. Therefore, there is only one force which makes some proteins to be "unhappy" in water, the hydrophobic force.

Entropical in nature, the hydrophobic force occurs, because some groups of atoms, known as hydrophobic groups, can not offer water the hydrogen bonding. Therefore, driven by the tendency to maximize the number of hydrogen bonds, the water molecules form organized clusters, known as water cages. Formation of these cages is entropically unfavorable. In general, the force, which drives two hydrophobic group to each other in water solution, thus decreasing the number of water molecules in cages, is called the hydrophobic force. This force minimizes the surface area of the hydrophobic

groups exposed to water. This minimization can be achieved by conformational changes in the protein, aggregation or by binding to some surfaces. In all cases the free energy gain from decreasing the water-accessible hydrophobic surfaces should be bigger than possible free energy loss of van der Waals contacts and dehydration of polar and ionized groups. That is why in general the interaction of hydrophilic and hydrophobic surfaces can not take place, the energy of dehydration of hydrophilic surface is simply too high. However, this type of interaction can take place, under certain conditions.

Under normal conditions at 273° K liquid water crystallizes to ice. Free energy of this process ΔG is equal to zero, because entropical disadvantage of organized structure is compensated by enthalpical gain of extra hydrogen bonds formation: $\Delta H=T\Delta S$. Thus, exchange of the environments for the hydrophobic groups of AFP from water cages to the ice surface appears to be reasonable since in ice the entropical disadvantage is already compensated. That can explain why WF AFP binds to the ice by its hydrophobic face only. Although not every protein, which has the hydrophobic face, would bind to the ice because the structure of the protein itself is crucial for that.

6.3 Structure-activity relationships

AFP should bind to ice surface in order to prevent ice crystal growth. We also demonstrated, that AFP should bind to ice by its hydrophobic surface and that the binding process requires surface complementarity between the hydrophobic side of AFP

and the ice surface, otherwise the loss of van der Waals contacts would not allow such binding. On the other hand, the binding requires the availability of AFP hydrophobic surface, which may be already involved in aggregation with another AFP molecule.

Thus, AFP should have a hydrophobic surface complementary to the ice, but this surface should not aggregate with that of another AFP molecule. This puts important restriction on the AFP hydrophobic binding surface, basically it should not be complementary to itself (see Figure 6.1). Consequently, AFPs should not bind to a "flat" ice surface, preferring asymmetrical rough one, such as [201]. In the case of a large and relatively flat hydrophobic surface, the introduction of some polar groups helps to avoid aggregation, by counterbalancing the strong hydrophobic force. Then polar groups can interact with water and ice surface, but can not do so with polar groups of other AFP molecules (see Figure 6.1.D). An example for this case is the insect AFP. At the freezing temperature as well as at the room temperature the insect protein does not form dimers. However by raising the temperature of the solution, this balance can be shifted moved to the aggregation stage, because the higher the temperature, the stronger the hydrophobic interaction. This effect is observed in the insect AFP solution, when AFP forms the dimer after temperature reaches 40^{o} C.

Another important issue is the solubility of AFP. AFP works in solution, therefore it should have enough polar and ionized groups to ensure its solubility. In addition, the

AFP molecule should be rigid, to maintain the ice binding hydrophobic surface in solution.

WF AFP fits, in our view, to an ideal AFP, since it has all features, which we described above. It has a hydrophobic surface which is due to 16.5Å distance between Thr residues is not complementary to itself. The salt bridge stabilizes the straightness of WF alpha-helix. The introduction of two additional salt bridges helps to make this AFP even more rigid. This had been demonstrated by series of CD experiments (Chakrabartty & Hew, 1991). Apparently, the salt bridge together with Asp and Asn residues help increase solubility and prevent aggregation. The mutagenic studies of Asn residues (Loewen et al., 1999) are also suggested involvement of these residues in solubility of WF AFP. The same group of scientist investigated role of Leu residues in WF AFP and came to the conclusion that Leu helped to prevent the α-helix aggregation process which is also known as "Alacoils". However effects of solubilization and aggregation were not addressed is out of quantitative consideration in this modeling study.

6.4 Why WF AFP binds better to [201] than to [111] surfaces?

Based on Chapter 6.3 it is reasonable to suggest that the higher affinity of WF AFP to [201] than to [111] surface of ice is a consequence of the structural restriction

which is applied to AFP. As we mentioned, in order to work, the binding surface of AFP should not aggregate with that of another AFP molecule. The [111] ice surface is a lot smother than [201], therefore by designing the AFP binding surface, which is fully complementary to [111] ice surface, Winter flounder risks to create AFP which would aggregate to itself (see Figure 6.1.A). We suppose that from the sterical point of view the best way to avoid aggregation would be the introduction of "spikes"(protrusions) on AFP binding surface, which should be long enough to prevent AFP dimer formation, but short enough to allow the binding to [111] surface (see Figure 6.1.C). Apparently, WF AFP is a compromised engineering solution for this problem. Any compromise requires the sacrificing, therefore the WF AFP is not optimal for binding to [111] ice surface. However, it is reasonable to assume that there is at least one surface from the whole variety of ice planes which has the best binding affinity to WF AFP, and that can be the [201] surface observable in the ice etching experiment.

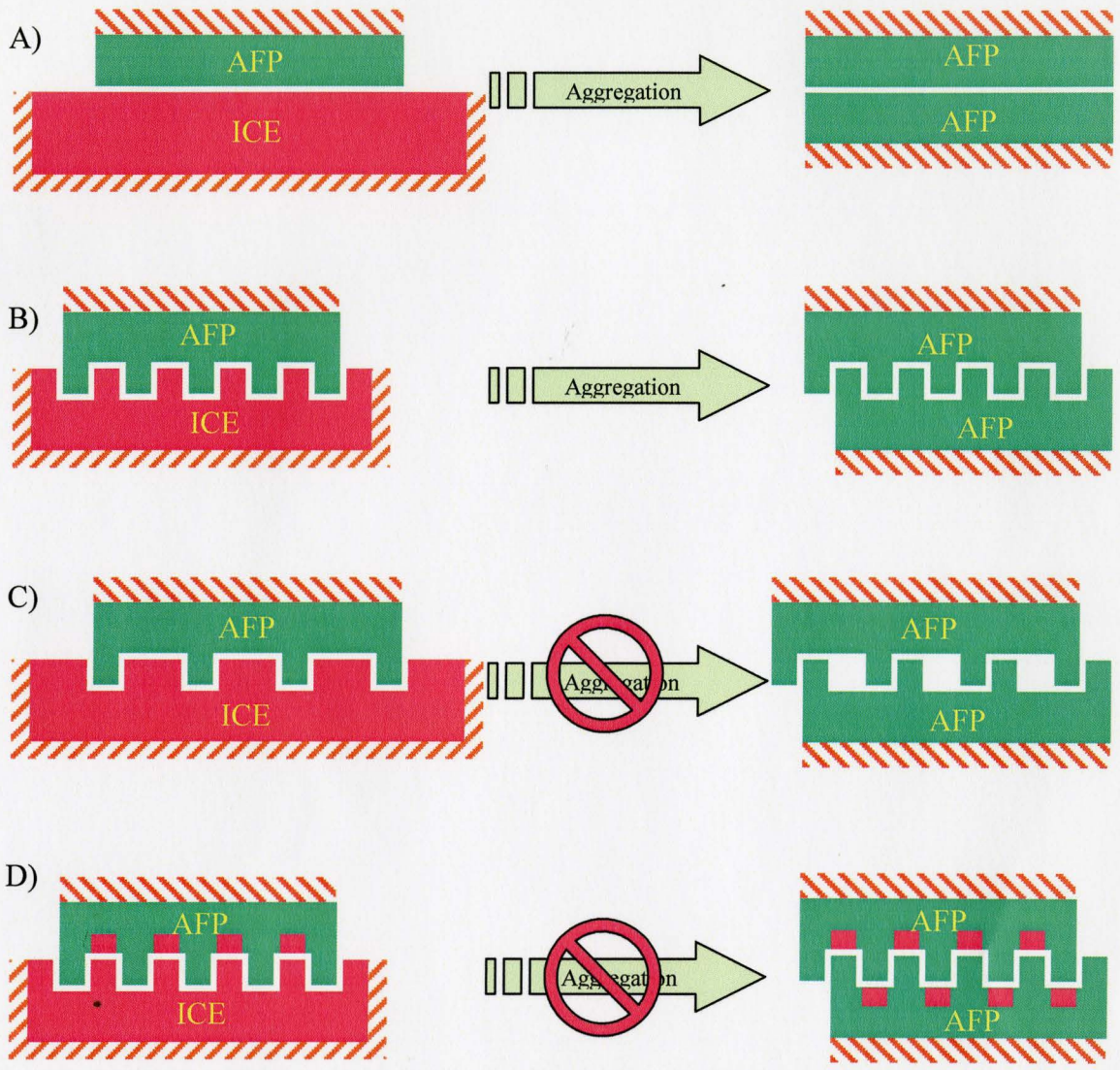

Figure 6.1 Possible aggregation and binding to ice surface scenarios for different AFP structures. A) "Flat" hydrophobic surface of AFP interacts with "flat" ice surface, however this structure of AFP also favors the AFP-AFP aggregation. B) Complementary to itself hydrophobic surface of AFP, naturally, favors the aggregation process. C) Possible conformation of AFP which allows interaction with certain ice surfaces, but not complementary to itself, therefore this AFP is not likely to aggregate. D) One more possible way to avoid aggregation – introduction of hydrophilic groups "inside" the hydrophobic surface. Upon binding of AFP on ice, formation of hydrogen bonds may partially compensate loss of contact with water for hydrophilic groups of AFP, on the other hand inability of hydrophobic groups to offer hydrogen bond unfavores the aggregation.

6.5 Binding energy of WF AFP and its mutants

The important part of our results were values of the binding energy of AFPs on two ice surfaces. Several force field parameters were developed by ourselves, based on the conclusion that the binding energy of WF AFP should be about 5 kcal/Mol (see Division 2.1). Consequently the found absolute value of wild type WF AFP binding energy can not be considered as an independent result. On the other hand, we can consider this process of adjusting of force field parameters as a calibration of the energy function to the experimentally observed value. Therefore the values of binding energy for WF AFP and its mutants on different ice surfaces (see Table 5.1) can be transformed using equation (2.4) and (2.12) to the fractional amount of AFP on ice surface ,θ (see Figure 6.2). Fractional density of AFP θ is also related to the experimentally observed fractional hysteresis ΔT_F (see Table 1.2), according to the equations (2.5) and (2.7). The correlation between theoretically predicted values of θ for different mutants of AFP and the experimentally observed fractional hysteresis ΔT_F can be considered as the measure of accuracy of our theoretical and computational approaches.

We can also use the values of the binding energy of of WF AFP to [201] and [111] ice surfaces to support our propose made in Division 3.4. The figure 6.3 illustrates the difference in fractional density θ on these two surfaces at the standard for ice etching assay concentration of WF AFP.

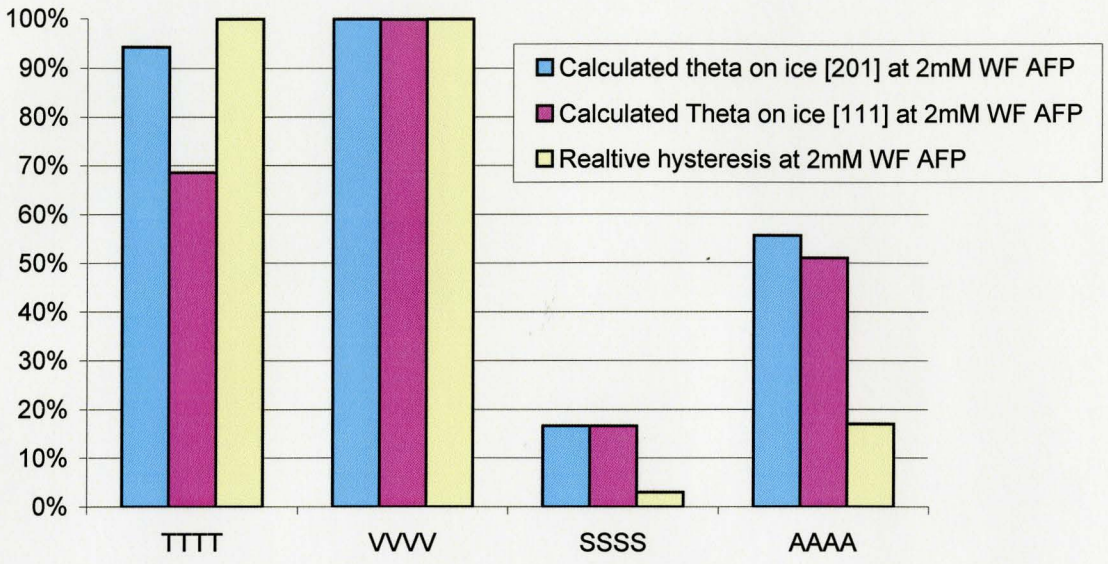

Figure 6.2. The calculated fractional density θ and experimentally observed temperature of thermal hysteresis (relative to WF) for WF AFP and its mutants

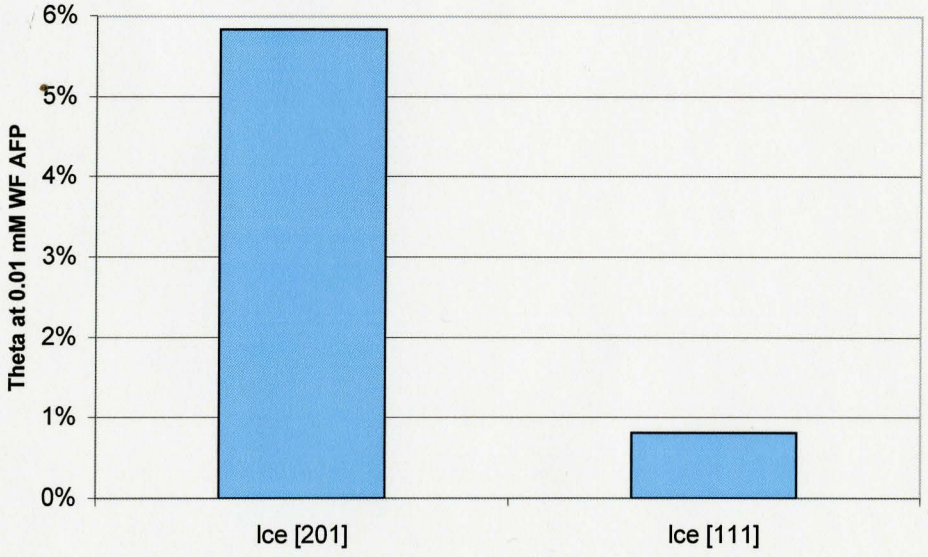

Figure 6.3. The calculated fractional density θ of WF AFP on [201] and [111] ice surfaces.

Chapter 7. Conclusion

The atomic-level mechanisms by which antifreeze proteins bind to ice are poorly understood. Until recently, the dominating theory was that the H-bonding is the major driving force of the binding (Raymond & DeVries, 1977; DeVries, 1984; Brooke-Taylor et al., 1996; Cheng & Merz, 1997). However, mutational experiments in which substitution of hydrophilic residues in AFP by the hydrophobic residues did not deteriorate the AFP-ice binding (Haymet et al., 1999) questioned this theory suggesting that the solvating effects may be involved. Obviously, computational molecular modeling studies were necessary to elaborate this suggestion.

In this study, we first estimated theoretically an approximate value of the free energy of AFP binding to ice and found it to be about -5 kcal/mol, a very small value as compared to the large energy of hydration of ice and AFP. This fact puts severe limitation on the choice of methodology of the simulation. Classical molecular dynamic computations with the explicit simulation of the system involving AFP, ice, and thousands of water molecules would require enormous computational resources to reproduce a small difference of two large energies. Less comprehensive MD simulations would hardly explain why AFP prefers the rigid water to the liquid one.

Therefore, we decided to employ new computational methods in which solvating effects are computed with using implicit substitutes of the explicit water molecules (Augspurger and Scheraga, 1996; Lazaridis and Karplus, 1999). The number of atoms in such a system is relatively small because thousands of water molecules are not included. Even more importantly, only tens variable degrees of freedom are necessary to describe the geometry of this system: position and orientation of AFP and side-chain torsions in AFP. This number of variables is negligibly small as compared to many thousands of degrees of freedom in the system involving explicit water molecules. The small number of variables opened a possibility to employ highly efficient Monte-Carlo minimization methods for the search of energetically optimal conformations of the system. The problem, however, was complicated by the absence of parameters describing energy of interacting of implicit waters with the melting ice. We calibrated these parameters to reproduce approximately the free energy of binding of AFP with ice.

Armed with this new methodology, we sought for the lowest-energy complexes of AFP and ice. Using the ZMM program, the thousands of MCM trajectories were launched from randomly generated starting positions and orientations of AFP. The analysis of the results allowed conclude that entropically favorable dehydration of hydrophobic groups of AFP, such as methyl groups in threonine, switching the hostile water environment to the ice surface is the major driving force of AFP-ice binding.

Along with this general conclusion, several structural problems were resolved by our modeling studies. Thus, we explained why WF AFP binds to the [111] ice plane more preferably than to other crystallographic planes. We explained interesting peculiarities of structure-activity relationships of natural analogs of WF AFP as well as their artificial mutants. We also proposed that the overall structure of AFPs evolved to find a compromise to bind to the "flat" ice surface but avoid self-aggregation.

Methodological aspects and results of this study, besides their direct relevance to the problem of ice-AFP interaction, may be pertinent to simulation studies of ligand-receptor and protein-protein interactions. Solvating and desolvating effects are increasingly recognized as most important component of such interactions (Camacho and Delisi, 1999; 2000). The methodology developed and tested during the course of this study may be used to simulate these systems.

Bibliography

Abagyan, R., and M. Totrov. (1994) Biased probability Monte Carlo conformational searches and electrostatic calculations for peptides and proteins. *J Mol Biol.* 235:983-1002.

Augspurger, J. D., and H. A. Scheraga. (1996) An efficient, differentiable hydration potential for peptides and proteins. *J Comput Chem.* 17:1549-58.

Baardsnes J, Kondejewski LH, Hodges RS, Chao H, Kay C, Davies PL. (1999) New ice-binding face for type I antifreeze protein. *FEBS Lett.*. 463(1-2):87-91.

Brooke-Taylor, C.A., Grant, G.H., Elcock, A.H. & Richards, W.G. (1996) Mechanism of action of antifreeze polypeptide HPLC6 in solution - analysis of solvent behavior by molecular dynamics. *Chem. Phys.* 204, 251-261.

Brooks, C. L., B. M. Pettitt, and M. Karplus. (1985) Structural and energetic effects of truncating long ranged interactions in ionic polar fluids. *J Chem Phys.* 83:5897-5908.

Brooks, C.L., Pettitt, B.M., Karplus, M. (1985) Structural and energetic effects of truncating long ranged interactions in ionic polar fluids. *J. Chem. Phys.* 83:5897-5908,.

Burcham TS, Osuga DT, Yeh Y, Feeney RE. (1986) A kinetic description of antifreeze glycoprotein activity. *J Biol Chem*; 261(14):6390-7

Camacho C. J., Weng Z., Vajda S., and DeLisi C.. 1999. Free Energy Landscapes of Encounter Complexes in Protein-Protein Association. *Biophys. J.* 76: 1166–1178.

Camacho C. J., Kimura S. R., DeLisi C., and Vajda S.. 2000. Kinetics of Desolvation-Mediated Protein–Protein Binding. *Biophys. J.* 78: 1094–1105.

Chakrabartty, A. & Hew, C.L. (1991) The effect of enhanced a-helicity on the activity of a winter flounder antifreeze polypeptide. *Eur. J. Biochem.* 202, 1057-1063.

Chakrabartty, A., Hew, C.L., Shears, M. & Fletcher, G. (1988) Primary structures of the alanine-rich antifreeze polypeptides from grubby sculpin, Myoxocephalus aenaeus. *Can. J. Zool.* 66, 403-408.

Chao, H., Hodges, R.S., Kay, C.M., Gauthier, S.Y. & Davies, P.L. (1996) A natural variant of type I antifreeze protein with four ice-binding repeats is a particularly potent antifreeze. *Protein Sci.* 5,1150 -1156.

Chao, H., Houston, M.E., Hodges, R.S., Kay, C.M., Sykes, B.D., Loewen, M.C., Davies, P.L. & SoÈnnichsen, F.D. (1997) A diminished role for hydrogen bonds in antifreeze protein binding to ice. *Biochemistry* 36, 14652-14660.

Chen, L., A. L. DeVries, and C. H. Cheng. (1997) Evolution of antifreeze glycoprotein gene from a trypsinogen gene in Antarctic notothenioid fish. *Proc Natl Acad Sci U S A.* 94:3811-6.

Cheng, A.L. & Merz, K.M. (1997) Ice-binding mechanism of winter flounder antifreeze proteins. *Biophys. J.* 73, 2851-2873.

Chou, K.C. (1992) Energy-optimized structure of antifreeze protein and its binding mechanism. *J. Mol. Biol.* 223, 509-517.

Dalal P, Sonnichsen FD. (2000) Source of the ice-binding specificity of antifreeze protein type I. *J Chem Inf comput Sci;* 40(5):1276-84.

Davies PL, Sykes BD (1997) Antifreeze proteins. *Curr Opin Struct Biol.* 7(6):828-34. Review.

DeLuca, C.I., Chao, H., SoÈnnichsen, F.D., Sykes, B.D. & Davies, P.L. (1996) Effect of type III antifreeze protein dilution and mutation on the growth inhibition of ice. *Biophys. J.* 71, 2346-2355.

Deng, G.J., Andrews, D.W. & Laursen, R.A. (1997) Amino acid sequence of a new type of antifreeze protein from the longhorn sculpin Myoxocephalus octodecimspinosis. *FEBS Lett.* 402, 17-20.

DeVries, A.L. (1974) Survival at freezing temperatures. In Biochemical and Biophysical Perspectives in Marine Biology (Sargent, J. & Mallins, D.W., eds), pp. 289-330. *Academic Press, London.*

DeVries, A.L. & Lin, Y. (1977) Structure of a peptide antifreeze and mechanism of adsorption to ice. *Biochim. Biophys. Acta* 495, 388±392.

DeVries, A.L. (1980) Biological antifreezes and survival in freezing environments. In Animals and Environmental Fitness (Gilles, R., ed.), *Pergamon Press, Oxford.*pp. 583-607.

DeVries, A.L. (1982) Biological antifreeze agents in coldwater fishes. *Comp. Biochem. Physiol.* B 73, 627-640.

DeVries, A.L. (1983) Antifreeze peptides and glycopeptides in cold-water fishes. *Ann. Rev. Physiol.* 45, 245-260.

DeVries, A.L. (1984) Role of glycopeptides and peptides in inhibition of crystallization of water in polar fishes. *Phil. Trans. R. Soc. Lond.* B 304, 575-588.

Duman, J.G. & DeVries, A.L. (1974) Freezing resistance in winter flounder Pseudopleuronectus americanus. *Nature* 247, 237-238.

Duman, J.G. & DeVries, A.L. (1976) Isolation, characterisation and physical properties of protein antifreezes from the winter flounder Pseudopleunectus americanus. *Comp. Biochem. Physiol.* B 54, 375-380.

Fletcher, G.L., Addison, R.F., Slaughter, D. & Hew, C.L. (1982) Antifreeze proteins in the Arctic shorthorn sculpin (Myoxocephalus scorpius). *Arctic* 35, 302-306.

Gibson, K. D., and H. A. Scheraga. (1967) Minimization of polypeptide energy. I. Preliminary structures of bovine pancreatic ribonuclease S-peptide. *Proc Natl Acad Sci U S A.* 58:420-7.

Go, N., and H. A. Scheraga. (1970) Ring closure and local conformational deformations of chain molecules. *Macromolecules.* 3:178-187.

Gong Z, Ewart KV, Hu Z, Fletcher GL, Hew CL. (1996) Skin antifreeze protein genes of the winter flounder, Pleuronectes americanus, encode distinct and active polypeptides without the secretory signal and prosequences. *J Biol Chem.*271(8):4106-12.

Graham LA, Liou YC, Walker VK, Davies PL. (1997) Hyperactive antifreeze protein from beetles. *Nature.* 388(6644):727-8.

Harding MM, Ward LG, Haymet AD. Type I 'antifreeze' proteins. Structure-activity studies and mechanisms of ice growth inhibition. *Eur J Biochem.* 1999 Sep;264(3):653-65. Review

Haymet, A.D.J. & Kay, P.A. (1992). Molecular dynamics simulation of a fish `antifreeze' polypeptide (AFP). Paper presented at the Society for Cryobiology 29th Annual Meeting (CRYO 0 92), *Itaca, New York,* Abstract 41.

Haymet, A.D.J., Ward, L.G., Harding, M.M. & Knight, C.A. (1998) Valine substituted winter flounder antifreeze ± preservation of ice growth hysteresis. *FEBS Lett.* 430, 301-306.

Haymet, A.D.J., Ward, L.G. & Harding, M.M. (1999) Winter Flounder `antifreeze' proteins: synthesis and ice growth inhibition of analogues that probe the relative importance of hydrophobic and hydrogen bonding interactions. *J. Am. Chem. Soc.* 121, 941-948.

Hew, C.L., Joshi, S., Wang, N.-C., Kao, M.-H. & Ananthanarayanan, V.S. (1985) Structures of shorthorn sculpin antifreeze polypeptides. *Eur. J. Biochem.* 151, 167-172

Hopfinger, A. J. (1971) Polymer-solvent interactions for homopolymers in aqueaous solution. *Macromolecules.* 4:731-737.

Hopfinger, A. J., and R. D. Battershell. (1976) Application of SCAP to drug design. 1. Prediction of octanol-water partition coefficients using solvent-dependent conformational analyses. *J Med Chem.* 19:569-73.

Jia, Z.C., DeLuca, C.I. & Davies, P.L. (1995) Crystallization and preliminary X-Ray crystallographic studies on type III antifreeze protein. *Protein Sci.* 4, 1236-1238.

Knight, C.A., DeVries, A.L. & Oolman, L.D. (1984) Fish antifreeze protein and the freezing and recrystallization of ice. *Nature* 308, 295-296

Knight, C.A., Cheng, C.-H.C. & DeVries, A.L. (1991) Adsorption of a-helical antifreeze peptides on specific ice crystal surface planes. *Biophys. J.* 59, 409-418.

Lal, M., Clark, A.H., Lips, A., Ruddock, J.N. & White, D.N.J. (1993) Inhibition of ice crystal growth by preferential peptide adsorption ± a molecular modeling study. *Faraday Discuss.* 95, 299-306.

Langmuir, I. (1918) The adsorption of gases on plane surfaces of glass, mica and platinum. *J. Am. Chem. Soc.* 40: 1361-1403.

Lazaridis, T., and M. Karplus. (1999) Effective energy function for proteins in solution. *Proteins.* 35:133-52.

Lee, B., and F. M. Richards. (1971) The interpretation of protein structures: estimation of static accessibility. *J Mol Biol.* 55:379-400.

Li, Z., and H. A. Scheraga. (1987) Monte Carlo-minimization approach to the multiple-minima problem in protein folding. *Proc Natl Acad Sci U S A.* 84:6611-5.

Li, Z., Scheraga, H.A. (1988) Structure and free energy of complex thermodynamic systems. *J. Mol. Struct.* 179:333-352,.

Liou YC, Davies PL, Jia Z. (2000) Crystallization and preliminary X-ray analysis of insect antifreeze protein from the beetle Tenebrio molitor. Acta Crystallogr D Biol Crystallogr. 6 (Pt 3):354-6.

Loewen MC, Chao H, Houston ME Jr, Baardsnes J, Hodges RS, Kay CM, Sykes BD, Sonnichsen FD, Davies PL. (1999).Related Articles Alternative roles for putative ice-binding residues in type I antifreeze protein. *Biochemistry.* 38(15):4743-9.

Maurer, M. C., J. Y. Trosset, C. C. Lester, E. E. DiBella, and H. A. Scheraga. (1999). New general approach for determining the solution structure of a ligand bound weakly to a receptor: structure of a fibrinogen Aalpha-like peptide bound to thrombin (S195A) obtained using NOE distance constraints and an ECEPP/3 flexible docking program. *Proteins.* 34:29-48.

McDonald, S.M., Tasaki, K., Brady, J.W. & Clancy, P. (1992). Molecular dynamics simulations of winter flounder antifreeze polypeptide (HPLC-6): stability features and mechanisms of action. Paper presented at the Society for Cryobiology 29th Annual Meeting (CRYO 0 92), *Itaca, New York*, Abstract 42.

Momany, F.A., McGuire, R.F., Burgess, A.W., Scheraga, H.A. (1975) Energy parameters in polypeptides. VII. Geometric parameters, partial atomic charges, nonbonded interactions, hydrogen bond interactions, and intrinsic torsional potentials of the naturally occurring amino acids. *J. Phys. Chem.* 79:2361-2381,

Nemethy, G., M. S. Pottle, and H. A. Scheraga. (1983) Energy parameters in polypeptides. 9. Updating of geometrical parameters, nonbonded interactions, and hydrogen bond interactions for the naturally occurring amino acids. *J Phys Chem.* 87:1883 -1887.

Ng, N.F., Trinh, K.-Y. & Hew, C.L. (1986) Structure of an antifreeze polypeptide Precursor from the sea raven, Hemitripterus americanus. *J. Biol. Chem.* 261, 15690-15695.

Ng, N.F.L. & Hew, C.L. (1992) Structure of an antifreeze polypeptide from the sea aven: disulfide bonds and similarity to lectin-binding proteins. *J. Biol. Chem.* 267, 16069-16075.

Noguti, T., and N. Go. 1985. Efficient Monte Carlo method for simulation of fluctuating conformations of native proteins. *Biopolymers.* 24:527-46.

Raymond, J.A. & DeVries, A.L. (1977) Adsorption inhibition as a mechanism of freezing resistance in polar fishes. *Proc. Natl Acad. Sci. USA* 74, 2589-2593.

Scholander, P.F., Dam, L.V., Kanwisher, J., Hammel, T. & Gordon, M.S. (1957) Supercooling and osmoregulation in Arctic fish. *J. Cell. Compar. Physiol.* 49, 5-24.

Scott, G.K., Davies, P.L., Shears, M.A. & Fletcher, G.L. (1987) Structural variations in the alanine-rich antifreeze proteins of the Pleuronectinae. *Eur. J. Biochem.* 168, 629-633.

Sicheri, F. & Yang, D.S.C. (1995) Ice-binding structure and mechanism of an antifreeze protein from winter flounder. *Nature* 375, 427-431.

Slaughter, D., Fletcher, G.L., Ananthanarayanan, V.S. & Hew, C.L. (1981) Antifreeze proteins from the sea raven, Hemitripterus americanus: Further evidence for diversity among fish polypeptide antifreezes. *J. Biol. Chem.* 256, 2022-2026.

SoÈnnichsen, F.D., DeLuca, C.I., Davies, P.L. & Sykes, B.D. (1996) Refined solution structure of type III antifreeze protein-hydrophobic groups may be involved in the energetics of the protein±ice interaction. *Structure* 1325-1337.

Weiner, S.J., Kollman, P.A., Case, D.A., Singh, U.C., Ghio, C., Alagona, G., Profeta, S. Jr., Weiner, P. A new force field for molecular mechanical simulation of nucleic acids and proteins. *J. Am. Chem. Soc.* 106:765-784, 1984.

Wen, D. & Laursen, R.A. (1992) Structure-function relationships in an antifreeze polypeptide: the role of neutral, polar amino acids. *J. Biol. Chem.* 267, 14102-14108.

Wen, D. & Laursen, R.A. (1993) Structure-function relationships in an antifreeze polypeptide ± the effect of added bulky groups on activity. *J. Biol. Chem.* 268, 6401-16405.

Wilson, P.W. (1994) A model for thermal hysteresis utilizing the anisotropic interfacial energy of ice crystals. *Cryobiology* 31, 406-412.

Yang, D.S.C., Sax, M., Chakrabartty, A. & Hew, C.L. (1988) Crystal structure of an antifreeze polypeptide and its mechanistic implica-tions. *Nature* 333, 232-237.

Zhang, W. & Laursen, R.A. (1998) Structure-function relationships in a type I antifreeze polypeptide ± the role of threonine methyl and hydroxyl groups in antifreeze activity. *J. Biol. Chem.* 273, 34806-34812.

Zhorov, B. S. (1981). Vector method for calculating derivatives of energy of atom-atom interactions of complex molecules according to generalized coordinates. *J Struct Chem.* 22:4-8.

Zhorov, B. S. (1983). Vector method for calculating derivatives of the energy deformation of valence angles and torsion energy of complex molecules according to generalized coordinates. *J Struct Chem.* 23:649-655.

Zhorov, B. S. (1993) Comparison of lowest energy conformations of dimethylcurine and methoxyverapamil: evidence of ternary association of calcium channel, Ca^{2+}, and calcium entry blockers. *J Membr Biol.* 135:119-27.

Zhorov, B. S., and N. B. Brovtsyna. (1993) Conformational analysis of d-tubocurarine: implications for minimal dimensions of its binding site within ion channels. *J Membr Biol.* 135:19-26.

Zhorov, B. S., and S. X. Lin. (2000) Monte Carlo-minimized energy profile of estradiol in the ligand-binding tunnel of 17 beta-hydroxysteroid dehydrogenase: atomic mechanisms of steroid recognition. *Proteins.* 38:414-27.